Haptic feedback in the steering system of the FRISC

A proof-of-concept

LTZ3 S.C.(Sophie) Schouten

August 15, 2018

Haptic feedback in the steering system of the FRISC

By:

LTZ3 S.C. (Sophie) Schouten

to obtain the degree of Master of Science
at the Delft University of Technology,
to be defended publicly on Monday August 27, 2018 at 10:00 PM

Student number: 4596692
Report number: SDPO.18.029.m.
project duration: November 13, 2017 - August 27, 2018
Thesis committee: ir. K. Visser, Rear-Admiral (ME) ret.
dr.ir. A. Vrijdag
dr.ing. S. Schreier

Contents

Summary

The FRISC is a high speed craft of the Netherlands Navy which came into use in 2012. Because these vessels sail with speeds up to 45 knots in inshore waters, a large amount of focus and accurate path following is needed for safe navigation, and due to large accelerations, there is a high level of physical strain. These two factors cause a high (prolonged) mental and physical workload which can heighten mental and physical fatigue, resulting in higher risks due to reduced alertness and mental performance. With this in mind, the focal point of this thesis is to increase the safety of the FRISC during high speed navigation by increasing the path following performance and reducing the level of fatigue through lowering the workload. With extensive literature research a possible solution was found to increase the safe navigation. Namely, haptic feedback which will decrease the workload and increase the path following performance. With this in mind, the following research question arises:

To what extent can haptic feedback, implemented into the steering system of the FRISC, contribute to safe navigation during (nightly) high speed inshore navigation?

A FRISC operates with high speeds in inshore waters, following a well prepared detailed planned route. During such an operation the FRISC is subject to performance shaping factors, factors "which influence the likelihood of an error occurring" [1]. With the use of the literature, a possible solution for almost all the factors, related to the FRISC, were found. This solution is a haptic feedback system which will lower the workload and increase the path following performance. An active guidance system is developed with two types of controllers (waypoint controller and XTE controller) to "advise" the operator with the correct rudder angle, to follow a preplanned route during high speed inshore navigation. The contribution of this thesis is tested by the implementation of a haptic shared control, and by investigating the cross track error and the workload. The results of the investigation of the XTE were unambiguous. The XTE controller lowers the mean and median XTE values by 20% and the absolute maximum value is lowered by 37% compared to manual control. The waypoint controller resulted in higher XTE values which means that manual control has the preference above the waypoint controller based on the XTE.
Furthermore, the participants indicated that the perceived workload was 37% and 44% lower with the use of the waypoint controller and XTE controller respectively. The physical workload was compared between the experience of the participants and the measured physical demand. This comparison resulted in the fact that the experience of the participants was not in line with the actual physical effort. The physical effort was the highest with the use of both controllers whereas the experience of the physical workload was the lowest. This was assumed to be less important than the perceived workload and therefore it did not influence the conclusion of haptic feedback lowering the workload.
Altogether, it is stated that the use of the correct haptic shared control system could increase the safety of navigating during (nightly) high speed inshore navigation.

Preface

This MSc thesis is written as the last part to obtain my master's degree in Marine Technology, with the track Design Production and Operation at Delft University of Technology. In all industries research is done on fully automated systems. However, this is not yet accepted in the empirical world and that is why another form of automation can be an interesting alternative, namely haptic feedback.
Haptic feedback is not yet extensively researched in shipping but could be an option to create more safety during inshore ship navigation. In my years after this master I will sail on navy vessels and during this job one must deal with safety at sea. Therefore, this subject is most appealing to me due to the common ground with my future job.
With as main goal to contribute to safer navigation, I developed a model in MATLAB Simulink which "advises" the operator a rudder angle to stay on the planned route. It was a tough process, but in the end I am looking back with a smile. I thank my supervisor Arthur Vrijdag who was very supportive and a great help with all my questions. Altogether I am proud of my delivered work and think the research could be helpful for further research.

S.C. (Sophie) Schouten

Delft, August 2018

List of Figures

List of Symbols

Symbol:	Description:	Unit:
d_{wol}	Distance to wheel over line	m
d_{XTE}	Distance cross track error	m
$dist$	Disturbance	-
e_{ψ}	Heading error	°
$F_{command}$	Forces human operator	N
F_{guide}	System forces	N
H_{ci}	Impedance of control interface	S
H_{nms}	Neuromuscular dynamics of the driver	S
K_f	Lookahead gain	-
pos_i	Position past waypoint	m
pos_{i+1}	Position upcoming waypoint	m
pos_{i+2}	Position waypoint after upcoming waypoint	m
pos_{ship}	Position ship	m
pos_{WOL}	Position wheel over line	m
pos_{WOP}	Position wheel over point	m
ref_{human}	Trajectory of the driver	m
ref_{sys}	Trajectory of the system	m
$v_{current}$	Current speed	kt
v_{ship}	Ship speed	kt
$vibr_{max}$	Maximum warning distance	m
X_c	Steering output	°
X_d	Course angle	°
X_e	Position error x-direction	°
X_{set}	Set-point position x-direction	m
Y_e	Position error y-direction	°
Y_{set}	Set-point position y-direction	m
β	Sideslip	°
Δ	Lookahead distance	m
δ	Actual rudder angle	°
δ_{set}	Set-point rudder angle	°
$\psi_{i->i+1}$	Bearing past waypoint towards upcoming waypoint	°
$\psi_{i+1->i+2}$	Bearing upcoming waypoint towards the waypoint after that	°
$\psi_{s->i+1}$	Bearing ship towards upcoming waypoint	°
ψ_{set}	Heading setpoint	°
ψ_{ship}	Ship heading	°

List of Abreviations

Abbreviation:	Description:	Unit:
BC	Boarding Craft	-
COG	Course Over Ground	°
DGPS	Differential Global Positioning System	-
DNC	Distance to New Course	m
ECDIS	Electronic Chart Display and Information System	-
FRISC	Fast Raiding and Interception Special forces Craft	-
GPS	Global Positioning System	-
GUI	Graphical User Interface	-
LOS	Line Of Sight	-
MARIN	Maritime Research Institute Netherlands	-
MCT	Maritime Counter Terrorism	-
NMEA	National Marine Electronic Association-	-
NSF	National Science Foundation	-
PID	Proportional, Integral, Derivative	-
PSF	Performance Shaping Factors	-
PWM	Pulse-width Modulation	-
PWO	Principal Warfare Officer	-
RADAR	Radio Detection And Ranging	-
RC	Raiding Craft	-
RIB	Rigid Inflatable Boat	-
RNoN	Royal Norwegian Navy	-
SCC	Support Craft Caribbean	-
SOG	Speed Over Ground	kt
STW	Speed Through Water	kt
SVI	Standard Variables Interface	-
UDP	User Datagram Protocol	-
WOL	Wheel Over Line	-
WOP	Wheel Over Point	-
XTE	Cross Track Error	m

Introduction

Since the end of 2012 the Royal Netherlands Navy sails with a high speed vessel named the FRISC (Fast Raiding Interception and Special forces Craft), Figure 0.1 [2] [11]. This high speed vessel is designed in two versions (lengths of 12 and 9.6 meters) and is used on board of surface vessels and by the marines. The FRISC is, according to the Operation Evaluations of the Netherlands Navy , a game changer with a high operational potential [12]. This vessel is used during counter drugs operations in the Caribbean and near the Dutch coast and it is used successfully during interceptions and suspected piracy.
Within the Netherlands the FRISC is used by NLMARSOF (Netherlands Maritime Special Operations Forces) for maritime special operations [12]. This high speed craft distinguishes itself by its large engine power accompanied by a vessel speed of approximately 45 knots. Three types of FRISCs are used within the Netherlands Navy: the Boarding Craft (BC), Raiding Craft (RC) and Support Craft Caribbean (SCC). All types are used for different purposes but can also be used for general operations such as replenishment, security, logistic operations and embarking/disembarking [13].

Figure 0.1: FRISC with operator and navigator [2].

During an operation the FRISC is at least manned by the operator and the navigator. The operator operates the controls while the navigator is mainly responsible for the safe navigation using an electronic nautical chart and radar.
Sailing a FRISC with high speeds, especially during inshore navigation, involves high risks. There are potential dangers above the water, think of buoys and vessels, as well as below the water, like shoals and wrecks. This results in the need of high path following performance, a high amount of focus of both crew members and requires intense concentration and rapid responses. The crew members continuously communicate with each other and monitor the operating systems. The integration of multiple sources of information may make navigation and collision avoidance more reliable but may also increase the (mental) workload [14].

Furthermore, the crew is subject to vibrations such as Whole-Body Vibrations and Repeated Shocks. Dependent on speed and sea state, forces of acceleration on the body can reach up to 15 G. These vibrations and forces create a high level of physical strain during an operation and can lead to high physical workload, and personal and material damage [12]. Prolonged mental and physical workload heighten mental and physical fatigue. Physical fatigue is accompanied by reduction of performance in the muscular system. Mental fatigue may influence various information processing functions such as listening, watching, and long and short-term memory. It may also lead to reduced alertness and reduced mental performance [15] [16].
It is clear that crew members of high speed vessels, such as the FRISC, are subject to fatigue. A tired crew will overlook dangers more easily due to the affected information processing function, which might create higher risks. With this in mind, the focal point of this thesis is to increase the safety during high speed navigation by reducing fatigue through lowering the workload and increasing the path following performance.
Note that this thesis focusses on the FRISC of the Netherlands Navy, but the results may be useful in other high speed crafts as well such as the NH1816 class of the Royal Netherlands Sea Rescue Institution (*KNRM*), the FRISC of the Dutch Military Police (*Marechaussee*) and Fast Patrol Boats.
Not only the crew of fast vessels must deal with a high concentration factor and risks (e.g. the possibility of a collision) during an operation. Similar risks occur in aviation, as well as when driving a car. In these industries much research has already been done to reduce the risks by using haptic feedback.
In aviation, adding a haptic flight director shows great potential by providing fast and continuous tactile information for manual aircraft flight control, causing the workload of the pilot and the path following performance to be much more accurate as compared to a visual flight director [17].
In the car industry as well, haptic feedback has already been successfully implemented using steering wheel guidance which shows a significant reduction in visual demand and a freeing of attention [7] [18].
The use of haptic feedback in other means of transport as shown above, are good examples of the benefits of using haptics. Therefore, it can be useful to research the extent of haptic feedback in fast vessels.
In this case, haptics in the steering system of the FRISC is an option to reduce the risks and increase the safety during inshore navigation. Correspondingly, in this master thesis an attempt is made to reduce the workload of the crew and increase the path following performance and thereby to increase the safety during (nightly) high speed inshore navigation with the FRISC. This will be done by implementing haptic feedback into the steering system of the FRISC. This choice is made because according to Abbink et al., 2012 [19] a future direction to explore for the maritime industry is haptic human-automation interaction, which has shown promise as a physical, bidirectional communication interface. This haptic human-automation interaction is based on clear communication of the actions of an automation system through forces on the control interfaces, merging the operator and the machine intelligence.
Furthermore, Hoeckx et al., 2017 [20] state that the benefits of haptic human-automation interaction include improvements in primary and secondary task performances at reduced physical and mental workload, and better awareness of the automation system status and

intent.
With this knowledge, haptic feedback may be a solution for an increase of safe navigation. Note that in this thesis the term *safe navigation* is intended as the ability to follow the planned route. Avoiding shoals, buoys, ships and other obstacles are omitted. With this in mind the goal of this thesis is to develop haptic feedback software to investigate if force feedback can reduce the workload, increase the path following performance and thereby result in an improvement of the safe navigation of the FRISC. This results in the following main research question:

To what extent can haptic feedback, implemented into the steering system of the FRISC, contribute to safe navigation during (nightly) high speed inshore navigation?

To answer the research question, firstly general knowledge of the FRISC is necessary. In Chapter 1 the operations performed with the FRISC are described, together with a section on how the operator and navigator manoeuvre during high speed navigation. The theory about haptic feedback is investigated and analysed in Chapter 2. This chapter gives examples of other industries using haptic feedback, examines the (dis)advantages of haptic feedback and shows which contributions it can or cannot make. The information about the FRISC in combination with the theory about haptic feedback is used to create an experimental setup to answer the research question. Chapter 3 shows the setup necessary to carry out this experiment. In Chapter 4 the procedures and calculations are described. Appendices B and C are used to explain the implementation in detail.
Important to mention is that due to the limited amount of time of this research, it is not possible to test various situations such as different weather conditions, multiple operations, various waterways, etc. Therefore, only a (nightly) high speed inshore navigation operation will be investigated on a narrow waterway with no waves. This is done to simplify the implementation of the haptic feedback into the steering system because the wave calculations are omitted. In Chapter 5 the experimental methods are discussed followed by the corresponding results in Chapter 6. The discussion, conclusion and recommendations are given in the last three chapters of this thesis.

1. The FRISC

In this chapter information about the FRISC (Fast Raiding Interception and Special Forces Craft) is presented. The first section provides general information about the multiple types of FRISC the Royal Netherlands Navy operates and what the different versions are used for in order to show the reader the large capabilities of the FRISC. Section 1.2 presents the navigation procedures on board a FRISC by the operator and the navigator. The risks during high speed inshore navigation will also be treated.

1.1 The FRISC in general

The FRISC is a high speed vessel used for multiple operations by the Royal Netherlands Navy. There are two versions in length: the 12 meter and the 9.6 meter FRISC [12]. The 12 meter version is divided into two types, the Boarding Craft (BC) and Raiding Craft (RC), with as main difference the propulsion. The 9.6 meter FRISC is categorised as the Support Craft Caribbean (SCC). Table 1.1 shows the specifications of the three types.

Table 1.1: FRISC-types [2] [3] [21].

	BC	**RC**	**SCC**
Length	12 meter	12 meter	9.6 meter
Beam	3.3 meter	3.3 meter	3.5 meter
Weight	max. 8 ton	max. 8 ton	max. 7 ton
Maximum speed	43 knots	40 knots	45 knots
Range	445 kilometres	370 kilometres	500 kilometres
Engine power	2 × 370 h.p.	2 × 435 h.p.	2 × 370 h.p.
Propulsion	2 × sterndrive	2 × waterjet	2 × sterndrive
Draft	1.15 meter	0.65 meter	1.15 meter

The range and speed of the Raiding Craft are significantly lower than those of the Boarding Craft or Support Craft Caribbean. This is caused by a lower system efficiency of the waterjet compared to the open water propeller due to higher internal losses [22]. This means that for the same speed, more power is needed causing a lower efficiency and a lower operating range. The two different sorts of propulsors do not influence the way of operating; this is the same for the three types.
Of course, a vessel can only operate safely when it is used within its limits. The sailing limits given in regulations of the Netherlands Navy (*Voorschrift Commando Zeestrijdkrachten* [13]) for the FRISC are as follows:

Table 1.2: Sailing limitations FRISCs [13].

Sea state/ wave height	**usage**	**9.6m FRISC**	**12m FRISC**
Sea state 1/2 (wave height till 0.5m)	Max. speed	3000 RPM - 35 kt	No limitations
	Max. rudder	75% (above, vessel will drift)	No limitations
	Time length	4 hours without physical discomfort, then a break due to concentration and strain	TBD
Sea state 3 (wave height 0.5 till 1.5m)	Max. speed	2300 RPM - 25 kt (sailing will be uncomfortable)	3000 RPM - 35 kt
	Max. rudder	50%	50%
	Time length	2 hours, then body will create more tension to resist the forces and knees, neck and back will hurt	TBD
Sea state 4 (wave height 1.5 till 2.5m)	Max. speed	1700 RPM - 15 kt	2300 RPM - 25 kt (dependent on the wave angle)
	Max. rudder	40%	40%
	Time length	1.5 hours then physically exhausted	TBD
Sea state 5 (wave height 2.5 till 4m)	Max. speed	1500 RPM - 10 kt (sailing "normally" not possible)	1700 RPM - 15 kt (dependent on the wave angle
	Max. rudder	50%	30%
	Time length	0.5 hours, physically very stressful	TBD

Worthy of note is that the FRISC is able to operate in sea state 4 and return to a surface vessel in sea state 5. In Table 1.2 a wide range of limitations of the FRISC are shown, but in this thesis only sea state 1/2 will be used as indicated in the introduction (no waves). To create a good visual of the FRISC, an overview of the vessel is given in Figure 1.1. This figure shows a side view of the Boarding Craft (top image) and the Support Craft Caribbean (lower image).

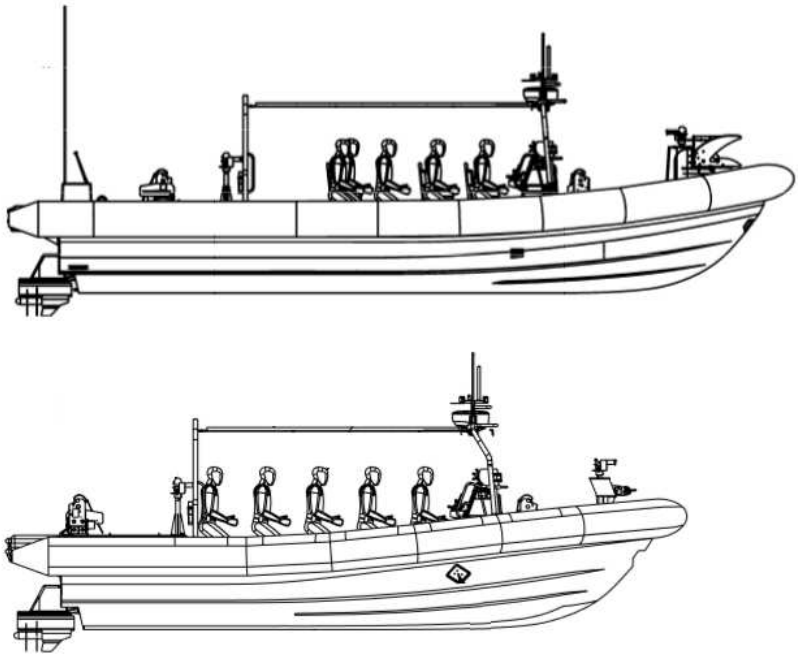

Figure 1.1: Profile FRISC, Boarding Craft (top) and Support Craft Caribbean [3] [4].

The three different FRISC-versions discussed in the beginning of this section can be used for specific operations but can also be used for general operations such as replenishment, security, logistic operations and embarking/disembarking [13]. To create some feeling with the FRISC-types, the specific operations and explanations belonging to the different versions are given below, Table 1.3.

Table 1.3: Specific operations belonging to the FRISC-types [23].

Operations	**BC**	**RC**	**SCC**
Shaping operations	×	×	×
Amphibious raids		×	×
River operations	×	×	×
Fleet protection	×	×	×
Patrol operations	×	×	
Transportation of staff and equipment	×		×
Special operations	×		
(MCT) Boarding operations	×		
Pursuit	×		

- Shaping operations: a pre-attack operation which contains, among others, reconnaissance, disarming mines, destroying obstacles and pre-landing operations;
- Amphibious raids: fast and short operations towards a specific goal followed by a planned retreat;

- River operations: operations on rivers and deltas. The craft transports staff and/or equipment or can be used as fire support craft;
- Fleet protection: the craft will operate near surface vessels (or surfaced submarines) and identify possible threats at a safe distance and eliminate when necessary;
- Patrol operations: during a patrol, suspicious vessels will be detected followed by identification;
- Transportation of staff and equipment: transportation of staff and/or equipment from a surface vessel towards a beach or a harbour, mainly from the Netherlands Antilles or Aruba. However, the operation area includes the complete Caribbean;
- Special operations: infiltration, withdrawals and fire support;
- (MCT) boarding operations: boarding operations performed on suspicious vessels or objects (e.g. oil platforms);
- Pursuit: aim is to reduce the distance to the suspicious vessel and to intercept this vessel.

As shown above, the three types can be deployed for many different operations. In this thesis the focus lays on high speed navigation. Because the purpose of this research is to improve the safe navigation and not to perform any other form of operation, the type of vessel used is irrelevant for the outcome of the results during this research.
To operate the FRISC and the above mentioned operations safely, the crew needs to perform an extensive and detailed preparation regarding navigation. The next section gives an insight how the vessel is operated and how the navigation is performed during high speed (inshore) navigation.

1.2 Navigation

During an operation the FRISC is at least manned by the operator and the navigator. The operator operates the controls while the navigator is mainly responsible for the safe navigation. The controls of the operator consist of the steering wheel and the throttles, one for starboard and one for port engine. The navigator uses an electronic map showing the nautical chart to navigate [21]. In addition to the electronic chart, a radar (Radio Detection And Ranging) is used to determine the presence of other objects and their course and speed [13]. These operating and navigation tools are positioned on the main console of the FRISC, Figure 1.2.
Note that in this picture the new "trial" navigation system of the brand Seacross is installed which is not yet implemented in all FRISCs. In Appendix A the "old" main console, together with its corresponding descriptions is shown in more detail.

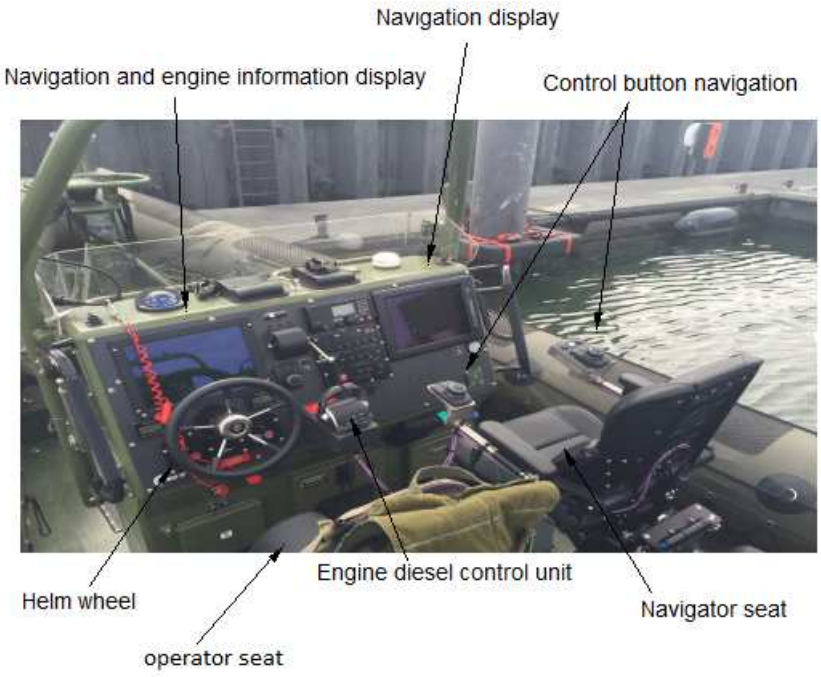

Figure 1.2: "New" main console.

Before the crew can use the tools on the main console and operate safely, a detailed route preparation is always done together with a pre-sailing briefing. Besides a detailed preparation, an important factor is the knowledge of the operator about his limits and the limits of his crew given the operating environment and the conducted operation. To accomplish a safe operation, the operator will be involved in the planning process by the commanding officers and planning personnel [13]. Note that this is only done during high speed inshore navigation.
During operations at open sea these preparations are not necessary as the environmental risks (objects and shoals) are less. In this case the FRISC operates from a surface vessel and is guided towards its goal by the Principle Warfare Officer (PWO) who is stationed onboard the surface vessel in the command centre.
When the planning process is finished, the inshore operation starts and the mentioned electronic chart and radar are used for safe navigation. It is important that the navigator always navigates during sailing, also with low speeds and with a low number of surrounding vessels.
During a high speed navigation operation (speeds of 35+ knots) the navigator communicates with the operator using short and clear standard terminology. To be able to communicate, the two crew members correspond through a headphone with an open line using VHF and HF communication. For clear communication four words are used by the navigator as a reminder which information must be given to the operator: Turning point (T), Head mark (H), Course (C) and Dangers (D). The way of navigating during high speed, using the electronic chart and the given letters is explained below based on Figure 1.3.

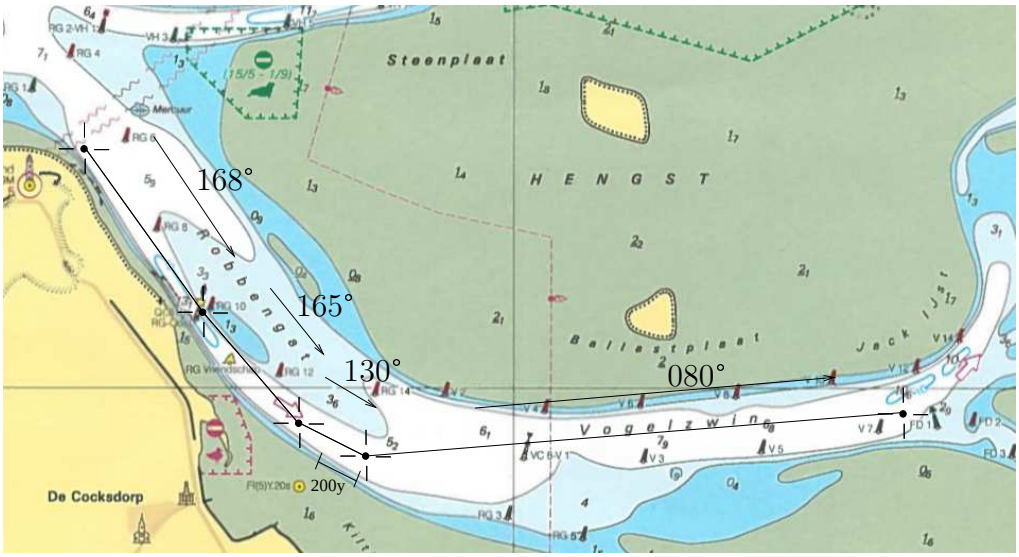

Figure 1.3: Example route FRISC north west of Texel.

Turning point (T): the point where the craft needs to turn to follow its prepared route. For example, the distance to the turning point from the 130° to 080° in Figure 1.3 is 200 yards. The navigator will tell the operator "*Turning point 200 yards, port 10*" meaning the turning point will be reached in 200 yards and when the turning point is reached turn with a rudder angle of 10° to port side.

Head mark (H): an "aiming" point which represents the steering direction. The head mark indicates the direction the operator needs to steer. The navigator will tell the operator "*Head mark lighthouse*" (this is not presented in Figure 1.3), which means the operator needs to steer in the direction of the lighthouse.

Course (C): represents the course of the planned route or the direction the navigator advises. The navigator will tell the operator "*Course 130*" this means the operator needs to steer course 130°, which the operator can check on the compass.

Dangers (D): a danger is an object which can be a risk for the safe navigation. A danger indicates an object that the craft will come across in the upcoming track(s), for example, other shipping, shoals or buoys. The navigator will tell the operator "*Danger, shoals starboard side 50 yards*" indicating a danger, in this case a shoal, on starboard side which will be passed in about 50 yards.

Besides the above described way of navigating, the FRISC-crew uses another method when sailing between buoys which indicate the waterway. The navigator "divides" the waterway into 10 parts, 1 is the left side of the waterway, 10 is the right side and 5 is the middle of the waterway. For example, the navigator will tell the operator "*straight 8*", meaning the operator needs to sail on the right side of the waterway, see Figure 1.4. In Figure 1.3 this method can be used during track 080° with buoys on both sides of the waterway.

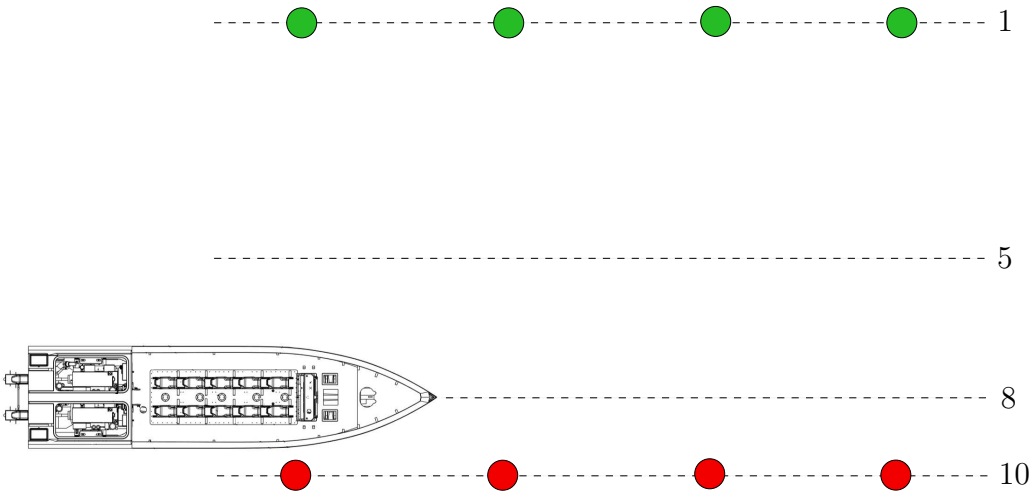

Figure 1.4: FRISC sailing *"straight 8"* in waterway.

Despite the detailed route preparations and the described way of navigating, high speed inshore navigation can be a great challenge, especially during the night. The dangers are, as mentioned, not only located above but also below the water. These dangers can easily be overlooked and the impact and damage can be substantial. This means that the crew needs to focus on many aspects at the same time resulting in a high workload.

1.3 Performance Shaping Factors

There is a difference in the way of sailing/navigating between high speed passenger crafts, pleasure crafts and naval crafts. This is probably due to different skill levels of the operators. It is presumable that there is a difference in the kind of training and the way of navigating between a professional and a skipper of a pleasure craft. The kind of accidents with these (professional and civilian) high speed crafts (HSC) however, are mostly similar. According to Antao and Soares., 2008 [24] high speed crafts are mostly subject to grounding, collisions and contacts. These three sorts of accidents cover the largest part of accidents with larger high speed ships (e.g. passenger catamarans). With small high speed vessels (e.g. RIBs or FRISCs), capsizing and ejecting passengers overboard are also common accidents.
A high speed vessel operating in sea-way, together with the combination of high speed, power and displacement can get dynamically unstable and can encounter large accelerations.
Furthermore, proper navigation for high speed vessels can be challenging due to the current navigational environment which is intended for more traditional (no high speed) crafts.
Additionally, when navigating at high speeds the corresponding risks will increase due to improper use of systems, such as the radar and to visibility issues [25]. With the use of these (intelligent) systems, the human becomes the weakest link in the system causing the operator to be the blame for most accidents [26]. These accidents caused by human error, have a mayor price tag and cost the marine industry $541 million a year [27] [28], not to mention the personal tragedy of injuries and loss of lives. These high costs and large number of accidents result in the need of thorough training, detailed route preparations

and knowledge about the environment and the reaction times of the vessel at high speeds [25]. For example, a vessel with a speed of 40 knots travels 20.58 meters per second (1 [kt] = 0.5144 [m/s]). This means that when the operator is looking at his systems or looks to the side for less than 5 seconds, the crafts is already a 100m further without the "knowledge" of the operator.
Furthermore, it can be difficult to follow the planned route precisely. A 10 degree deviation from the planned route for 5 seconds with a speed of 40 knots creates a cross track error (XTE) of 17.86m. This reflected on the FRISC, which navigates at high speeds in inshore areas where the safe sailing area is limited, can be of significant risk.
With no proper training, knowledge or route planning, the chance of accidents increases.

There is a large difference between civilian shipping and navigating with (inshore) naval vessels [28].
However, examples of accidents with high speed pleasure crafts can show the risks concerning operating with small high speed vessels. The first example is powerboat Sea Snake which crashed onto a cliff while entering a restricted navigational area during the night [29]. Secondly, the rigid inflatable boat (RIB) Sooty grounded with a large speed during the night on the rocks [30]. Other examples of grounded RIBs were found in [31] [32] [33]. On board of the RIB Milly, people were launched into the water when the vessel made an intended hard turn. Important to note is that, in this case, the owners were not aware of the dangers involved in taking high speed turns [34]. These examples show the importance of well-prepared navigation and knowledge of the impact of different actions at high speeds.
A naval vessel uses strict procedures and rules, resulting in safer navigation. Even with the right use of all the systems and procedures, operating high speed crafts is never free of risks. The high speeds do make it difficult for the operator to monitor all different systems at once, not miss anything and follow the planned route precisely.
To prevent accidents such as grounding and wrong rudder movements, force feedback can be a possible solution. By preparing a route in a chart-system, the steering system can generate a recommended rudder angle to steer in the right direction. To limit wrong rudder movements, due to lack of knowledge with high speeds, a rudder limiter can be implemented which prevents full rudder at high speed.
In the next part of this section the haptic feedback as a solution for these sorts of accidents is given.

As mentioned before, there is a large difference between civilian (pleasure) shipping and naval vessels. In the next part of this section the differences between navigating a civilian craft and a naval vessel are explained. Furthermore, an analysis, done by Gould et al., 2006 [28] about Performance Shaping Factors (PSF) in accidents that occurred in the Royal Norwegian Navy (RNoN) is discussed.
In the research of Gould et al., 2006 five reasons are identified about the difference between civilian shipping and (RNoN) naval vessels.

1. The tasks of naval vessels are unique and the operational demands are mostly more intense;

2. high speed naval vessels operate more often in shallow waters which can be poorly

marked or can be complicated at high speeds;

3. the navy works with shift systems causing crew members to have less sleep;
4. naval crew members are mostly younger and have a different educational background than merchant skippers.
5. the naval crew on the bridge operates with larger crew sizes and uses other navigation principles than most merchant vessels [28].

These differences are based on findings of the Norwegian Navy but are applicable to other navies with high speed crafts operating in the inshore waters as well.
In this thesis, where the FRISC is researched in the environment of inshore waters, it is assumed that the first four differences shown above are also suitable for the Netherlands FRISC. Because the FRISC is operated by just two people, the fifth difference is not applicable to this research.
The accidents researched in the article of Gould et al., 2006 are in inshore waters. The crew needs to be able to perform multiple tasks simultaneously and must deal with a great level of uncertainty [35].
With the above knowledge, Gould et al., 2006 did the analysis about high speed accidents by using performance shaping factors. These are factors "which influence the likelihood of an error occurring" [1]. These PSFs are based on the hypothesis that the surrounding conditions can be seen as individual factors which influence the way human act. The conditions, together with their corresponding factors, do not have any control over the outcome of the performance of the human and an error, but do influence the result [36]. In other words, the performance of the individual is assumed to be influenced but not determined by PSFs. To reduce the probability of an error, the use and identification of PSFs can be of high value [1].
In the analysis of Gould et al., 2006 the performance shaping factors of Kim and Jung (2003) [37] are used to identify the list of PSFs which are applicable to the navigation accidents with high speed vessels within the Norwegian Navy. To give a small insight into the list, multiple PSFs are given (Table 1.4) but for the full list of PSFs used in the analysis, see Gould et al., 2006 [28].
The list is divided in four main groups, human, system, task and environment (e.g. working capabilities, hardware system, procedures and working environment respectively) which are again divided into subgroups with more detailed items, Table 1.4 [28] [37].

Table 1.4: List with performance shaping factors [28].

Main group	**Subgroup**	**Detailed items**
Human	Cognitive characteristics	*Cognitive states* • Attention • Skill level *Temporal cognitive states* • Operator diagnosis • Perceived perception • Perceived consequences • Operator expectations
	Physical and psychological characteristics	*Physical states* • Fatigue *Psychological states* • Task burden
Task	Procedures	*Procedure* • Required time for completion • Number of simultaneous tasks *Task type* • Required level of cognition *Task attributes/requirements* • Amount of required information • Information load • Task difficulty • Perceptual requirements • Physical requirements • Speed • Precision
System	Man-machine interface	*Panel/screen layout* • Visibility
	System states	*System states* • level of automation
	Phenomenological characteristics	*Operational characteristics* • Time pressure
Environment	Physical working conditions	*Physical constraints* • Temperature/humidity/pressure • Vibration *Timing aspects* • Time of day • Time on duty
	Team and organization factors	*Team-related factors* • Adequacy of distributed workload

The three most common PFSs found in navigation accidents of the RNoN were operator expectations (77%), perceptual demands (74%) and attention (66%). Most of the factors found could be linked to the main group *human* and to subgroup *cognitive characteristics* [28].
To find performance shaping factors which can be related to the FRISC, Table 1.4 is used. Seven detailed items are selected to describe why these specific items can contribute to less accidents with the FRISC. Note that these factors are chosen with a subjective opinion by the writer, resulting in the possibility of other outcomes when the factors are chosen differently [37].

- Attention: due to the high speeds the FRISC navigates with, attention and focus are pivotal. When attention reduces, the situational awareness is less and the chance to overlook possible risks increases.
- Operator expectations: when the expectations of the operator of the upcoming events differ from the reality, the operator may make a poor assessment. For example, when an operator does not expect a shoal, he does not react to it and may run aground.
- Fatigue: as mentioned in the introduction, prolonged mental and physical workload heightens mental and physical fatigue. It will result in a reduction of performance in the muscular system, and in less alertness and reduced mental performance.
- Number of simultaneous tasks: this will lead to more mental workload which will result in higher mental fatigue. The integration of multiple sources of information may make navigation and collision avoidance more reliable but may also increase the (mental) workload, which again can result in fatigue [14].
- Information load: a lot of information needs to be processed during an operation. Because of the high speeds of the FRISC, only a short amount of time is available to do so. This results in a high mental workload causing even more fatigue.
- Precision: the high speeds result in short reaction times and the margin of error reduces. Therefore, operating in inshore waters need high path following performance to minimise the risks.
- Vibrations or shocks: lead to physical workload and strain which will result in fatigue.

The seven factors chosen above mostly result in high workload and fatigue. The expectations of the operator, his attention and path following performance are also important.
The point of focus of this thesis, as mentioned in the introduction, is to increase the safety during high speed navigation by reducing fatigue through lowering the workload and by increasing the path following performance.
The performance shaping factors chosen from the list in Table 1.4 and the focus of this thesis accord with each other for a large part. In the next paragraph, every given PSF is discussed and it will be shown that a possible solution to lower the likelihood of an error occurring is available with the implementation of haptic feedback.

1.3.1 Solutions to PSFs with haptic feedback

A possible solution to lower the number of *simultaneous tasks* and the *information load*, is to reduce the number of tasks and to help the operator to follow the indicated route accurately. A great potential to do so is the implementation of haptic feedback on the steering system. The force feedback advises the operator the correct rudder angle, resulting in a reduction of the number of tasks and in the minimization of looking at the electronic chart during operation. This will lead to a reduction in workload and consequently in less fatigue.
Furthermore, haptic feedback can increase the *precision* of the steering actions of the operator. To increase the *attention* of the operator is difficult, however to minimise the effect of less focus can be an option. As mentioned before, when an operator is distracted for 5 seconds with a speed of 40 knots, the vessel has advanced 100 meters and can have a cross track error of almost 20 meters with a steering fault of 10°. When introducing haptic feedback, the chance of a route deviation reduces when the attention lowers.
Haptic feedback can also be of help to improve the *operator expectations*. The operator "feels" the advice of the system in the steering wheel, limiting the unexpected dangers during sailing.
To reduce the influence of the *vibrations/shocks* felt by the crew, other measures need to be taken. Better seats with better suspension are a possibility. Another solution can be found in the haptic feedback, however not implemented on the steering wheel but on the throttles. A speed advise or speed limitation can be given through feedback to the operator, resulting in lower accelerations and less physical strain.
Altogether, haptic feedback can be a solution to reduce the likelihood of an error caused by the multiple PSFs. In this case the focus is mainly on force feedback in the steering system to follow an indicated route. To get more insight in the basics of haptic feedback, in the next chapter the background, definition and the categories of haptic feedback are discussed.

2. Haptic feedback

The word haptic is derived from the Greek word "haptikos" which means the sense of touch [38]. According to Hoeckx et al., 2017 [20] the word is used to indicate haptic devices which are designed to display forces to the user or to represent the physiology of human perception (through tactile sensors in the skin and through proprioceptive sensors in the muscles, tendons and ligaments).
The development of force feedback was the start of haptic systems. The initial applications were used in the nuclear industry as manipulators for teleoperation to access remote and dangerous locations [39]. The project GROPE of Fred Brooks in 1967 developed the first visual haptic system [40]. He enabled the user to gain knowledge by feeling the bonds between molecules and interact with them. In 1987 the visualisation sector took off after an article of the NSF (National Science Foundation) in Visualization in Scientific Computing [41]. During the launch of Windows and the Macintosh desktop, researchers started to develop haptic displays. The progression and availability of the PHANTOM device and GHOST software activated the real growth of haptic systems. After the release of GHOST (the first haptic library) in 1997, the sector of haptic visualisation systems has multiplied and is still increasing [42].

Much research on haptics is done. The majority of which is about haptic feedback implemented in cars, airplanes or robotics. Unfortunately, not much attention went to research about haptic feedback onboard ships to improve the control of the vessels [20].
A main difference between a ship and a car, besides for example the influence of current or waves, is the reaction time of the systems. To be able to navigate a large vessel, the operator needs to think ahead. This originates from the fact that, a large ship is a slow response system with slow dynamics and long reaction times, i.e. there is a long delay between giving the control input and achieving the desired effect. A car, on the contrary, is a fast response system. A car immediately reacts when the driver gives a steering input and less forward-thinking is necessary. The FRISC however is difficult to place under a fast or slow response system. Compared to a large merchant vessel, the FRISC is a fast response system but compared to a car it is a slow response system. To be able to use the information available in this research, the FRISC will be assumed to be a fast response system.
Furthermore, a vessel, as used in this thesis, is controlled in almost the same way as a car (steering wheel and gas pedal/throttle). Therefore, information given about haptics will be according to papers about haptic feedback in cars.
In the first part of this chapter the types of haptic systems are discussed (i.e. warning systems, systems using passive constraints and active guidance). This is followed by two variants of shared control systems. Furthermore, multiple research articles and their applicability are viewed to get an insight in the existing research.

2.1 Haptic systems

Haptic systems can be divided into three types: warning systems which use vibrations, systems using passive constraints to create a natural feel and guidance systems using ac-

tive constraints which deploy continuous forces [18] [20] [43] [44].
A warning system merely informs the driver about an unintended situation detected by the system and does not produce any form of direction guidance to the driver [44]. Vibrations implemented on the right or left side of the steering wheel however, can be used to warn the driver of an upcoming lane departure on a certain side [45] [46].
The guidance system, as the word indicates, provides the driver with continuous guidance and supplies the driver with information about an appropriate action. This means that a guiding force communicate both the direction and the magnitude of the recommended action [44]. In an example of lane keeping, continuous haptic feedback is given when the intention of the automation is to go back to the lane centre [18].

2.1.1 Warning system

As already mentioned, a warning system indicates a situation the automation does not approve of but does not inform the driver about the direction he has to steer to. The information is given via vibrations (high frequency, small amplitude) to the driver and can be done through the driver seat, the seat belt or the steering wheel [44] [45]. When steering wheel torque of equal extent is applied, steering wheel oscillations are induced. These vibrations are indicating to the driver that a steering reaction is needed [45].
In most articles one speaks of oscillations in the steering wheel rather than vibrations in the seat belt or the driver seat. Beruscha et al., 2011 [45] indicates that only studies with vibrations on the left or right half of a steering wheel were found and no implemented oscillations at the whole steering wheel. These vibrations at the left and right half of a steering wheel are referred to as directional steering wheel vibrations.
So, what can be the use and what is the effect of using such a warning system in a car? Petermeijer et al., 2015 [44] evaluated 70 empirical studies on haptic assistance in driving and their results indicate that warning systems provide short-term benefits such as a reduction in reaction time, an improved performance and a reduced mental workload. An important aspect is that the effect of the signal is considerably influenced by the content (i.e. frequency and amplitude) of the signal. A downside of a warning system is that it can be wrongly interpreted causing drivers to steer in the wrong direction.
A warning system can be used in two different ways. First it can indicate the deviation from the planned route, for example, the steering wheel starts vibrating when the vessel has a certain deviation from the route and increases in intensity during a larger error. Another possibility is that it can be used to indicate any sort of future danger. In both cases a warning system can be helpful to increase the safe navigation.

2.1.2 Passive constraints

Systems with passive constraints are built with the concept that they need to be operated by the operator; it is a hands-on device and its initial force is applied by the operator. In other words, if the driver does not exert a force on the controls, the system does not react either [5] [43]. The device can only exert forces to redirect or limit the motion of the system. This means that passive constraints are not capable of giving a guiding force. Additionally, passive dynamics are used to give a natural feel to the driver. For example, a damper can be used to simulate the resistance of the steering wheel and to create a more natural feel similar to an actual steering wheel on board of a vessel [20].

Passive constraints can be of large interest for, for example, a remotely controlled tug. When it is accompanying a vessel and it must push this vessel towards the quay it is possible to let the operator feel the moment of touch. Another example is that the system lets the operator feel the position of the propellers to indicate the moment full throttle can be given in the correct direction.

2.1.3 Active constraints/virtual fixtures

Contrary to a warning and passive system, a guidance system uses active constraints, also known as virtual fixtures. The driver "feels" the indication through forces provided by the automation system [44]. The forces can, for example, be used to guide the driver along some sort of optimal trajectory [18].
Another example is force feedback in the gas pedal where the forces are designed to continuously provide the driver with information in a car-following situation (two cars are behind each other) [19]. Note that in this case, also passive constraints are used. In this specific example not only a force is applied but the gas pedal is also designed with variable stiffness. The stiffness is used to decrease or increase the level of authority of the driver. The closer a lead car, the higher the stiffness of the gas pedal and the less driver authority [19]. This means that when the stiffness is very high the driver has no authority at all, it can be seen as an automatic control system and when the stiffness is almost null, the driver authority of the driver is at its maximum and the system has no influence at all. When both the driver and the automation have control, one can speak of shared control. In Section 2.2 the notion of shared control is elaborated.
Virtual fixtures can be divided into two main constraints namely, regional constraints (forbidden region virtual fixtures) and guidance constraints (guidance virtual fixtures) [5] [47].
The *regional constraints* support the operator with information about no-go zones, zones where he cannot operate safely. The system only provides active guidance when the no-go zone is in sight. These constraints will reduce risks, material damages and will create avoidance.
The *guidance constraints* indicate the optimal path to follow the specified route. The guidance system immediately activates when leaving the indicated route. The operator can overrule such an advice [5]. Figure 2.1 shows the regional and guidance constraints.

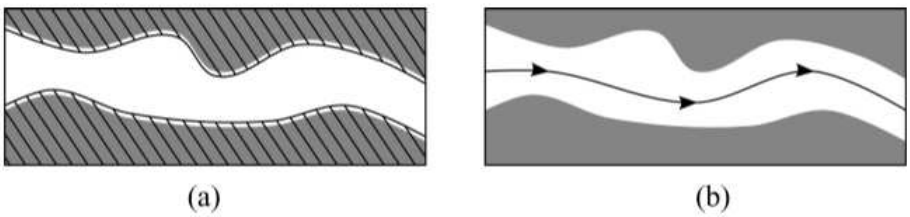

Figure 2.1: Example (a) regional and (b) guidance constraints. Obstacles are shown in grey and the constraints in black [5].

To realize one of the constraints mentioned, attractive or repulsive constraints are used. The *repulsive constraint* is used to stay in the safe zone and avoid the no-go zone. The operator will feel a force which prevents him to go to the no-go zone.

The *attractive constraint* will guide the operator towards the indicated route. Note that in this case, the operator already deviated from the route before the system reacts. Figure 2.2 shows the repulsive and attractive constraints

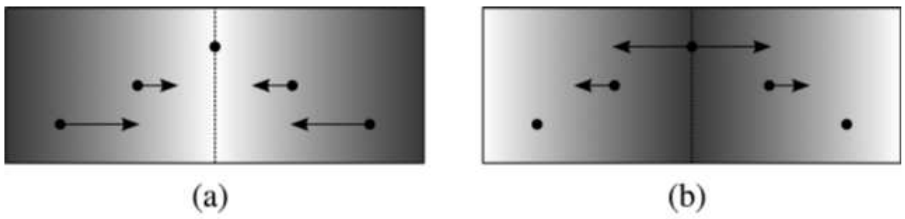

Figure 2.2: Example (a) attractive and (b) repulsive constraints. The constraint acts at the line, with permitted regions shown in lighter colours and restricted regions shown in darker colours. Arrows show the direction of "encouraged" motion [5].

To provide the driver with the required constraints specified above, the driver must "feel" the information provided by the system. In case of following the optimal trajectory and lane keeping, the warning system, as mentioned, could use the seat, seat belt or steering wheel to provide information to the driver. When using a guiding system with virtual fixtures, only the steering wheel is an option due to the fact the only constant contact of the driver is the steering wheel [45]. According to Beruscha et al., 2011 [45] most authors agree that haptic signals at the steering wheel provide the best information concerning vehicle lateral guidance based on the compatibility of the location of the stimulus and response. Consequently, the steering behaviour of the driver could best be influenced at the steering wheel.
Whether a guidance system, just like a warning system, is effective depends on the design parameters, i.e. if the exerted guidance forces are linear or quadratic. Also the differences between objectives of the driver and the automation influence the effectiveness of the system [44]. Less differences result in a more effective guidance system. For example, when a driver judges the situation as safe but the automation does not, the driver may turn it off. Or when a driver wants to overtake a lead car but the system wants to keep the car in its lane, the system and the driver disagree and an unsafe situation or even a collision may occur. Therefore, it is important that the system and driver agree. This will lead to a decrease in mental workload and visual demand of the driver.
Furthermore, the level of authority plays a role; the positive effects are higher with a higher amount of haptic authority. This is however, not yet accepted in the world.
Furthermore, guiding systems lead to a decrease in reaction time and an increase in overall performance [44].
An important note is that the use of active constraints can also have a negative side as it can lead to less awareness, over-reliance or even loss of skill by the driver [7] [44].
In case of the FRISC, active guidance could be useful. The guidance constraints in combination with the attractive constraints will cause the vessel to follow the route more precisely, resulting in a smaller chance of grounding and an increase in safety. This does not however, provide the operator with a large safe zone, the operator does not know where the dangers are but knows where they are not.

The regional and repulsive constraints, on the other hand, do provide the operator with an indication of the dangers. This results in a larger safe operating zone which can be of use for certain operations. In both cases the constraints provide an increase in overall performance.
In total, the overall performance of a driver using a warning system and/or a guidance system will improve, resulting in reduced reaction time and reduced mental workload [44].

2.2 Shared control

As mentioned before, the stiffness of a system influences the control authority of the driver. The driver has full control when there is no stiffness and has no control when the stiffness of the system is at its maximum. In both extreme cases there is no shared control. A combination of both however, is possible (shared control) and is shown in Figure 2.3 which indicates the possibilities in the Level of Haptic Authority (LoHA) [19].

Figure 2.3: Haptic shared control facilitates the communication of authority between human and automation from fully automated to full manual control [6] [7].

So why is shared control applicable and useful for this research? The use of a shared control system, which keeps the driver in the loop, can mitigate the issues belonging to a warning or/and guidance system such as over-reliance, loss of skill and loss of situational awareness [19] [44] [48]. Therefore, it is useful to get more insight in a shared control system and to discuss the applicability in a car or vessel.
In the past ten years, multiple advanced assistance systems in cars have been built around the idea of shared control between the automation system and the driver to improve the lateral motions of the car.
However, to combine the machines precision and the adaptability of the driver can be difficult due to the control tasks which are susceptible to human error and the wide-ranging limitations of the totally automated tasks. A solution for the latter can be a shared control system [49].
Two types of shared control systems can be used[8]. The first type is “blending” or “input-mixture” shared control (Figure 2.4), which affects the input into the control system [50]. It is a mixture of the output of the automation system and the output of the control interface based on the results of the human input. For example, in some lane keeping systems, when the actions of the driver do not interfere with the goal of the assistance system, no extra forces are generated. When the system does not agree with the driver, an additional guiding force is given by the system to ensure the car will follow the guidance of the system [8]. The driver, in this case, is not able to overrule the automation and may not even be aware of the activity of the system [7] [8] .

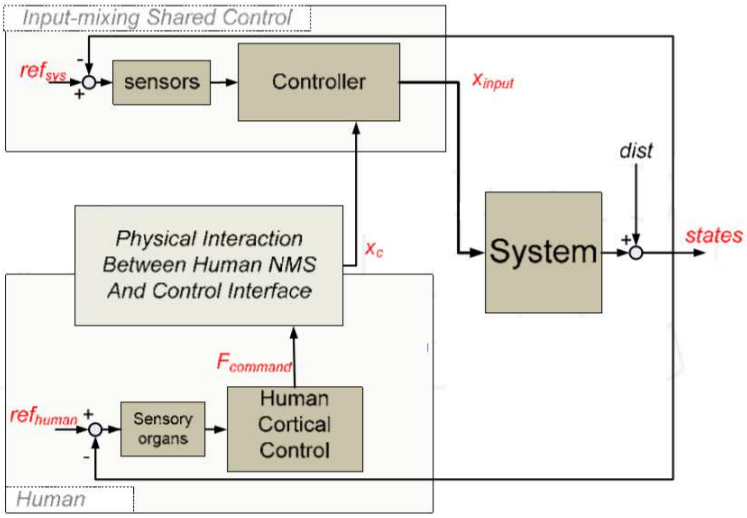

Figure 2.4: Blending/Input-mixture shared control scheme [8].

With:
$dist$ = disturbance;
$F_{command}$ = forces human operator;
H_{ci} = impedance of the control interface;
ref_{human} = reference trajectory of the driver;
ref_{sys} = reference trajectory of the system;
X_c = steering output.

The second type, which can be a solution to the challenge of combining the precision of the machine and the adaptability of the driver, is haptic shared control (Figure 2.5). Haptic shared control can be defined as a system which continuously and simultaneously shares the control authority with the human controller. Together they determine the input (forces) of the controlled system [7] [19] [49] [51].
The concept of haptic shared control is to retain the human controller in the direct manual control loop while the continuous support of an automation system is provided to avoid criticalities of the controlled system in the environment [7]. The system allows both the human and the automation to exert forces on the control interface of which the output remains the direct input to the vehicle. For that reason, the human controller continuously feels the forces given by the automation system [7].

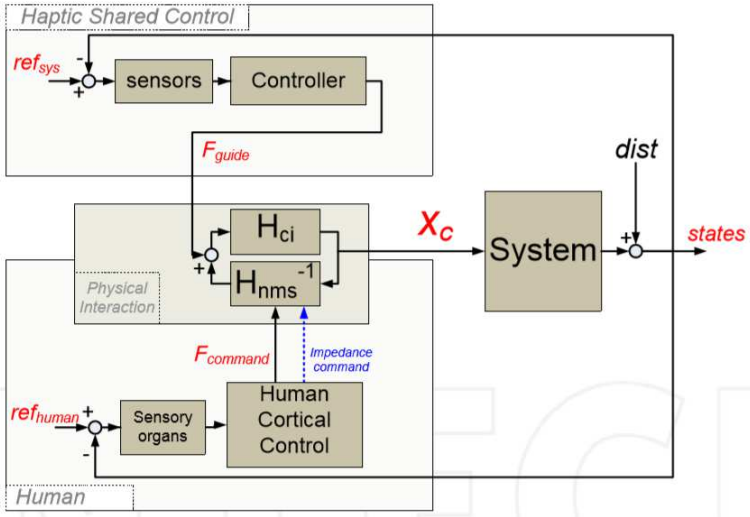

Figure 2.5: Haptic shared control scheme [8].

With:
$dist$ = disturbance;
$F_{command}$ = forces human operator;
F_{guide} = system forces;
H_{ci} = impedance of the control interface;
H_{nms} = neuromuscular dynamics of the driver;
ref_{human} = reference trajectory of the driver;
ref_{sys} = reference trajectory of the system;
X_c = steering output.

A previous example mentioned but not determined as a haptic shared control system, is a lane keeping assistance system. This system operates by adding a motor on the steering wheel which provides torques [7] [8] [18]. The human controller stays in control and is aware of the actions of the system and can choose to overrule (steer in another direction or provide more force in the indicated direction) the activity of the system at any time [7] [8] [51].

2.3 Lane-keeping

Since this thesis focusses on safe navigation of the FRISC, i.e. the path following performance and assuming a high speed vessel can be compared to a car, several papers and current applications about the implementation of lane-keeping have been surveyed. With the information found, a research method is designed to find answers to the main research question given in the introduction.

2.3.1 Lane-keeping on the road

In multiple papers about lane-keeping, different methods are used to keep a car in the correct lane. Some of these methods will be discussed in this paragraph. Note that only lane-keeping is considered and changing lanes is omitted.

In the research about lane-keeping in most of the articles, forces to get back to the centre of the lane are used. This can however be achieved in multiple ways.
In the papers of Mulder et al., 2008, 2010 [52] [53] a controller was used which provided force feedback based on lateral error to the lane centre 0.7 seconds ahead and stiffness feedback based on the current lateral error. It was assumed that there was a constant steering input of the driver [7]. The lateral error at that lookahead time was translated to forces, to communicate the optimal steering angle [19].
In Mulder et al., 2012 [7] the speed was fixed to focus on the steering behaviour of the driver. One of the reasons was that the differences in chosen speed of the drivers would complicate the comparisons of the results between the drivers [7].
Petermeijer et al., 2015 [44] also looked at a force feedback system in a car by surveying several studies. They stated that "in most studies the force exerted by the system was either a function of an external variable that represented the current position of the vehicle with respect to the road (e.g. deviation from lane centre), or used a lookahead principle, which determined the future position of the vehicle with respect to the road (e.g. time to line crossing)".
In Griffiths and Gillespie, 2005 [18] the deviation from the centre of the lane was used to produce continuous haptic information (torques) about the tendency of the system to return the car to the lane centre. An example is a steering wheel with a "home" position. The steering wheel is "attached", by virtual springs created by the automatic controller, to a moving home angular position which matches the recommended steering direction by the automation. In this case the driver can feel the recommended direction of the system [18].
In the paper of Saleh et al., 2013 [49] a lane assist model was developed based on the hypothesis that drivers use visual information to recognize upcoming curves and the position of the car on the road in relation to the edge lines. Drivers use "near" vision to keep the car in the centre of the road and "far" vision to account for upcoming curves. Also with this lane assist model, the results showed a reduction in the variability and average of lateral deviation and the lane departure risk [49].
An extract of the latter example of a lane assistance system is nowadays implemented in cars on the road. For example, Volvo developed Lane Keeping Aid [54], Volkswagen uses Lane Assist [55] and Audi has Audi Active Lane Assist [56]. In all examples the basic principle of the assist system is to use a camera placed in the centre upper edge of the windshield which detects the white lines of the road and uses small steering wheel torques to help keep the car in lane and create more safety [57].
These examples of lane assist systems are based on visual white lines on the road and are therefore impossible to use during navigation on water. An extraction of lane-keeping, a maximum cross track error of a planned route or the water between buoys however, can be used as a "lane".
Furthermore, the examples where force feedback is used to limit the deviation from the lane-centre are applicable to high speed vessels following a planned route. It is also a possibility to use the above two examples together.
Table 2.1 gives an overview of the similarities and deviations of a car and the FRISC. With this table it is possible to see in one glance where the developed haptic model can be the same or needs to deviate from a lane-keeping system of a car.

Table 2.1: Car vs. FRISC.

Car		**FRISC**
	Similarities	
centre lane keeping	$<->$	track keeping
obstacle avoidance	$<->$	obstacle avoidance
stay away from emergency lane	$<->$	safe water limits
external impacts (wind, rain)	$<->$	external impacts (wind, rain, waves, current)
fast response system	$<->$	assumed to be fast response system
low reaction time	$<->$	low reaction time
operates in all visual conditions	$<->$	operates in all visual conditions
	Deviations	
no drift	$<->$	drift
operator under low amount of stress	$<->$	operator sometimes under high amount of stress

With Table 2.1 an indication can be made of the algorithms needed to develop a Simulink model for the FRISC to be able to give the operator information about the route. This model exists of the experimental setup with required algorithms. Before the algorithms are described in detail, the experimental setup in which the algorithms will be implemented is outlined in the next chapter.

3. Experimental setup

The previous part of this thesis gave information about the FRISC and described the advantages of a shared control system using haptic feedback and virtual fixtures. Merely the literature is not enough to answer the research question. Therefore, to answer the research question an experimental setup is created and haptic algorithms are tested. This setup can be divided into three parts indicated in Figure 3.2 (i.e. a real-time controller (Bachmann), the haptic levers used by the operator and the simulator software) are described in the upcoming sections. An overview of the experimental setup used in this thesis is shown in Figure 3.1. The three individual parts are described in the forthcoming part of this chapter.

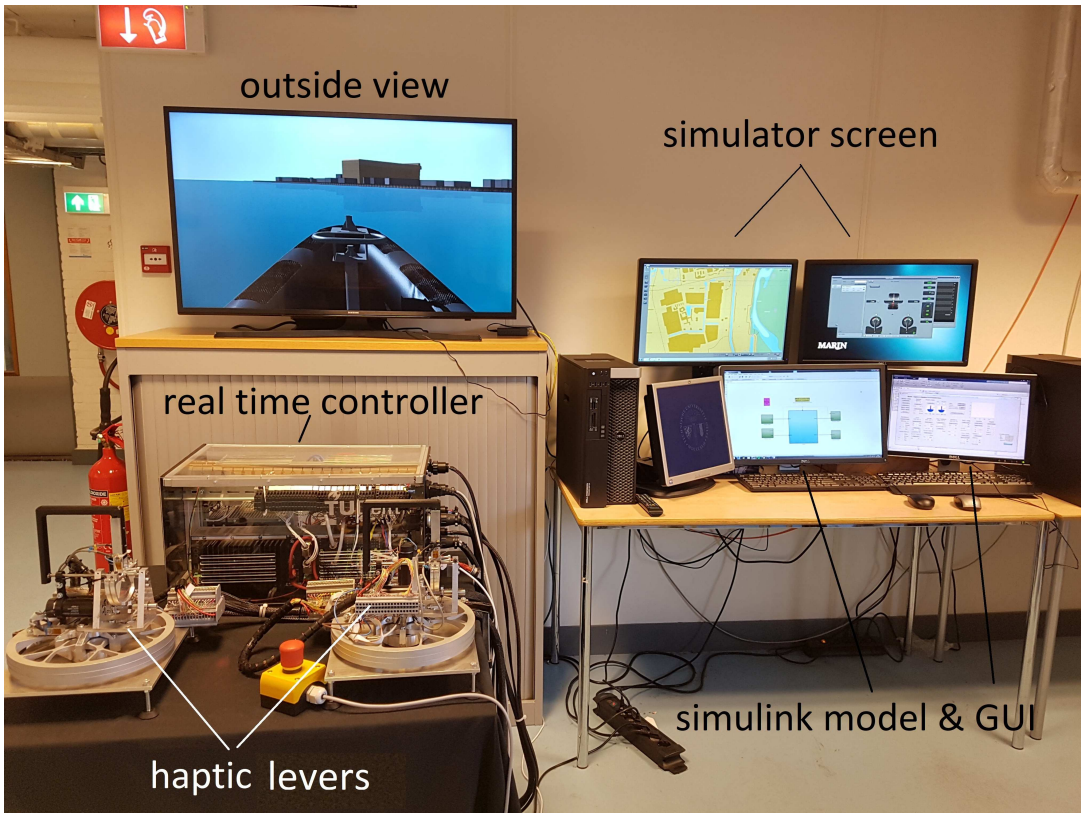

Figure 3.1: Overview experimental setup.

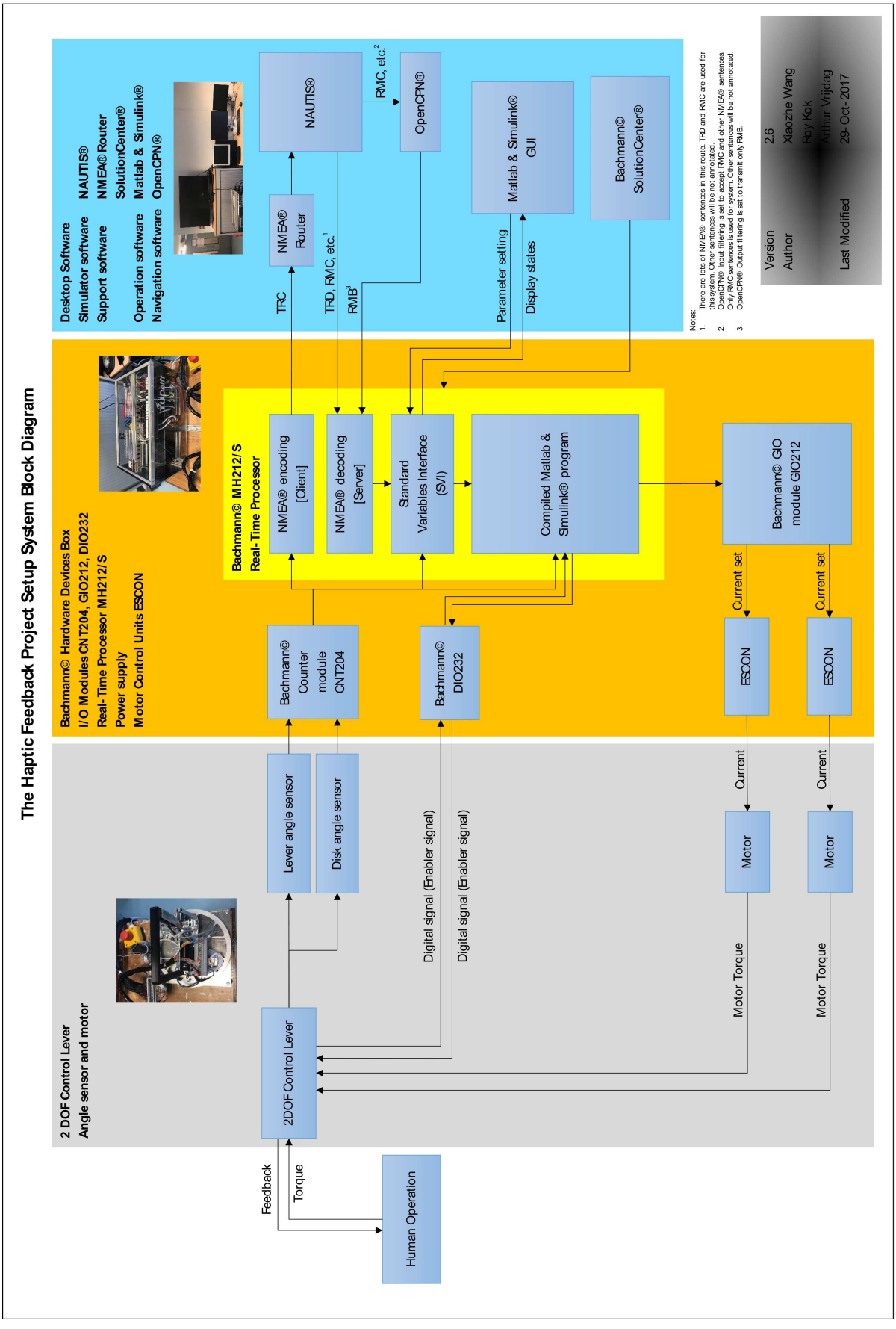

Figure 3.2: The Haptic Feedback Project Setup System Block Diagram.

3.1 Real-time controller

As can be seen in Figure 3.2, to control the haptic levers and to be able to directly act to the visuals observed by the human operator, a real-time controller is used. In the case of this experimental setup, a Bachmann system is used to encode and decode NMEA-sentences (National Marine Electronics-Association) to communicate with the (MARIN) simulator to read information about the status of the ship (e.g. rpm or azimuth) [20], and to translate lever angles calculated in a compiled MATLAB Simulink model to torques used by the Maxon motors. These different parts given in Figure 3.2, are described separately.
The counter module (CNT204) contains four counters for single line pulse generators and where two channels can be used as inputs for incremental encoders (generates a pulse signal whose frequency indicates the velocity of displacement) [58]. This module sends information to the real time processor (MH212/S) where the decoding/encoding of the NMEA-sentences take place [59], the process data (SVI variables) is mapped [60] and where a compiled MATLAB Simulink model is used.
In this setup, NMEA 0183 (NMEA, 2000) is used. It defines an electrical interface and data protocol for communication between marine instrumentation [61]. It communicates information about the current status of the ship (e.g. rudder angle and speed) towards the Bachmann and it sends information from the Bachmann (e.g. rudder set-point) towards the simulator.
The communication of the NMEA-sentences (sending and receiving) goes over the Ethernet with the UDP protocol [20]. The decoded and encoded sentences are received from/sent to the NMEA router in the simulator software (Paragraph 3.3.1) where the information is used to control the ship in the simulator. The SVI variables can be set as a preferred constant which can be used in the compiled Simulink program.
To be able to use the MATLAB Simulink model, and to use the model in combination with the levers and the simulator software, the model is compiled and sent to the Bachmann. Note that the model cannot be changed after compiling, values however can be changed but only using the GUI or the solution centre. The compiled MATLAB Simulink model is linked with a Digital Input/Output Module (DIO232) which is thereafter linked to the control levers. In this setup however, this connection between the DIO and the levers is not used. Additionally, the compiled model is connected to a universal I/O module (GIO212) which measures or outputs different types of signals [62]. In this case a current is set which thereafter goes through the ESCONS, which are PWM (pulse-width modulation) servo controller (i.e. motor control units), to output the correct current to the electric motors that drive the haptic levers to provide the operator with the correct haptic feedback.

3.2 Haptic Levers

The leftmost of Figure 3.2 are the haptic levers which are operated by a human operator. These two haptic levers are designed by the Delft Haptics Lab and built to control the speed and heading of a vessel.
To influence the azimuth angle, the levers are mounted on a rotational disc. On this azimuth angle disc, the rpm-lever is mounted. Both rotations, azimuth angle and rpm, are actuated by Maxon motors through a cable transmission. Note that these rotations

are done without noticeable play [20]. The motors are provided with a current from the ESCONSs based on the calculated rudder set-point and the motors deliver the correct torque to the levers. The amount of torque delivered is determined in the compiled MATLAB Simulink model(Paragraph 3.3.2) to advise the operator of, in this case, a rudder set-point to follow a planned route.
The position of the levers is used as input to the real-time controller which forwards the signal to the ship simulator software resulting in movements of the vessel in the simulator. The position is influenced by the feedback forces provided by the automation and by the human operator. This means that the operator "feels" the forces provided by the handles but can also exert a force on the handles himself.

3.3 Software

3.3.1 Ship simulator

The real-time processor sends, as mentioned, the encoded NMEA-sentences towards the software. The NMEA-router uses the encoded sentences for the simulator software. In this thesis a simulator with DOLPHIN software from MARIN is used. DOLPHIN is MARIN its new generation manoeuvring simulator software designed for interactive simulations of many types of nautical operations. Two operation examples are seakeeping in multiple environments, and nautical safety and operability studies.
This software can be used for Full Mission Bridges but can also, as in this case, be used for a small simulator setup [63].
The simulator can show a route with waypoints positioned on an electronic chart, ship information and multiple windows can be opened to adjust the simulation. For example, multiple sorts of vessels can be used for training and the environment (such as current and wave height) can be adjusted.
In this thesis, the FRISC is used and the environment is set to no waves with a constant current. Besides the input settings, the simulator can also indicate ship information (e.g. speed, heading and position) and ships movements (i.e. roll, pitch and heave). Important to mention is that a simulator never has the exact same response as the real vessel.
In the case of this research, the ship model and its hydrodynamic model used during this research are of a fast small vessel, not specifically of the FRISC. The assumption however, is made that this model, with its vessel properties and hydrodynamics, are a good approximation of the FRISC (type boarding craft). This is based partly on the properties of the vessel used in the simulator:

- Displacement: 7 ton;
- Loa: 14 meter;
- Beam: 3.3 meter;
- Draught: 0.5 meter;
- Installed power: diesel;
- Propulsion: 4 fixed propellers;
- Speed 43 knots.

Furthermore, it is possible that the manoeuvring capabilities of the vessel in the simulator are a bit different than that of the real ship. For example, during sailing on a real ship, the propellers have a wheel effect. This is probably not the case based on the small differences in diameter of a port or starboard turning circle tested in the simulator, Figure 3.3.

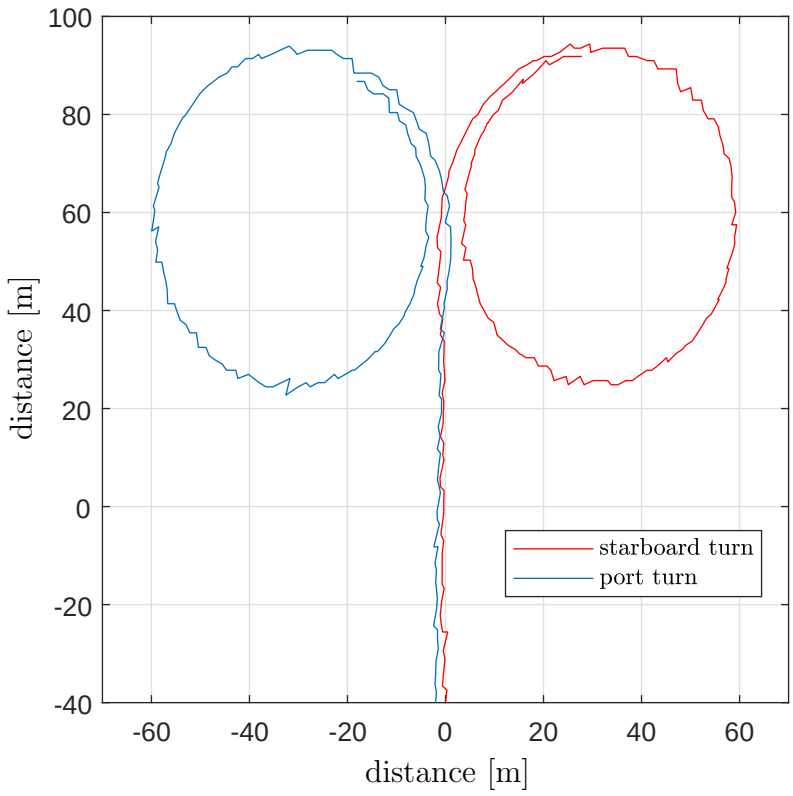

Figure 3.3: Port and starboard turn (v = 20 [kt], δ = 20 [deg]) of the FRISC in the simulator.

The ship information (e.g. speed, heading and position), provided by the simulator is decoded by the NMEA-decoder where after it is used in the compiled Simulink model to calculate the haptic feedback.
Additionally, the point of view of the operator is provided to create a more realistic simulation environment during testing.

3.3.2 Model

The MATLAB Simulink model is connected to the real time processor where it is compiled to be used during the tests.
An already existing model developed by Frank Hoeckx., 2017 [20] is expanded for haptic feedback in a FRISC during high speed inshore navigation.
The model is created in such a way that the craft is able to follow an indicated route with the possibility of using one of two different control laws (waypoint and XTE controller), and one of the two control options, which are an autopilot or a haptic shared control system. In Figure 3.4 an overview of the model is shown.

In the waypoint indicator the position of the ship is compared to the route and the position of the upcoming waypoint, and the bearing to the upcoming waypoint is determined. The bearing is the direction to steer from one point to another point, in this case from ship to waypoint. This bearing is used in the control laws to determine the rudder set-point.
When the set-point is known, it can be used as an input for either the autopilot or haptic shared control setting. The autopilot follows the rudder set-point by only moving the rudder angle and not the levers. With the use of haptic shared control, it is possible to let the operator feel warning signals and guidance constraints. In the next chapter the individual parts are described in more detail.

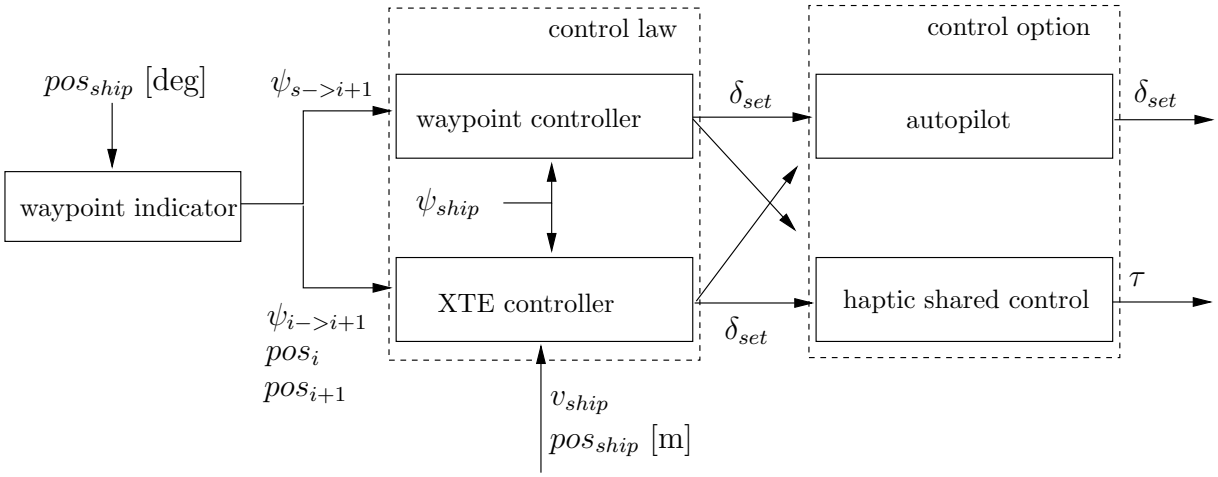

Figure 3.4: Overview Simulink model.

Additionally, the GUI (Graphical User Interface) developed by Frank Hoeckx is expanded. In this GUI the multiple aspects in the model can be turned on or off. For example, the two control laws can be turned on or off and the autopilot or levers can be activated.
All the different parts in the Simulink model are described extensively in Appendix B. In Appendix C the GUI and the multiple buttons are explained.
In Chapter 4, the procedures together with the calculations used in the Simulink model are described, starting with an overview of the waypoint indicator.

4. Procedures

This chapter elaborates on the details of the model made in MATLAB Simulink. As mentioned, an already existing model is expanded to be able to find an answer to the research question given in the introduction. In the previous paragraph it was shown that the model consists out of multiple parts: the waypoint indicator, the control laws (waypoint and XTE controller) and the control options (autopilot and haptic shared control). In this chapter, the model is explained according to these parts, starting with the waypoint indicator.
Before this model is described it is important one knows more about the development of a route. The development of a route, also called path determination is described in the forthcoming section.

4.1 Path determination

To specify a planned route of a surface vessel, waypoints are used and given as x and y coordinates and other waypoint properties such as speed and heading can be defined.
According to Fossen, 2011 [9] during route planning, multiple criteria can be implemented. In this research two of these criteria are applied and specified below.

1. Mission: the craft should move from some starting point (x_0, y_0) to the terminal point (x_n, y_n) via the waypoints (x_i, y_i).

2. Feasibility: each waypoint must be feasible, in that it must be possible to manoeuvre to the next waypoint without exceeding the maximum speed and turning rate.

When the waypoints are known, the correct and fastest way to follow the route is known. In shipping it is common to use the results of Dubins, 1957 [64] who used straight lines and circle arcs to connect waypoints. Fossens, 2011 [9] summarized Dubins results as:
"The shortest path (minimum time) between two configurations (x,y,ψ) of a craft moving at constant speed U is a path formed by straight lines and circular arc segments."

Figure 4.1 gives a good insight in the use of Dubins path. The circles between two straight lines give the desired turning rate of the ship to go to its next course [9].

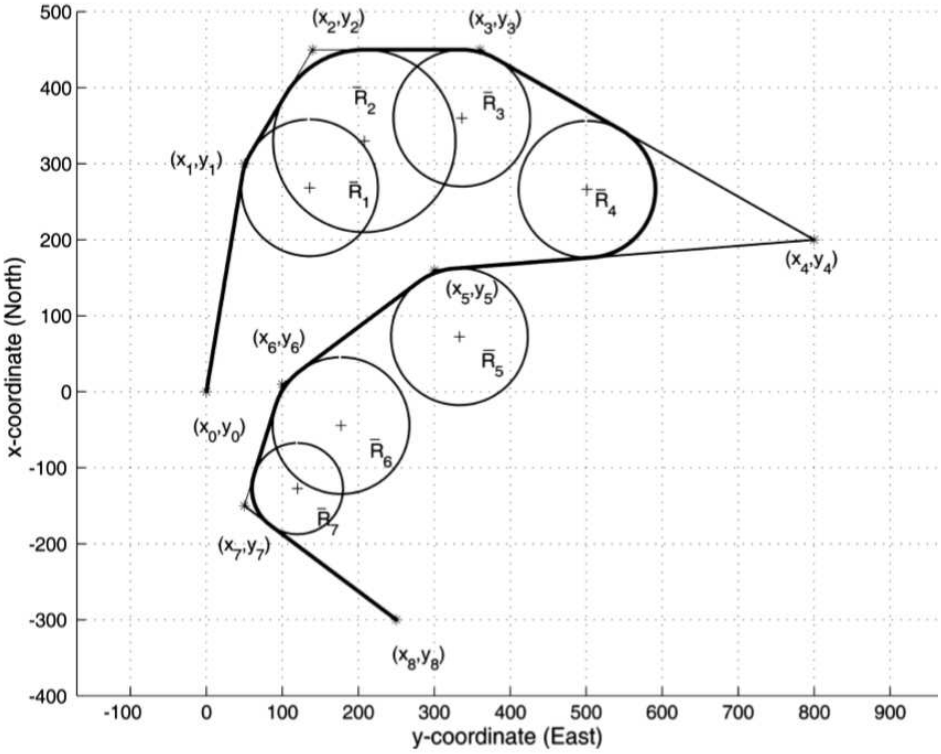

Figure 4.1: Straight lines and inscribed circles used for waypoint guidance [9].

Furthermore, the circles can be specified based on the speed or rudder angle wishes of the operator. The point where the circle and the straight line meet is the wheel over point, this is the point where the ship should turn to its next course. The determination of the position of the wheel over point is based on the radius corresponding to a certain speed and rudder angle and is given in Paragraph 4.2.2. First the waypoint indicator such as shown in Figure 3.4 is described.

4.2 Waypoint indicator

The waypoint indicator, as the word suggests, indicates the position of three relevant waypoints surrounding the vessel, i.e. the past waypoint (wp_i), the upcoming waypoint (wp_{i+1}) and the one after that (wp_{i+2}), and shifts at the correct moment to the next relevant waypoints.
These waypoints are selected out of a predetermined list of waypoints from the complete route (waypoint database) and are given in degrees of latitude and longitude. Thereafter, the waypoints are converted to meters with as origin the first waypoint of the route which is to simplify the usage in the rest of the model.
The conversion and selection are conducted in the first part of the waypoint indicator, Figure 4.2. The calculations conducted in the waypoint indicator with the output of the waypoint selector are explained in the upcoming part of this section.

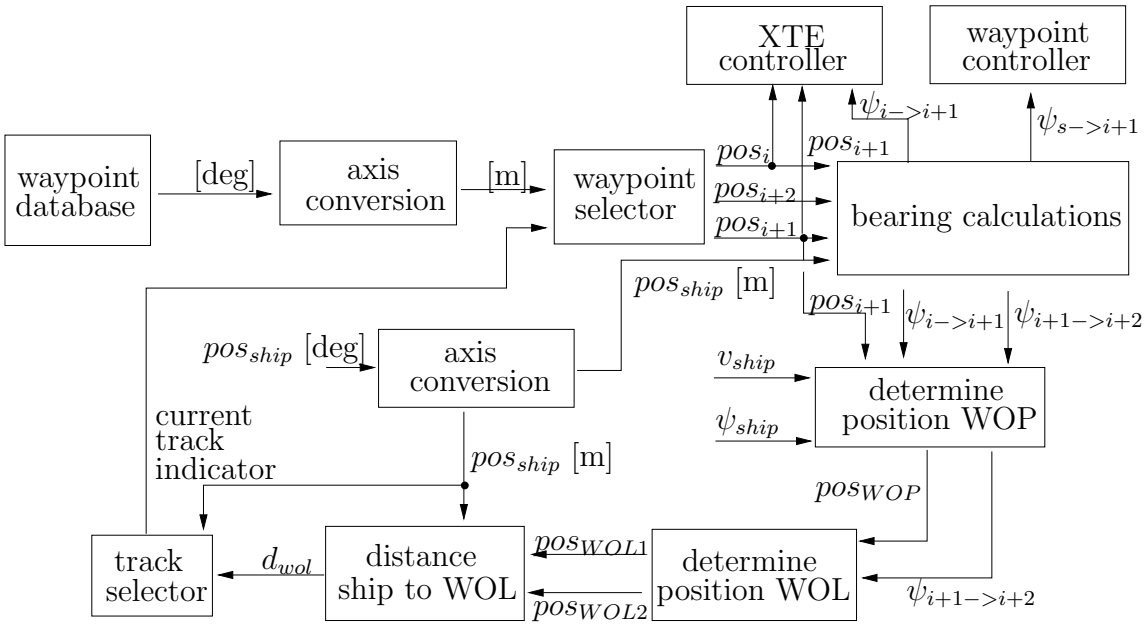

Figure 4.2: Waypoint indicator.

With:
d_{wol} = distance to wheel over line;
pos_i = position past waypoint;
pos_{i+1} = position upcoming waypoint;
pos_{i+2} = position waypoint after upcoming waypoint;
pos_{ship} = position ship;
pos_{WOL1} = position wheel over line, point 1;
pos_{WOL2}= position wheel over line, point 2;
pos_{WOP} = position wheel over point;
v_{ship} = ship speed;
$\psi_{i->i+1}$ = bearing past waypoint towards upcoming waypoint;
$\psi_{i+1->i+2}$ = bearing upcoming waypoint towards the waypoint after that
$\psi_{s->i+1}$ = bearing ship towards upcoming waypoint;
ψ_{ship} = ship heading.

4.2.1 Bearing calculation

The bearing calculator is used to determine multiple bearings/set-points which are used in the rest of the MATLAB Simulink model. A bearing (ψ in Figure 4.3) is indicated as a direction from one point to another point and is given in degrees (0-360°). These points can vary from, for example, a ship or waypoints. When the positions of the first and second point are known, the bearing can be calculated. In this example, the first point is a vessel and the second point a waypoint.

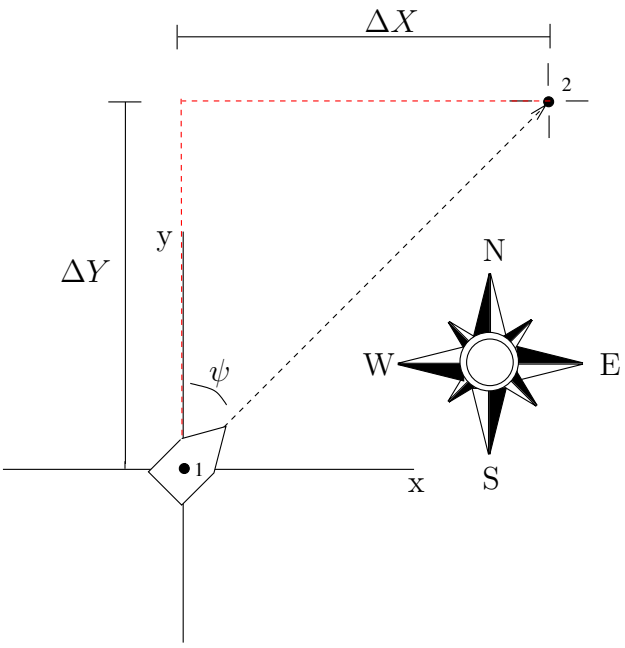

Figure 4.3: Bearing calculation.

Before the calculation can be executed, one needs to know the basics of latitudinal and longitudinal coordinates. A coordinate is built up out of degrees [°], minutes ['] and seconds ["]. The degrees in longitudinal direction run from -180° to 180°, that in latitudinal direction from -90° to 90°, and in both directions the minutes run from 0-60 and the seconds from 0-60. The relation between the three is given below [65].
Note that generally, the minutes and seconds are used as one. This means that the seconds are used as decimals for the minutes and run from 0-99.

1 degree = 60 arcminutes
1 arcminute = 60 seconds = 1852 meters

The calculation can be split into multiple steps. These steps are based on an example with random coordinates of the ship and waypoint given below. The coordinates are given in two variants, one in degrees, minutes and seconds, and the other in degrees with only minutes.

Coordinates ship = 49°42'38"N 005°01'06"E or 49°42.63'N 005°01.10'E
Coordinates waypoint = 51°36'08"N 007°92'07"E or 51°36.14'N 007°92.12'E

Step 1: The coordinates, degree of latitude and longitude of point 1 and 2, are converted to meters. In longitudinal direction, to convert from degrees to meters the degree of latitude must be considered. Therefore, the longitudinal coordinate needs to be multiplied by the cosine of the degree of latitude (Equation 4.2). For the waypoint coordinates only the result is given.

ship:
49°42.63'N = 49.7105°N
005°01.10'E = 5.0183°E

$$49.7105 * 1852 * 60 = 5523830.76[m] \tag{4.1}$$

$$5.0183 * 1852 * 60 * \cos\frac{49+51}{2} = 365840.49[m] \tag{4.2}$$

waypoint:
51°36.14'N = 51.6023° = 5734047.58[m]
007°92.12'E = 8.5353° = 596874.23[m]

Step 2: The length of ΔX and ΔY in Figure 4.3 are calculated.

Difference in longitudinal direction, ΔX:

$$596874.23 - 365840.49 = 231033.74[m] \tag{4.3}$$

Difference in latitudinal direction, ΔY:

$$5734047.58 - 5523830.76 = 210216.82[m] \tag{4.4}$$

Step 3: With the lengths of ΔX and ΔY, the bearing is calculated. Note that the answers are between 180° and -180°, i.e. when the answer is negative, +360 has to be added to get the correct bearing.

$$\psi = \arctan 2(\Delta X, \Delta Y) = 47.70[deg] \tag{4.5}$$

With the above three steps, the bearing between two points can be calculated. This calculation is used to determine the bearing from the ship towards its next waypoint ($\psi_{s->i+1}$), the bearing from the previous towards the upcoming waypoint ($\psi_{i->i+1}$), and from the upcoming waypoint to the waypoint after that ($\psi_{i+1->i+2}$). The calculations used in the Simulink model are shown in Appendix B.

4.2.2 Wheel over point

With the known bearing from ship to waypoint, the turning point to a next course can be determined. This turning point needs to be calculated to determine the correct position of the turning point of the ship to the next waypoint. Such a point is called the Wheel Over Point (WOP).
A WOP can be calculated in multiple ways. Two examples are given, the first possibility uses advance (the distance the vessel moves along its original course from the time the rudder is put over until the new course is reached) and transfer (the distance the vessel moves perpendicular to the original course during the turn). The second possibility is to use the distance to a new course (DNC), which is the distance between the WOP and the upcoming waypoint [65].

As mentioned in Section 4.1 the route is built up out of straight lines and circle arcs. Therefore, the turning circle of the craft has to be taken into account. To determine a turning circle, a turning circle test has to be executed (Figure 4.4). This test provides information about the manoeuvrability of a vessel including the tactical diameter, advance, transfer and time to change heading to 90 and 180 degrees [66]. The radius of the circle can be found to determining the DNC.
Note that the standard IMO (International Maritime Organization) test is done with maximum steering angle (δ_{max}=25° onboard a FRISC). To determine more extensive values of the distance to new course, the test is also done with other speeds and rudder angles.

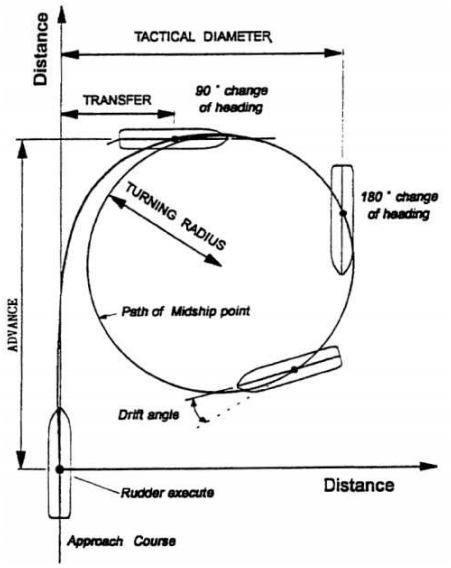

Figure 4.4: Turning circle test [10].

It is assumed that the vessel follows a circular path during a turn (Dubins path). To determine the radii of the circles for different speeds and rudder angles, the FRISC in the simulator is used. First, the speed of the ship is set as a constant and the rudder angle is changed (2, 5, 10, 15, 20 and 25 degrees). Then the rudder angle (δ) is set and the speed is changed from 10-40 knots with steps of 5 knots.
Note that not 25 knots is used but instead 22.5 knots. This is because the FRISC in the simulator is starting to plane above approximately 23 knots and a constant speed of 25 knots was not able to be accomplished, therefore a speed of 22.5 knots is used. Figures 4.5 and 4.6 show two examples of a turning circle graph which are used to determine the turning radii.

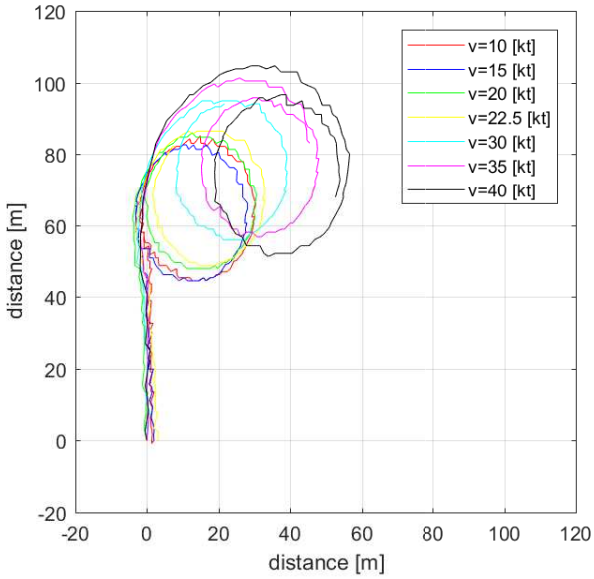

Figure 4.5: Full turning circle manoeuvre, rudder angle 25 degrees.

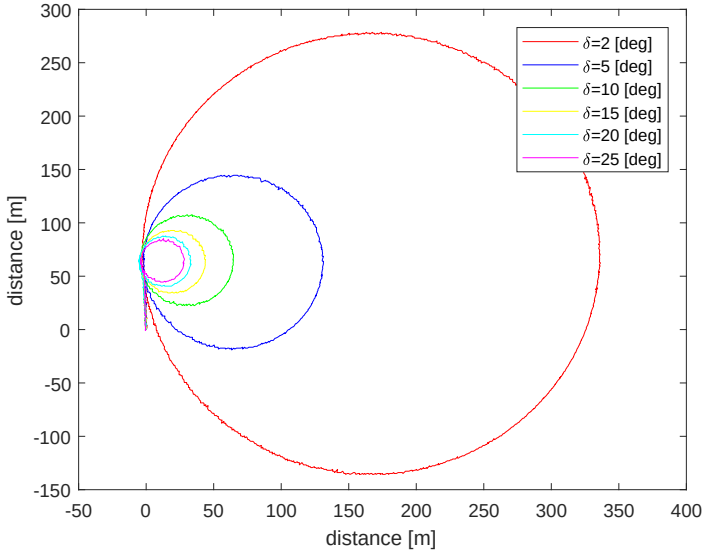

Figure 4.6: Full turning circle manoeuvre, speed 10 knots.

Figure 4.5 shows that when the vessel sails with different speeds and uses a constant rudder angle during a turn, the drift of the vessel changes. The length of the first 180 degrees of the circle arc increases with a higher speed. The rest of the turning circle, after the first 180 degree turn, differs much less for every speed.
When a constant speed is used instead of a constant rudder angle, Figure 4.6 shows that the turning circles are clearly round. The drift of the vessel during the complete turn is the same. The differences in circle sizes appear due to the different rudder angles used. For both the figures it shows that a higher speed or a smaller rudder angle result in a larger turning circle.

The multiple turning circles measured for the different speeds and angles are logged and the corresponding radii are put into a lookup table (Figure 4.7) to be able to use them during the simulation when a certain speed and rudder angle are attained.
Note that there is no data of rudder angles smaller than 2° because it is assumed that with a difference between tracks of 2°, it is not needed to use a WOP to follow the route precisely.

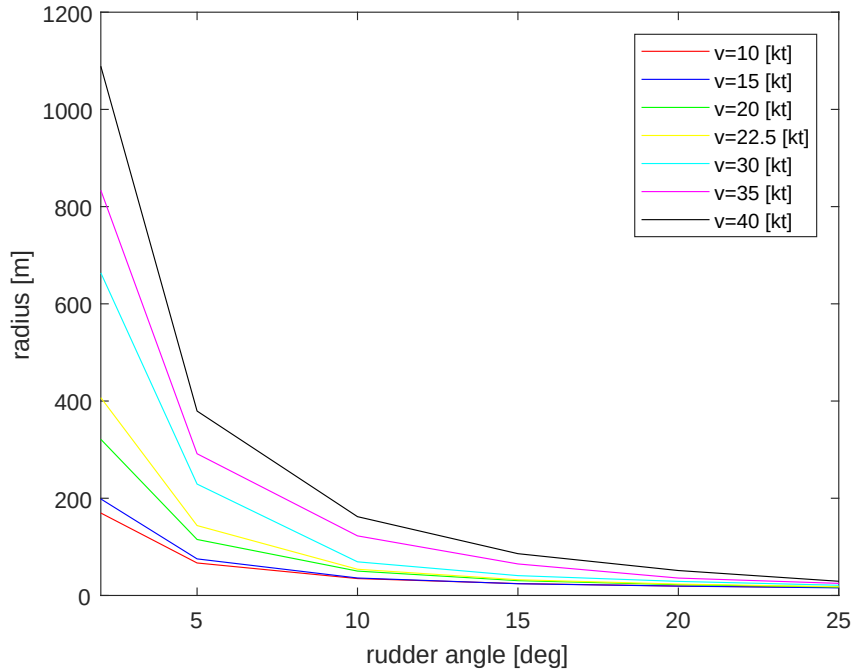

Figure 4.7: Lookup table radius turning circles.

With the radius obtained from the lookup table, the distance from waypoint to WOP (q in Figure 4.8) can be calculated. The equations used are given below. To be able to calculate this distance, the heading and the next bearing must be known.

$$X = R\sin(\alpha) \tag{4.6}$$

$$Y = R\cos(\alpha) \tag{4.7}$$

$$Z = R - Y \tag{4.8}$$

$$q = X - \frac{Z}{\tan(\alpha)} \tag{4.9}$$

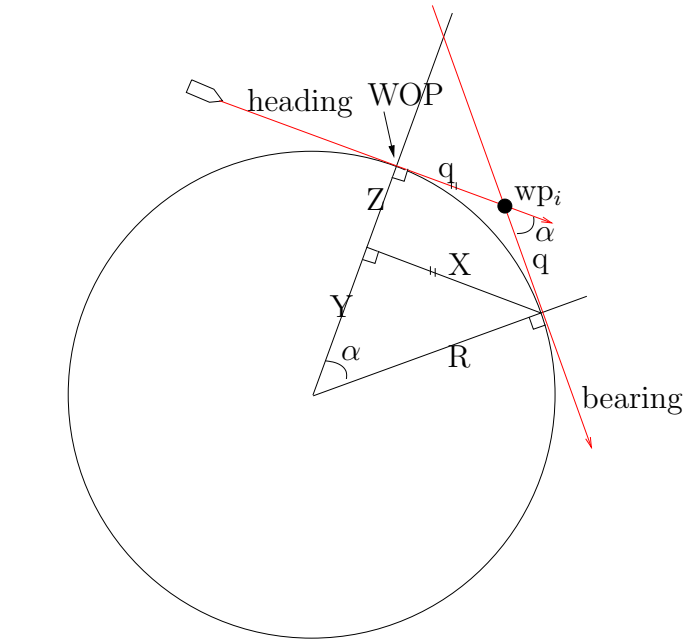

Figure 4.8: Determination distance waypoint to wheel over point.

In the calculations given above the assumption is made that the vessel, after indicating a rudder angle, will turn immediately. A ship has a (small) delay before it starts turning and therefore this has to be taken into account.
The reaction times of the FRISC during a turn are determined for speeds of 10-40 knots with steps of 10 and for two rudder angles, 5 and 25, are used. This is because the assumption is made that when the reaction time differs, this is the largest difference in reaction time. Investing this reaction times result in no big differences and the average of these 8 reaction times (0.996 seconds) is used and implemented into the Simulink model. Figures 4.9 and 4.10 show an example of the determination of the reaction time of the vessel, the rate of turn and the heading of the vessel.

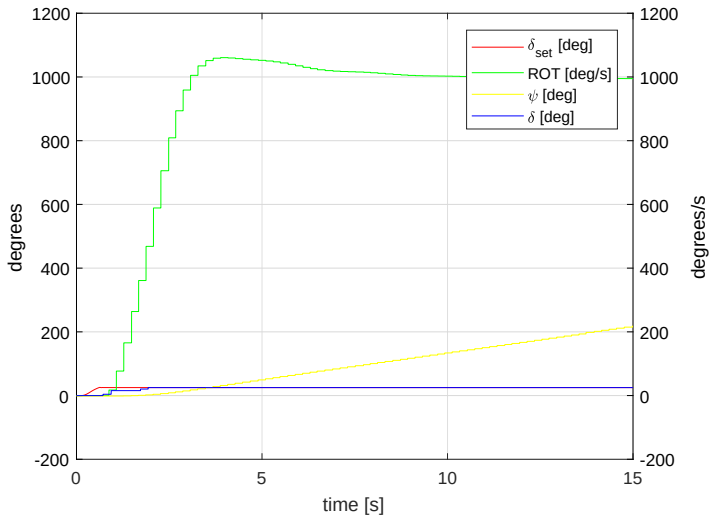

Figure 4.9: Overview of turning reaction with speed 10 knots and rudder angle 25 degrees.

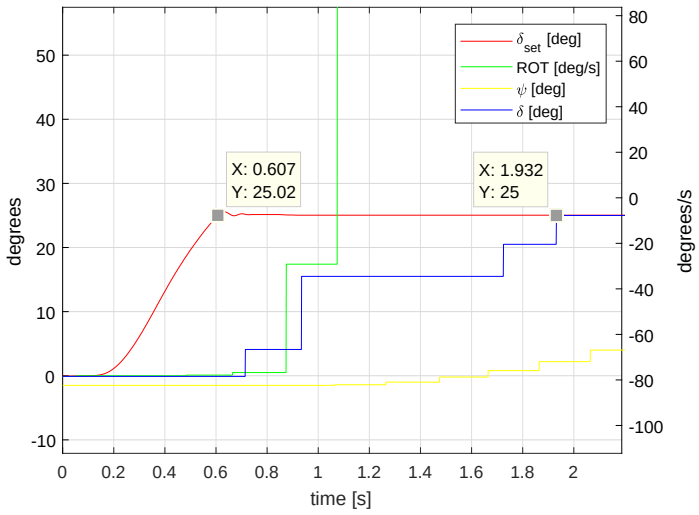

Figure 4.10: Detailed view of turning reaction with speed 10 knots and rudder angle 25 degrees.

Note that the WOP is only used to turn a vessel to its next course when the ship follows a certain route exactly. When the vessel deviates from its planned route (sails starboard or port side of the route), the ship cannot turn exactly at the WOP. Therefore, to make sure the vessel turns at the correct moment to follow the planned route after its turn, a Wheel Over Line (WOL) is introduced.

4.2.3 Wheel over line

The WOL, just as the WOP, determines the turning point of a vessel from one track to its next track (the dashed green line in Figure 4.11). When the vessel crosses the WOL the ship should turn.
The WOL is a line parallel to the next course line and is intersecting the WOP. When the vessel turns with its planned settings at the WOL, it proceeds exactly at its next course line. When a vessel starts turning earlier or later than the indicated WOL, the ship will follow an, in this case, inside or outside turn respectively. Note that this is true for Figure 4.11, this means that following an inside or outside turn is depending on a port or starboard turn.
To indicate the turning point, the distance from the ship towards the WOL is determined. This distance calculation is explained in the forthcoming paragraph.

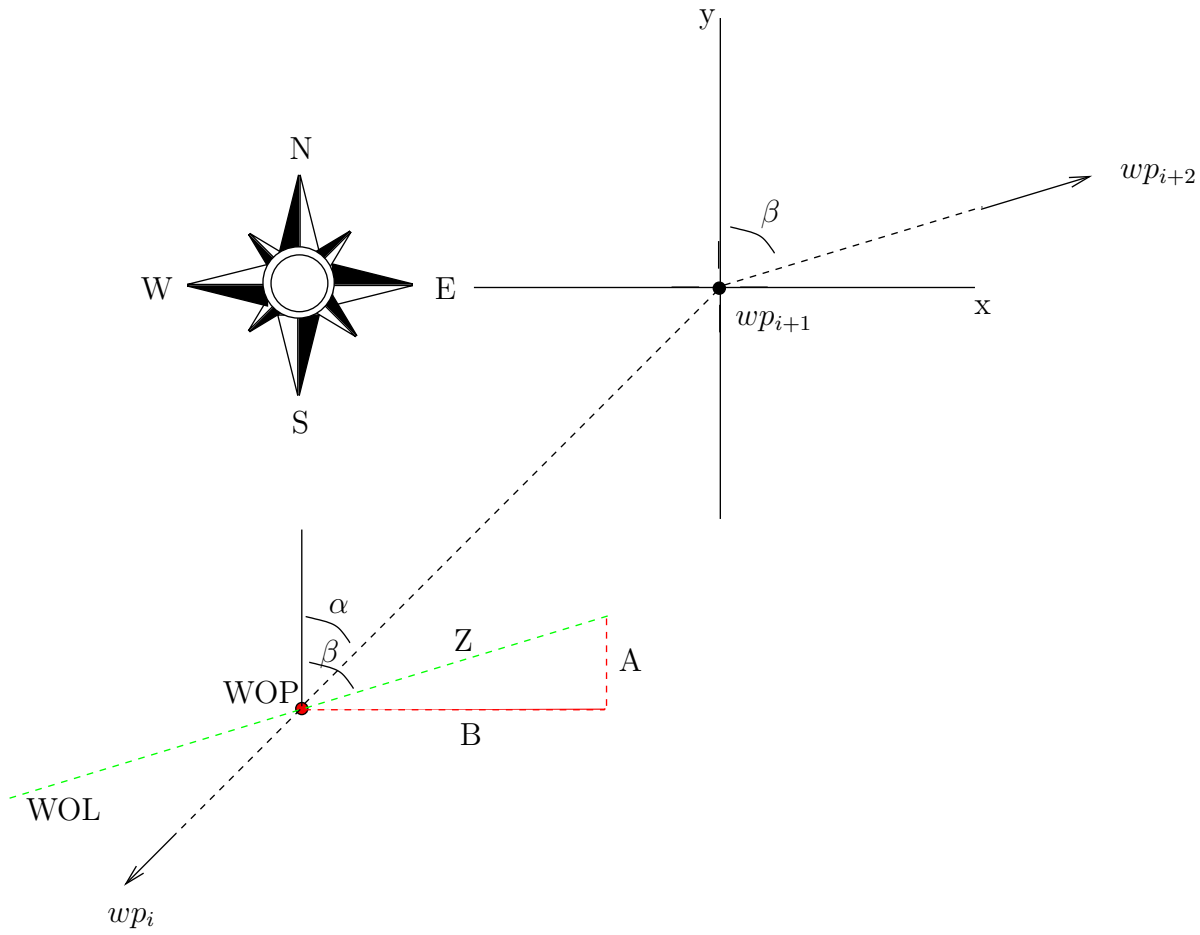

Figure 4.11: Determination wheel over line.

4.2.4 Distance ship to WOL

When the ship is within a 3 meter distance of the WOL, the craft must start turning. The vessel needs to be within 3 meters of the WOL to make sure the line is always detected by the vessel due to the update rate of the vessel position of 5 Hz and the maximum speed of 40 knots ($20.576/5 = 4.115$ [m/sample]). This distance is multiplied with a safety margin of 1.5 resulting in 6 meters, 3 in front and 3 meters behind the WOL.
This results in a possible turning point error of a maximum of 3 meters. With this update rate, it is possible that the vessel starts turning 3 meters too early of too late.
To indicate the turning position, the distance between vessel and WOL is calculated with the following equation [67] and is sent to the track selector.

$$d_{wol} = \frac{|(x_2 - x_1)(y_1 - y_0) - (x_1 - x_0)(y_2 - y_1)|}{\sqrt{(x_2 - x_1)^2 + (y_2 - y_1)^2}} \tag{4.10}$$

With:
x_0, y_0 = position vessel;
x_1, y_1 = position point 1 WOL;
x_2, y_2 = position point 2 WOL.

4.2.5 Track selector

When the distance from ship to WOL is within 3 meters, the vessel needs to turn to its next course. The track selector focusses on the distance from ship to WOL and when this distance is within the given limit, the current track indicator is raised by one to select the correct relevant waypoints.
The tracks (course line between two waypoints) are divided into a number from 1-n (in this Simulink model from 1-10), Figure 4.12 shows an example of the first two tracks. The numbers 1 and 2 indicate track 1 and 2 respectively. In this example it is assumed the vessel sails on the first track (i=1), therefore the first waypoint is i, the second i+1 and the third i+2. When the craft is within a distance of 3 meters of the WOL of track 1, the current track indicator is raised by one (i=2) and the waypoint indication shifts to the next three relevant waypoints (i+1 becomes i and i+2 becomes i+1 etc.).

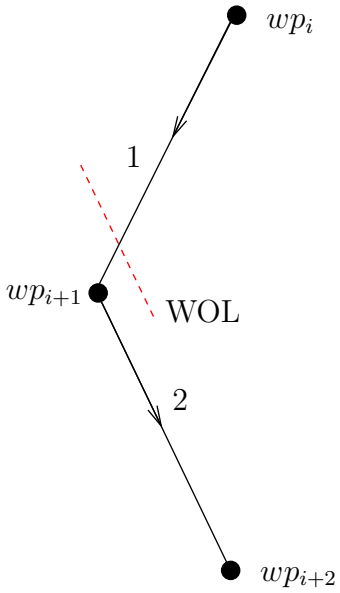

Figure 4.12: Track selector.

4.3 Control laws

As mentioned, the automation is designed to follow an indicated route. To be able to do so, a control law is used. In this thesis two control laws are created (waypoint controller and XTE controller) to calculate the rudder set-point to follow a planned route as precisely as possible. This rudder set-point is thereafter used as an input for the control options (autopilot or the haptic system).
Because the control laws are used to calculate a rudder set-point, multiple basic control laws are surveyed [68] [69] [70] [71]. These various laws are combined to design a general control law to follow a planned route, the result is shown in Figure 4.13 and described below.
To follow a planned route, the position of the vessel is compared with the position set-point (X_{set}, Y_{set}), resulting in the position error. The position error (X_e, Y_e) is used to determine the heading set-point (ψ_{set}) of the vessel. With the heading set-point, the heading error (e_ψ) is determined. The heading error is calculated by subtracting the ship heading (ψ_{ship}) from the heading set-point. To create a smooth reaction of the vessel, a

PID-controller is used and to have the correct maximum steering angle a limiter is implemented.
To use the rudder set-point as input for the simulator, the value is converted with an NMEA-encoder so the simulator can use this as rudder input. Thereafter, the simulator sends the actual heading of the vessel through an NMEA-decoder and this value is again used to subtract from the heading set-point.
Additionally, this general control law can be used when a vessel needs to go in one direction. In the model an option to insert a heading set-point (0-360 degrees) is implemented and can be adjusted in the GUI. This can be useful to test the movements of the ship, for example to find the right PID-values.
An important note is that the control law described, is used for both the waypoint and XTE controller however, just the waypoint controller uses the total control law with a position set-point (upcoming waypoint) as shown in Figure 4.13. In the XTE controller the heading set-point is not calculated based on the position error but based on the Cross Track Error (XTE). The calculated set-point in the XTE controller is used in the same manner as shown in Figure 4.13 where it is used to determine the heading error and where it passes the PID-controller and the limiter before it is sent to the simulator. Both the waypoint controller and XTE controller are described in the forthcoming paragraphs.

Figure 4.13 with:
e_ψ = heading error;
X, Y = position ship;
X_e, Y_e = position error;
X_{set}, Y_{set} = position set-point;
δ = actual rudder angle;
δ_{set} = set-point rudder angle ;
ψ_{set} = heading set-point;
ψ_{ship} = actual heading.

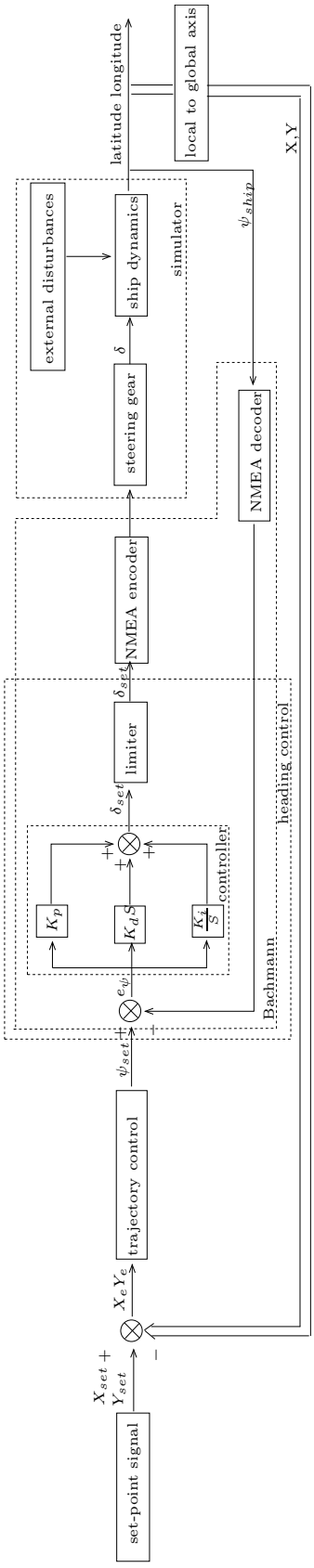

Figure 4.13: General control law scheme.

4.3.1 Waypoint controller

The waypoint controller is used to steer the vessel from the current position of the ship towards the upcoming waypoint. By comparing a heading set-point, in this case the bearing from ship to waypoint ($\psi_{s->i+1}$) and the ship heading (ψ_{ship}), the heading error is determined.

$$e_\psi = \psi_{s->i+1} - \psi_{ship} \tag{4.11}$$

Furthermore, in the model it is possible to indicate a deadband on the calculated heading error. When it is not necessary to redirect the heading continuously this is an option. In the case of inshore navigation, it is of importance the vessel follows the indicated route as accurately as possible and therefore, no deadband is used during the experiments. The determined heading error is used as input for the PID-controller and is thereafter sent to the limiter which calculates the rudder set-point ($delta_{set}$). This rudder set-point is used as input for the autopilot or for the haptic shared control system. The waypoint controller, with in- and outputs, derived from Figure 4.13 (part heading control), is shown in Figure 4.16.

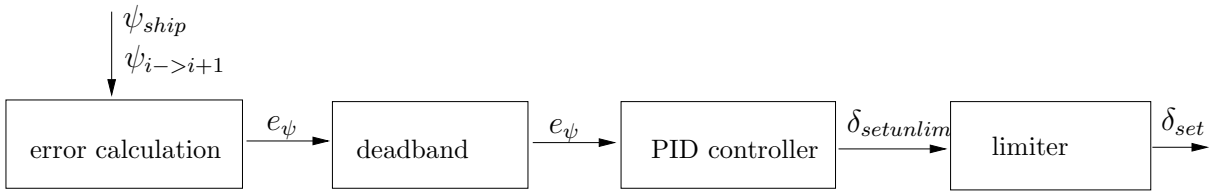

Figure 4.14: Waypoint controller.

Because the vessel has the upcoming waypoint as aiming point in the waypoint controller, the ship does not return to its course line based on the rudder set-point when it is deviated from track by, for example, waves or current. A large XTE can be dangerous when there is, for example, a shoal between the upcoming waypoint and the current position of the ship.

4.3.2 XTE controller

The second control law, the XTE controller, can be a solution to create a model which dissolves this track deviation. The track deviation, also called the cross track error (XTE) which is the distance between the position of the craft and the course line, is calculated with Equation 4.12 [67]. In the regular formula the absolute value is used to calculate the absolute distance. In this case, the absolute sign is removed to be able to determine on which side (starboard (+) or port (-)) of the course line the ship is located.

$$d_{XTE} = \frac{(x_2 - x_1)(y_1 - y_0) - (x_1 - x_0)(y_2 - y_1)}{\sqrt{(x_2 - x_1)^2 + (y_2 - y_1)^2}} \tag{4.12}$$

With:
x_0, y_0 = position vessel;
x_1, y_1 = position wp_i;
x_2, y_2 = position wp_{i+1}.

When the XTE=0, the vessel has converged to its course line and the ship is sailing "on" track. This leads to the following associated control objective for straight-line path following [9]:

$$\lim_{t\to\infty} XTE(t) = 0 \tag{4.13}$$

According to Fossen, 2011 [9] lookahead-based steering can be used to steer along the LOS (Line Of Sight) vector and is valid for all XTEs without computationally intensive methods. Therefore, the lookahead principle is used in the XTE controller.
The following calculations based on Figure 4.15, are used to determine the heading set-point [9]. Note that when the environmental forces (e.g. wind, current and waves) are zero the sideslip angle $\beta = 0$ and thus the heading set-point is equal to the heading of the ship (Equation 4.17). In the case of this research, the sideslip is not taken into account during the calculation. This means that with a constant current, as used during the experiments, the ship heading (ψ_{ship}) differs from the course over ground (COG) and the vessel does move in another direction than the calculated heading set-point (ψ_{set}) which results in a continuous heading error.
In this research, with a constant current of 3 knots and a maximum vessel speed of 40 knots, this means that the maximum error between the COG and ψ_{ship} is $\tan^{-1}\left(\frac{3}{40}\right) = 4.3$ degrees.

$$\psi_{set}(xte) = X_p + X_r(xte) \tag{4.14}$$

$$X_p = \psi_{i->i+1} \tag{4.15}$$

$$X_r(xte) := \arctan\left(\frac{-xte}{\Delta}\right) \tag{4.16}$$

$$\psi_{set} = \psi_{ship} + \beta \tag{4.17}$$

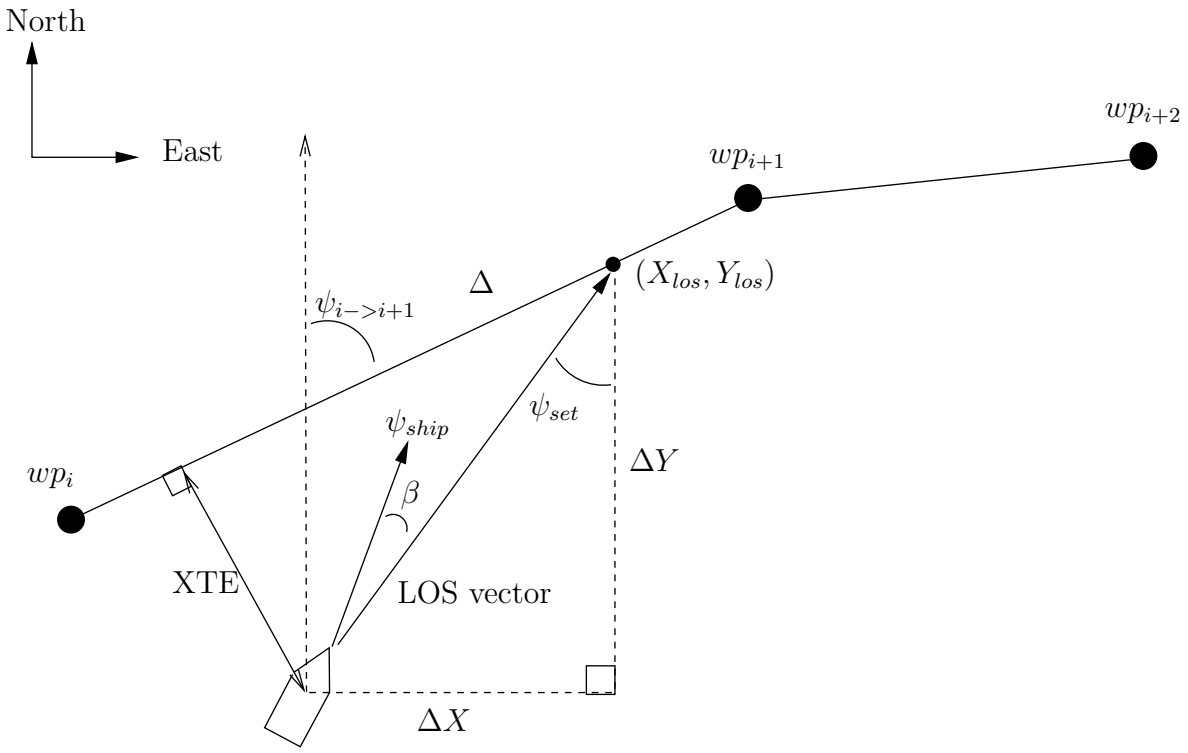

Figure 4.15: LOS guidance [9].

To create a stable system, the values for the lookahead distance (Δ) need to be chosen carefully. The Δ-value is small when the vessel has a large XTE, resulting in a more aggressive steering behaviour to decrease the XTE faster. When the lookahead distance is too large, the vessel is close to its course line and the system can overshoot or get unstable [72] [73].
In this thesis the lookahead distance is subject to the velocity of the vessel $\Delta = K_f * U$. The gain K_f is set to 2 and is determined by trial and error. A too large gain led to a too aggressive steering reaction, a too small gain led to a too slow vessel reaction. When the heading set-point is calculated, it is compared with the heading of the vessel and the heading error (e_ψ) is determined, Equation 4.11. This error is used as input for the PID controller and is sent to the limiter which calculates the rudder set-point (Figure 4.16). In Appendix B the corresponding calculations conducted in the MATLAB Simulink model are shown.

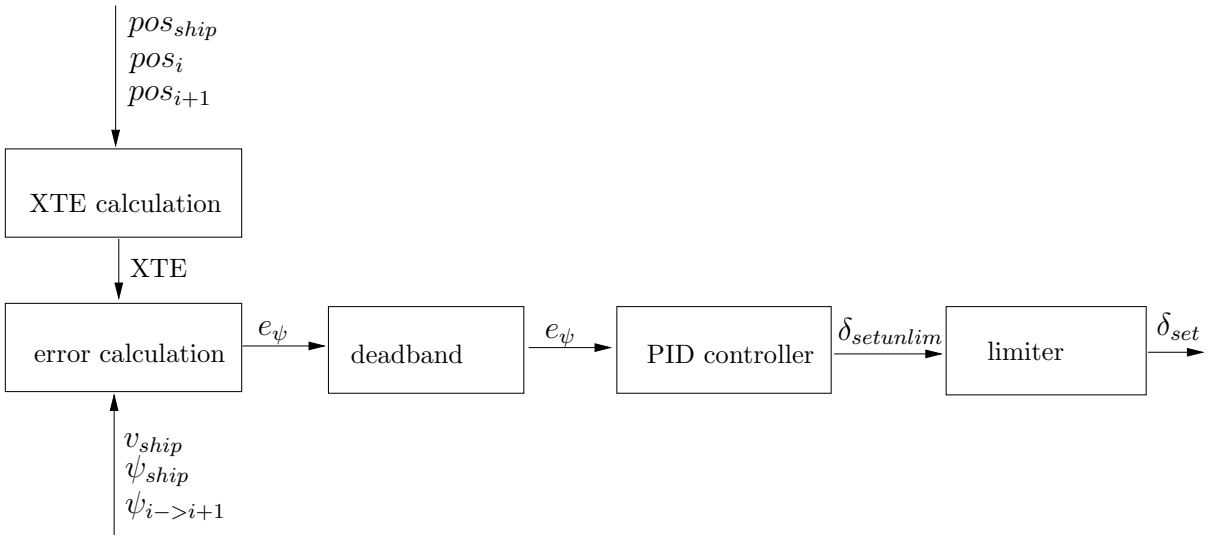

Figure 4.16: XTE controller.

Both the waypoint controller as well as the XTE controller, calculate the rudder set-point. This means that both the control laws have to be used separately to be able to guarantee the correct rudder set-point input.
The automation can use the rudder set-point to gain the correct rudder angle with the use of two different control options. The first and most simple option is the use of an autopilot, the haptic shared control system is the second option. Both options are described in the last part of this chapter.

4.4 Control options

4.4.1 Autopilot

The autopilot, as the word indicates, follows the indicated route automatically. The rudder set-point determined by one of the control laws is transferred directly as input to the simulator. With the correct NMEA-sentence, the rudder in the simulator becomes similar to the rudder set-point. In this case, the rudder angle is determined within the Simulink model without any movement of the levers.
Furthermore, when the levers are moved in azimuth direction, they do not influence the rudder angle of the vessel. The ship speed however, does have to be indicated by the levers.
With the use of the autopilot, no feedback is transferred to the operator and he is not able to feel the direction of the rudder set-point. When the operator does want to feel the advice of the system, the haptic shared control system needs to be used.

4.4.2 Haptic shared control

To be able to let the operator feel the advice of the system, the force feedback needs to be transported via the levers. Therefore, the lever control must have the right settings and must be developed in such a way that the exact feedback of the system is communicated to the operator in the right manner.

The control law calculates the rudder set-point and this set-point is used as an input for the haptic system. The calculated set-point is compared with the lever angle which result in a lever error. This lever error is converted to a torque which is transferred to the levers, i.e. the levers move in the direction of the rudder set-point.
For example, when the rudder set-point is +3, the lever will move towards +3 due to the indicated torque. Because of inertia of the levers, it does not stop exactly on +3 degrees. Therefore, a lever deadband of 1 degree is used to make sure the lever does not stay moving around the indicated angle (from +2 to +4) when it has a small overshoot. With the movements of the lever in the hand of the operator, the operator feels the advice of the system and is able to follow the indicated route more precisely. Figure 4.17 shows the amount of torque relative to the lever error.

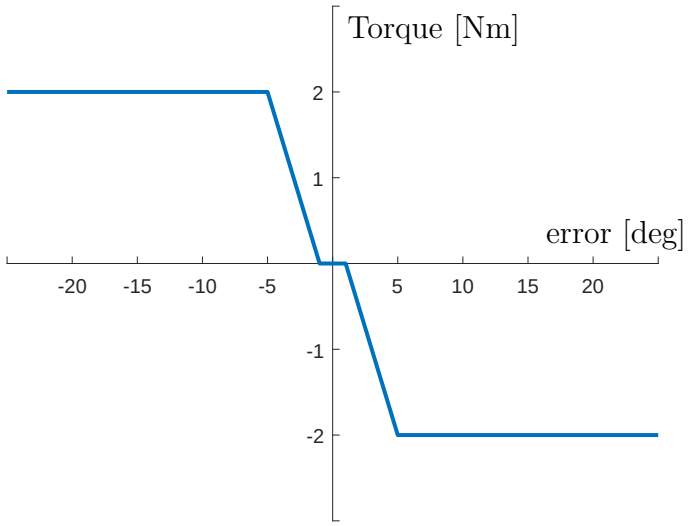

Figure 4.17: Force feedback relative to lever error.

Furthermore, the haptic control system can be used as a warning system. It uses the XTE to determine the warning point. A warning to the operator can be indicated when the vessel deviates from its course line with a certain distance. Three values, $0.625 * vibr_{max}$, $0.875 * vibr_{max}$ and $vibr_{max}$ are indicated with different vibrations (difference in frequency) from low to a higher intensity respectively. The distances between the different warnings are chosen in such a way that the operator does have some operating space but is warned when the deviation gets to large. The maximum warning distance ($vibr_{max}$) can be adjusted depending on the minimum safe distance from the track. In Appendix B the complete model of the haptic shared control system is described.

5. Experimental methods

This chapter elaborates on methods used during the experiments conducted in this thesis. The instructions given to the subjects are discussed, followed by an explanation of the design of the experiment and information about the participants who conducted the experiments. The last paragraph of this chapter shows the procedures followed during the experiments.

5.1 Design

The experiment is conducted based on a within subjects, repeated measures design. The participants performed three experiments in three support conditions: manual control (A), haptic shared control based on the waypoint controller (B) haptic shared control based on the XTE controller (C).
The experiments were counter balanced across participants using a Latin square to ensure the learning effects were reduced to a minimum [74]. The order of experiments for each participant is shown in Table 5.1.
Furthermore, to reduce the learning effect each participant conducted a training run with manual control to get acquainted with the reaction of the ship.

Table 5.1: Experimental design.

Participant	1^{st} **Condition**	2^{nd} **Condition**	3^{rd} **Condition**
1	A	B	C
2	B	C	A
3	C	A	B
4	C	B	A
5	A	C	B
6	B	A	C

Additionally, the experiments are conducted during sunset with constant precipitation resulting in a moderate view, Figure 5.1. The direction of the route sailed by the participants is indicated by red and green buoys on the port and starboard side of the route respectively.

5.2 Task instruction

The goal of the task is to minimize the XTE, the error between the position of the vessel and the indicated route. The current XTE during an experiment is not shown to the participants. An electronic chart with the implemented route and the position of the craft is shown together with a visual of the point of view of the operator, Figure 5.1.
Furthermore, the direction of the route is indicated with buoys on the port and starboard side of the route. These buoys do not show the exact route. To follow the route, the heading direction of the ship is influenced by one lever. The azimuth direction of the lever

corresponds with the rudder set-point of the vessel in the simulator.
Additionally, the levers are set in a fixed rpm direction, resulting in the same vessel speed ($\approx$ 35 knots) during each experiment.
Before the experiments were conducted, the participants were asked to fill out a general questionnaire about their age, gender and sailing experience. This general questionnaire is given in Appendix D.

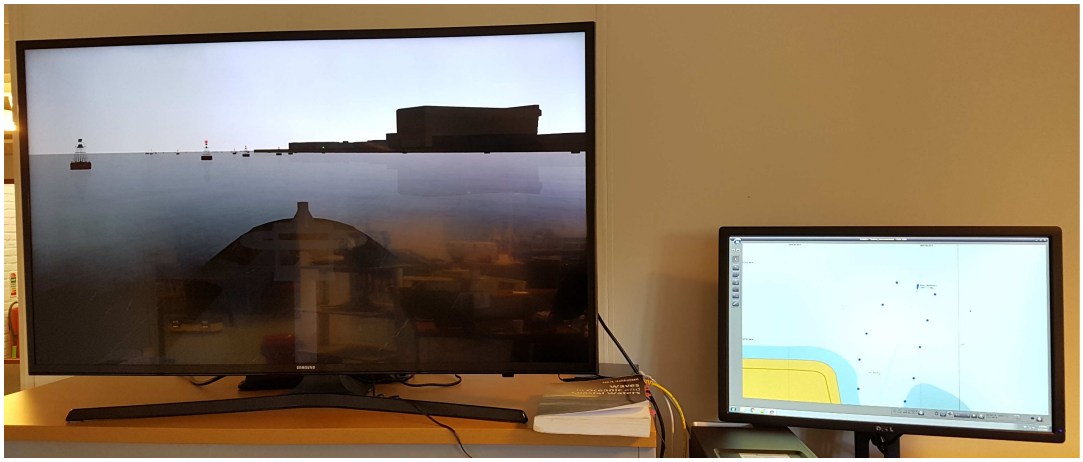

Figure 5.1: Operators point of view and electronic chart.

5.3 Participants

Six participants (3 women and 3 men) participated in the experiments, five with sailing experience but without a navigation license and one with a license. The latter participant is a FRISC operator in the Royal Netherlands Navy. Her test results are compared with the other participants to show if experience with sailing this particular vessel in real life has an influence on the results. These results are analysed and it is determined if this research can be relevant for the Netherlands Navy (or other companies using high speed crafts during inshore navigation).

5.4 Procedure

The experiments are conducted with a constant lever angle resulting in a speed through water of approximately 35 knots. The speed over ground is influenced by a 315° current. The current force acting on the vessel differs per track depending on the depth of the seabed.
To be able to compare the results, multiple data is saved and is shown below.

- Time [s];
- Position ship [deg];
- Cross track error [m];
- Lever angle [deg];
- Rate of turn [deg/s];

- Ship heading [deg];
- Rudder angle [deg];
- Speed through water [kt];
- rudder set-point [deg].

The saved data is analysed to compare the results. As mentioned, the task given to the participants is to follow the indicated route as precise as possible, i.e. limit the XTE during the experiment. Therefore, the XTE will be examined.
Additionally, the experienced and measured workload will be analysed. All values used, are absolute values unless indicated otherwise. The absolute error is used to prevent port (negative) and starboard (positive) errors to cancel each other out. It is not relevant if the error is on the port or starboard side of the route.
The results are compared between the three conditions. A good result will increase the safe navigation by decreasing the workload and increasing the path following performance.

6. Results

The data was analysed for all participants using the three conditions separately. Because the goal of the task during the experiment was to minimize the XTE, this error is explored in different aspects.
Furthermore, the perceived workload of the participants is determined by using the NASA-TLX questionnaire [75]. To compare the perceived and the measured workload, the physical workload is viewed. This means that the measured lever movements during a run are compared with the physical workload perceived by the participants.
All figures are given in the same order of conditions, first the waypoint controller, followed by manual control and the XTE controller. Note that, as indicated in Table 5.1, the participants conducted the multiple experimental conditions in a different order.
The experiments are performed by sailing a preplanned route for every condition. This means that all participants sailed three times, two times with haptic feedback and one with manual control. The route is placed east of Den Helder from north to south with, as mentioned, a current to the north west. The route is shown in Figure 6.1 with the first waypoint as the origin. The total distance of the route is 4160 meters and the participants have an average finishing time of 255 seconds.

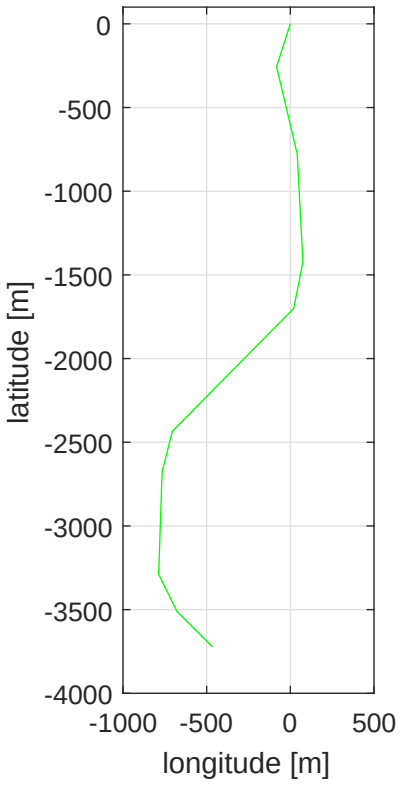

Figure 6.1: Sailed route.

6.1 Path-following performance

During the experiments, the XTE over time is measured. Figure 6.2 shows the XTE over time for all participants and the mean (bold line) of all participants over time. The figures were viewed to see if there were large unexpected differences between the conditions during the experiments.

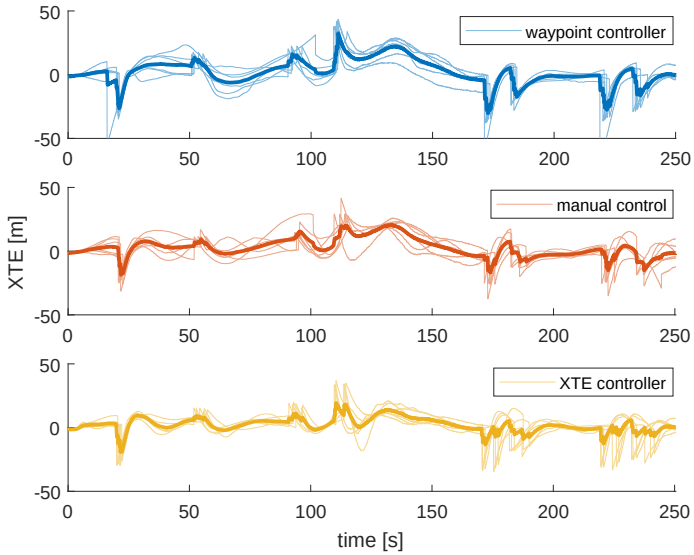

Figure 6.2: XTE of all participants and the mean of all participants over time.

The curve of the mean XTE of the three conditions have the same trend, this means that no large unexpected differences between the conditions are found and it is assumed the data can be used to examine the results.
The graphs in the figure show multiple steep peaks. These peaks are related to the starboard (+) and port (-) turns during the route. The peaks arise during the transition from one track to next one. An option to eliminate the peaks is to use a preplanned route with curves instead of connecting straight lines by waypoints. This means that the curves are taken into account during the determination of the XTE. This will result in a more reliable XTE measurement. In this thesis, the mean absolute value will be high due to high values in the XTE data obtained during a track transition.
To get a better insight in the results, the XTE is viewed in more detail. To do so, the mean absolute XTE values per participant and the mean XTE value per condition are used. Figure 6.3 shows the boxplots together with the mean absolute XTE values per participant. This means that per boxplot six mean XTE values (*) are used to create one boxplot. The three plus signs (+) in the plot represent the mean absolute XTE for the six participants per condition.
The figure shows that the participants performed worse with the use of the waypoint controller compared to manual control, i.e. the minimum error, the median and the standard deviation are higher than with manual control.
The XTE controller on the other hand, does lead to better results. The boxplot of the XTE controller shows that the maximum XTE value measured is still lower than the median of manual control, the standard deviation is also smaller. This means that based on the

information gathered from Figure 6.3, the XTE controller lowers the XTE compared to manual control whereas the waypoint controller increases the error.
Note that just six participants performed the experiment and therefore, the graph could show different results when more participants take part. One outlier can have a large influence on the results with a small group of participants. For example, it can be seen that the FRISC operator had a relatively high mean value with the use of the waypoint controller. In her case, the run with the waypoint controller was her first run which is of influence on the results as was mentioned before. When this high mean value of the FRISC operator is seen as an outlier and this value is cancelled out, the graph changes. The position of the boxplot, the median and the mean in the figure will lower. The vertical length of the box decreases from 3.4 meters to 2.9 meters, the median lowers from 8.1 to 7.1 meters and the mean lowers with 0.5 meters. This does not have a very large influence because the results of the waypoint controller compared to manual control change but it still shows a better result with the XTE controller.
Nevertheless, it does show that the data of one participant affect the results. In this case the removal of the outlier results in less difference between the waypoint controller and manual control.

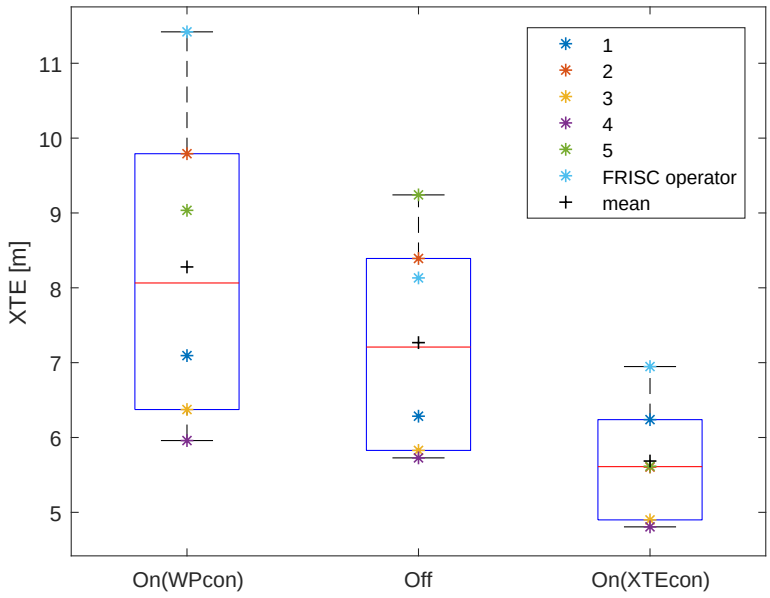

Figure 6.3: Boxplot mean absolute XTE.

Figure 6.3 shows that the use of the waypoint controller did not lower the mean cross track error relative to manual control. This is because the participants were asked to limit the XTE but the waypoint controller leads them towards the next waypoint instead of back to the route. This results in a negative influence of the force feedback on the performance of the participants.

The XTE controller however, does show in all cases an improvement relative to the other two conditions. The mean and median absolute XTE of the XTE controller, show an improvement of more than 20% compared to manual control. Notable is the fact that participant 5 is the only person who had a higher mean with manual control than with the waypoint controller. This can be explained by the fact that manual control was his first run and the practice run was too short for him to get used to the vessel reaction.
Figure 6.3 shows the mean absolute XTE values per participant. To gain more information about the three conditions, the maximum XTE values per participant are viewed.
Not all maximums shown in Figure 6.2 give the correct XTE value. To obtain the correct value, the maximums are determined in such a way that the errors caused by the transition from one track to the next track, when passing the wheel over line, are not taken into consideration. This is because the arising peak indicating the XTE, does not match the actual XTE at that moment.
Figure 6.4 shows an example of such a peak during manual control and Figure 6.5 shows the wrong XTE measurement.

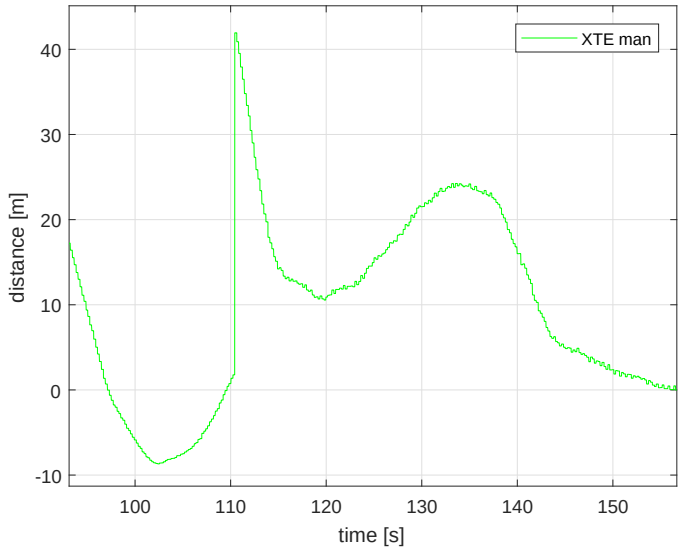

Figure 6.4: XTE peak during track transition.

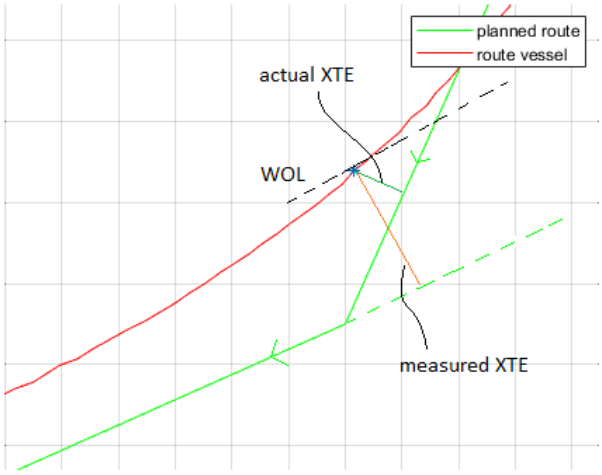

Figure 6.5: XTE during track transition.

Figure 6.5 shows that just after passing the WOL, the XTE changes and the perpendicular distance towards the new track is used as the XTE. This is not correct because the craft did not pass the waypoint yet. This is why the transition peaks are excluded. With this exclusion it is possible that when the steep transition peak would not be there, another (large) peak could be at the same position which is not being detected using this method. The maximum XTE values per participant determined as described above, are shown in Figure 6.6.

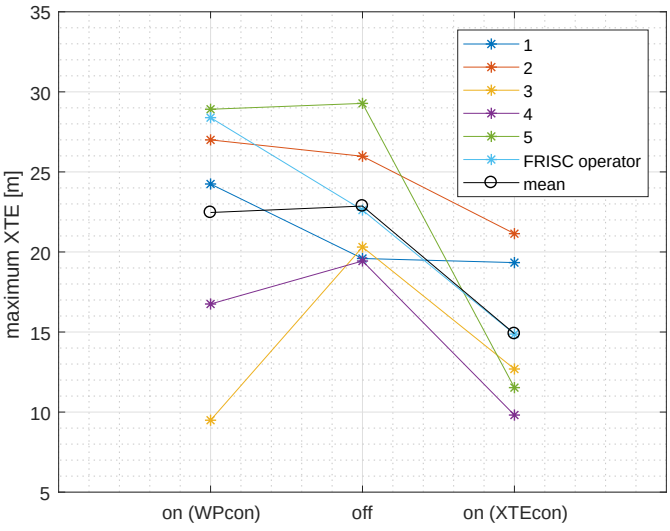

Figure 6.6: Maximum absolute XTE.

Figure 6.6 shows that the absolute maximum values per participant for one condition, differ quite a lot. When using the XTE controller the values are in general the lowest, resulting in the lowest mean value, approximately 37% lower than the with the use of the other two conditions. The figure also shows that with the use of the waypoint controller or with the use of manual control, the mean values of the maximum do not differ much. Again, it can be shown that the result of one participant has a large effect at the mean

value of a condition. When the maximum value of participant 3 with the use of the waypoint controller is seen as an outlier and cancelled out, the mean value will increase from 22.5 to 25 meters. This results in a higher mean maximum value of the waypoint controller compared to manual control. Again, this does not influence the result of the XTE controller compared to manual control but it shows the sensitivity of the data with a small testing group.
An important note is that the results given in Figure 6.3 are not obtained with the correct XTE values. The peaks for every turn are included and therefore the boxplots would be lower when these peaks were excluded. The relation between the three conditions would probably be the same. This assumption is not substantiated because it is not obvious where the peaks end. When all peaks are cancelled out, it could be that to less or too much data points are taken into account.
Additionally, the relative frequency of the XTE for the three conditions during the experiments is shown in Figure 6.7. All the XTE values per condition over time are put together as one experiment. This means that the values shown in Figure 6.7 are the XTE values of the six participants.

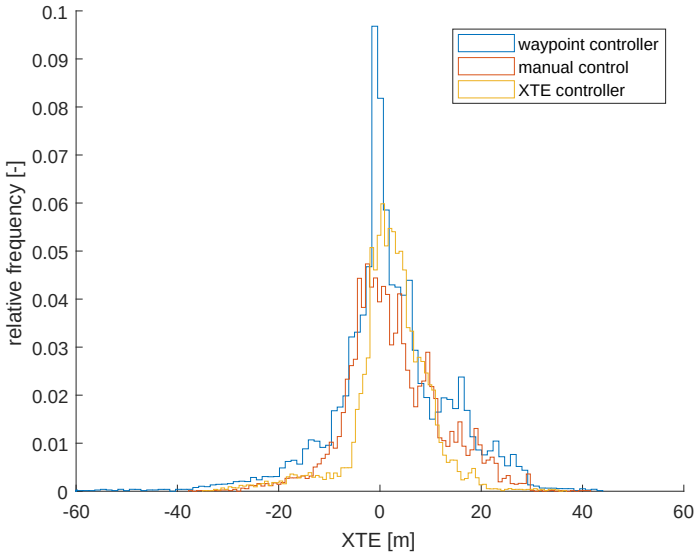

Figure 6.7: Relative frequency XTE during the experiment for all participants.

Preferably, the distribution resembles a normal distribution and shows a very small and high peak around XTE=0. Than the XTE has for the largest part of the time, the smallest value. The coupling with the normal distribution is made because the assumption is that the distribution of the XTE data resembles the normal distribution. It is assumed that the peak of the distribution lays on the right side of XTE=0 because the current force is "pushing" the craft to the right side of the route. In neither of the cases shown, the distributions resemble the normal distribution precisely. Therefore, the condition with the narrowest peak around XTE=0 has the best result.
The figure shows that the three distributions show similarities to a normal distribution but are not the same. The waypoint controller and manual control show the least resemblance with a normal distribution, mainly due to the peaks at an XTE of 18 meters and that of

5 meters respectively. The XTE controller shows the largest resemblance with a normal distribution.
Furthermore, for all conditions the figure shows that the largest part of the distribution is located right of XTE=0. This is due to the current force (315°) pushing the vessel to the right. The largest peaks of the conditions differ in location because the conditions do not all match a normal distribution as precise. Figure 6.7 shows that the waypoint controller and manual control do have their largest peak around XTE=0 but these peaks are not narrow. This means that the chance of sailing with a larger XTE is higher. The XTE controller has its largest peak at the right side of XTE=0 but does not have any other large peaks with large XTEs. This distribution shows the narrowest peak, resulting in a small XTE value with a high relative frequency.
Not all XTE data of every participant follows the trend of the distributions shown in Figure 6.7. Two examples are given in the next part of this chapter.
Figure 6.8 shows the gained XTE data of participant 1. This figure shows that the data with the use of the waypoint controller, just as shown in the overall data, has the widest distribution with a large peak around XTE=0. The rest of the distribution of the waypoint controller shows that it cannot be compared to a normal distribution due to the large peaks with a high XTE value. Manual control and XTE controller, during the experiments of participant 1, do not show a large difference in width where they did in Figure 6.7. The largest difference are the two peaks around XTE=0 during manual control whereas the XTE controller shows more resemblance to the normal distribution.

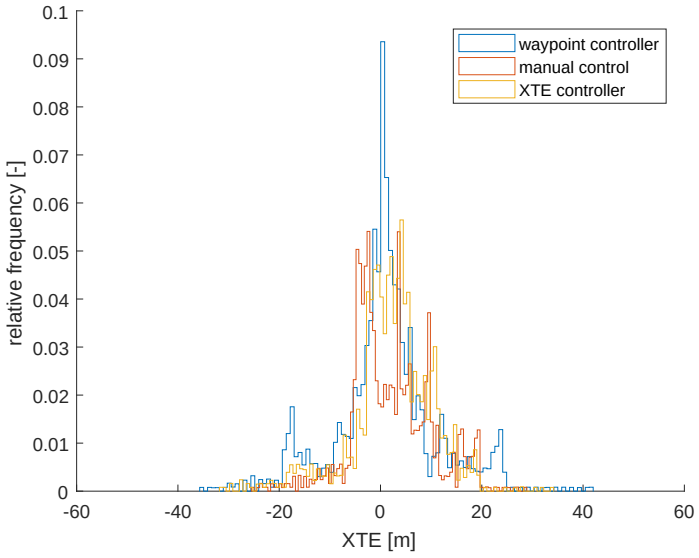

Figure 6.8: Relative frequency XTE during the experiment for participant 1.

The XTE data of participant 5 (Figure 6.9) does show that the width of the conditions is the same as shown in Figure 6.7. The XTE controller has the smallest distribution with its peaks at the right side of XTE=0 whereas manual control and the waypoint controller show wider distributions. All the three distributions shown in Figure 6.9 do not resemble the normal distribution due to the fact that a lot of peaks with a high relative frequency are located at positions with a large XTE.

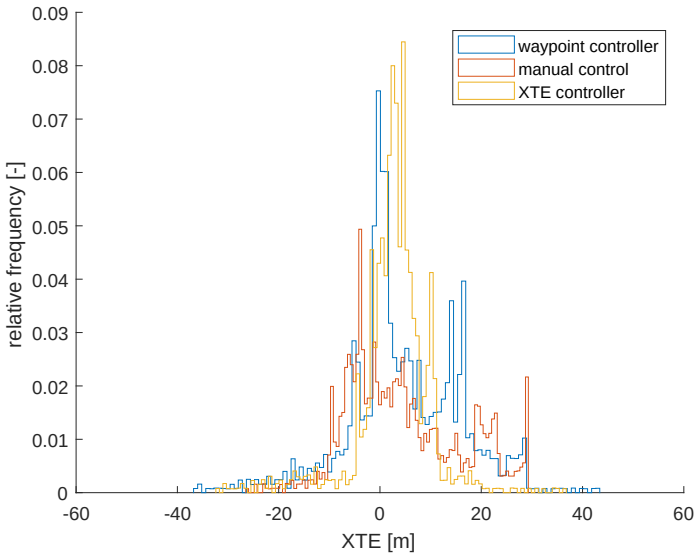

Figure 6.9: Relative frequency XTE during the experiment for participant 5.

Figure 6.8 and 6.9 show that the distributions are rather different compared to the overall data shown in Figure 6.7. This means that the results shown in Figure 6.7 do not resemble all the participants and the results per participant can differ quite a lot.

6.2 Workload

The above given results show information about the XTE. To determine the workload perceived by the participants during the experiments, the participants filled out the NASA-TLX questionnaire for each condition (Appendix E). Note that no weight number for each factor contributing to the workload is applied to the ratings of the participant to prevent biased results. The results of the perceived workload are shown in Figure 6.10.

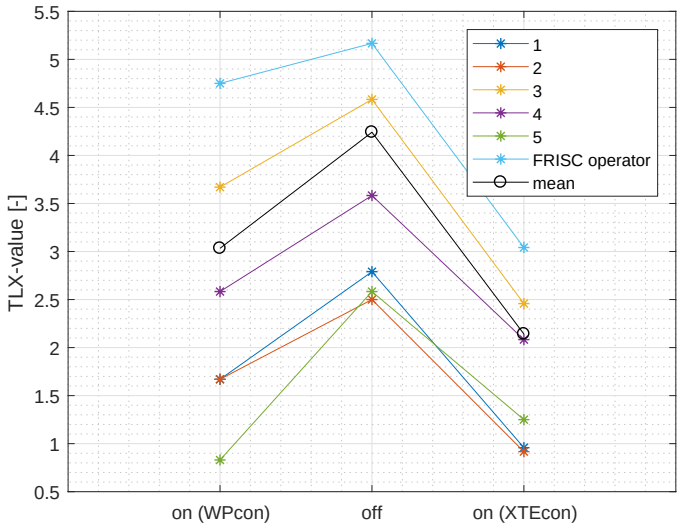

Figure 6.10: Perceived workload.

The results in Figure 6.10 are obvious. Participants perceived a lower amount of workload with the use of the two haptic feedback controllers. The waypoint controller and the XTE controller showed, with this test group, a decrease in perceived workload of approximately 28% and 50% respectively.
The question now is, if the results of the perceived workload correspond to the measured workload. Therefore, the measured physical workload is compared to the perceived physical workload. The measured physical workload is determined by investigating the movement of the lever and the amount of torque generated by the lever. Note that the latter only shows the comparison between the two haptic controllers.
The first part of the physical workload (lever movement) is determined by using the sum of the absolute value of the derivative of the lever angle during the experiments. Figure 6.11 shows the total lever movement per run per participant.

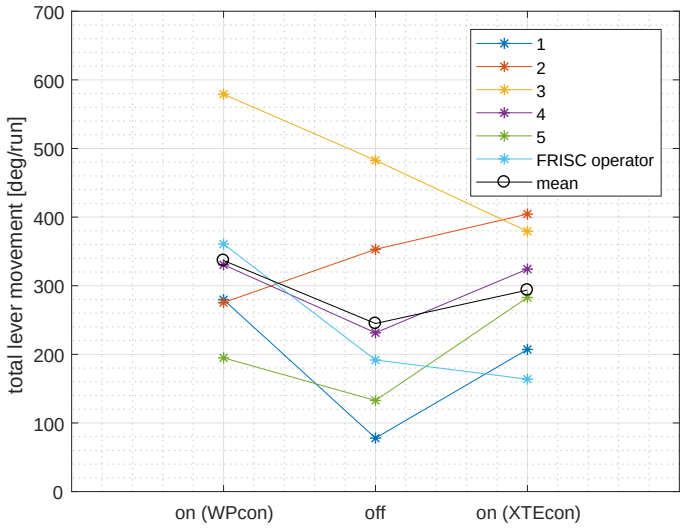

Figure 6.11: Total lever movement.

The second part of the physical workload, the torque, is determined by linking the lever error (lever angle minus rudder set-point) to the corresponding amount of torque. Of course the amount of torque delivered during manual control is zero, the other two conditions are shown in Figure 6.12.

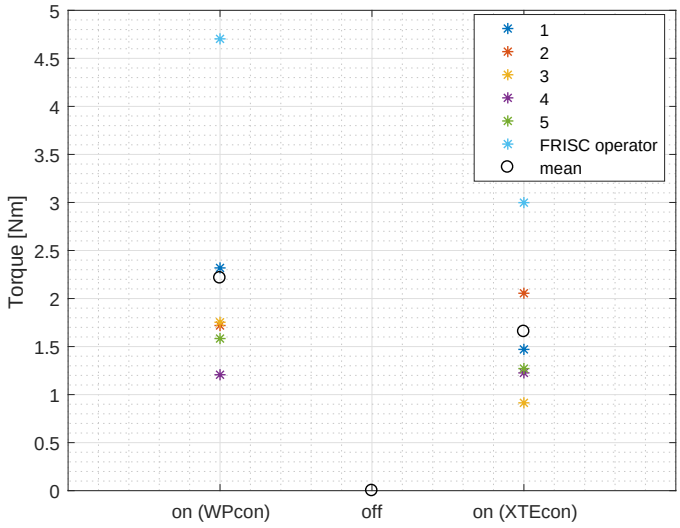

Figure 6.12: Mean torque.

Figure 6.11 shows that with the use of both controllers, the participants on average, moved their lever more than during manual control. This was to be expected since both controllers give continuous feedback and the operator reacts to this advice.
During manual control the operator adjusts his course less, resulting in less lever movement. This means that, determined from Figure 6.11, the physical workload is lowest during manual control and approximately equal when using one of the haptic feedback controllers. This might be caused by the force of the lever provided by the automation. This is however not the case; when the resulting movement is determined by subtracting the movement of the advice and the actual movement, it reveals an even larger resulting lever movement.
Figure 6.12 shows that the automation generates a bit more torque with the use of the waypoint controller compared to the XTE controller. This means that the operator had to resist more force during the waypoint controller resulting in a higher physical workload. Altogether, the total measured physical demand is higher with the use of a haptic controller compared to manual control, the waypoint controller shows the highest amount of workload.
When the results of the lever movements are compared to the physical demand perceived by the participants, it shows that the physical workload does not correspond with the perceived physical workload. The actual physical workload determined out of the lever movement is approximately 27% and 17% higher for the waypoint controller and XTE controller compared to manual, whereas the perceived workload is approximately 37% and 44% lower for the waypoint and XTE controller respectively compared to manual control. Because in this thesis it is assumed that the actual physical workload during the experiments does not lead to muscle fatigue, the perceived workload is assumed to be of main importance. Leading to a decrease in workload while using a haptic shared control system.

7. Discussion

During this research an active guiding system is used to follow an indicated route.
However, when a high speed naval vessel is conducting inshore operations, the operator wants to use as much operating space as possible. Nevertheless, during this research a path following method was used. This is due to lack of chart information and the time limitation. A possibly better option to increase safety during inshore high speed navigation, is creating a larger operating space by indicating safe zones. This means the haptic system indicates the safe zones and does not permit the vessel to sail into the forbidden zones (regional constraints). To do so, the system should use repulsive constraints to "push" the vessel from a forbidden zone instead of attracting the vessel towards an indicated route. The haptic system only assists when the situation is getting unsafe instead of constantly assisting the operator when deviating from track, as it is done in this research.
To create a safe haptic system, with attractive or regional constraints, the correct position of the vessel must be known. The position of the vessel is calculated from GPS information. This means that when the GPS receives incorrect data, a GPS-error occurs and the haptic system does not deliver the correct information, i.e. the system assumes the ship is not in the position it actually is. This position error will result in incorrect haptic feedback.
Furthermore, a GPS signal has an accuracy of 15 meter which can result in a too large error when sailing in inshore waters. DGPS on the other hand shows a more accurate position, it has an accuracy of approximately 10cm [76], this is however not used onboard the FRISC.
In this research, it is assumed that there is no GPS signal error (no GPS error or noise was applied during the experiments), so the position of the vessel used in the model is accurate. Note that the update rate of the vessel in the simulator is 5Hz which means that the model calculates with a position delay of 0.2 seconds. This has been taken into account during the determination of the WOP and WOL. This delay results in a possible error of maximum 3 meters, the maximum distance between the ship and the WOL before turning.
For the calculation of the XTE this delay is not taken into account causing the model to calculate with an XTE of the last time step. This should not be a large problem in this research; even with a perpendicular course angle compared to the route, the XTE could differs approximately 4 meters. Note that it is not logical to sail perpendicular to the planned route but when a haptic system would be implemented into a real vessel this could be taken into account.
Furthermore, the output of the control laws can be determined with different vessel information (i.e. Course Over Ground (COG), heading, Speed Over Ground (SOG) and Speed Through Water (STW)). This information can be based on the GPS signal (COG and SOG) or based on the (gyro) compass (heading) and the speed log (STW). The different values do have an impact on the output calculated in the control laws, i.e. a different rudder set-point value is determined when the COG instead of the heading is used. The rudder set-point calculated in the XTE controller is also dependent on the vessel speed. This means that the speed input, SOG or STW, result in a different rudder set-point. This

difference has less influence on the rudder set-point compared to the difference between the COG and the heading.
The difference between the use of the COG or the heading is based, with a correct GPS signal, on the update rate of the signal. The GPS signal has an update rate of, in general 1 Hz whereas the heading is updated continuously (in this research both values have an update rate of 5Hz).
With the use of the COG, the control law uses the actual movement of the vessel, whereas the heading provides the control law with only the heading of the vessel which differs from the actual movement of the ship. This means that with the use of the COG, the sideslip is taken into account while this is not the case when the heading is used, Figure 7.1.

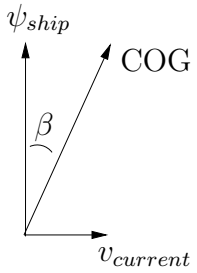

Figure 7.1: Sideslip β.

This difference can be divided into sailing on a straight path and sailing during a turn during the route.
When the COG is used instead of the heading during a straight part of the route, the control law will be more accurate. The system uses the actual movement of the vessel while with the use of the heading the rudder set-point is based with a movement error which is equal to the sideslip. In this research the maximum movement error is 4.9 degrees, i.e. while sailing 35 knots with a current of 3 knots.
During turns, the use of the heading is more accurate than the use of the COG. Because the GPS signal has an update rate of 1 Hz whereas the heading is updated continuously, the COG value has a delay. This means during a turn, with the use of the COG, the vessel uses an input value with 1 second delay which will probably lead to an overshoot and a more instable system during a turn. When the heading is used, the turn will pass smoother due to the continuous update rate. Note that the system does not take the current into account.
In this research the choice is made to use the heading and the STW as input for the control laws. This results in stable system during the turns but a heading error during the straight lines.
Note that the complete calculation is based on the vessel position determined from the GPS signal. Therefore, it can be argued that the COG and SOG can be used in the haptic system. When the vessel position is incorrect the system does not provide the correct haptic feedback. This means that either the GPS information is correct, i.e. the position, COG and SOG are correct, or the information is incorrect and the haptic system cannot be used at all because it will provide the operator with the incorrect feedback.
The choice during this research is however, to use the heading and STW as input for the control laws. This is because the system can also be used as a simple autopilot. In the shipping industry the heading based on the (gyro) compass and the STW are usually used in autopilots. Therefore, in this research the heading and STW were used.

Another point of notice is that the developed haptic system is only tested during inshore high speed navigation with only environmental interference from a constant current and no waves. The PID-values are determined with no waves as well, so the values are probably only applicable to these specific environmental circumstances. If the system should be implemented onboard an actual FRISC, the system must be tested in waves. When waves are added during testing, the system can get unstable which can be resolved by adjusting the PID-values in the right settings. It is possible that for each wave height other values are needed.
Furthermore, the haptic levers used during this thesis cannot be compared to an actual steering wheel and throttle onboard of a FRISC. It is possible that the results found during the experiments will differ when other steering equipment, equipment more comparable to the FRISC, is used. Therefore, it could be an option to use the motion platform of a high speed vessel developed by MARIN which has already been used by the Royal Netherlands Navy. The use of this motion platform will result in more reliable results.
Additionally, just the force feedback is tested during this research. When also the warning system implemented in the model is used, other results are possible. In this research the use of the warning system was not covered to get an unambiguous result about the influence of force feedback and due to the limited period of time. When one wants to test the warning system, two options are possible. The first option is to test the warning signals solely. The other option is to test the combination of the force feedback with the warning signals. Note that it is of interest that the results of just the warning signals are known before the combination is tested.

8. Conclusion

Implementing the correct haptic shared control system in the steering system of the FRISC contributes to safe navigation during (nightly) high speed inshore navigation. This means that it leads to a better path following performance and a decrease in perceived workload. In this chapter the conclusion is drawn to what extent the haptic system contributes to safety during high speed navigation. The conclusions are divided into a part about path following performance and a part about the workload.
Altogether it can be stated that haptic feedback, implemented into the steering system of the FRISC, contributes to safe navigation during (nightly) high speed inshore navigation by increasing the path following performance and decreasing the workload.

8.1 Path following performance

The XTE data from the participants as shown in Figure 6.2, influence the results shown in Figure 6.3. Due to the high XTE peaks during the track transition the position of the boxplots are higher than when these peaks are omitted. The position for the conditions relative to each other will stay the same.
From the boxplots shown in Figure 6.3 it can be concluded that the XTE controller, based on the mean, median and standard deviation, has the best results compared to the other two conditions. It shows a smaller boxplot, i.e. lower standard deviation, and it shows that the mean and median of the XTE reduces over 20% compared to manual control. The waypoint controller on the other hand, increases the mean and median of the absolute XTE due to the contrast between the goal of the task and the feedback of the waypoint controller. This means that the waypoint controller only shows a worse influence on the XTE whereas the XTE controller shows a 20% improvement compared to manual control. This results in the fact that the XTE controller contributes to an increase in the path following performance compared to manual control.
Figure 6.6 shows the absolute maximum XTE values attained during the experiments. These values, calculated with the elimination of the XTE peaks during track transition, show that the mean value of all the participants using the XTE controller is 37% lower than with the use of the other two conditions. This is of advantage during inshore navigation because rivers with small navigable areas can be safely reached.
A distribution with the relative frequency of the mean XTE values is shown in Figure 6.7. The XTE controller shows the highest peak a bit at the right of XTE=0 (due to the current) and the smallest peak compared to the waypoint controller and manual control. This means that the relative frequency of low XTE values is the highest with the use of the XTE controller and will increase the path following performance. The waypoint controller shows worse results, larger distribution width and multiple high peaks, compared to manual control.
Altogether, it is shown that the use of a correct haptic shared control system, in this case the XTE controller, increases the path following performance, based on the mean and median of the XTE with 20% and based on the maximum XTE value with 37% during high speed inshore navigation.

8.2 Workload

The workload also contributes to safe navigation. The perceived workload by the participants is measured according a NASA-TLX questionnaire. The questionnaire showed that the perceived workload is reduced with the use of a haptic feedback system (both the waypoint and XTE controller). Figure 6.10 shows that the perceived workload with the use of the waypoint and XTE controller lowers with 37% and 44% respectively.
The measured physical workload was compared with the perceived physical workload based on the lever movement per run. This measured physical workload showed the opposite result. The amount of lever movement with the haptic controllers was higher than with manual control whereas the perceived workload was lower with the use of haptics.
Because the perceived workload is assumed to be of main importance, it can be stated that the perceived workload during high speed inshore navigation with the use of a haptic shared control system, reduces with approximately 40%.

9. Recommendations

In this thesis it is examined to what extent a haptic feedback system in the steering system of the FRISC contributes to safe navigation during high speed navigation. This is done by comparing two control laws (the waypoint and XTE controller) with each other and with manual control.
Because the research can be more extensive and the model more precise, the next sections provides the reader with clear recommendations. The recommendations are divided into a part about the Simulink model, the hardware and the experiment.

9.1 Simulink model

The MATLAB Simulink model uses the waypoint coordinates given by the MARIN simulator. The coordinates are put into the Simulink model by hand. To create a more user-friendly system, the electronic chart must be coupled with the haptic system. Resulting in the fact that the route preparations can be conducted with the use of the electronic chart, and after that the haptic system uses the chosen waypoints as input. With this approach, route preparations stay the same as before and no extra work has to be done.
Furthermore, the model is depended on the update rate of the position of the vessel and the system delay. Therefore, this has to be taken into account and for every system these values should be examined.
Not only the update rate and system delay lead to a less accurate system. Also the turning radius and the vessel reaction are of importance. In this Simulink model, the lookup table used to determine the position of the WOP is created for multiple speeds and rudder angles. Not all possible values are implemented in the lookup table. To make a more accurate system, all combinations, i.e. rudder angles 1-25 degrees and speeds 1-40 knots, have to be used in the lookup table. The wheel effect has to be taken into account as well. This means that two lookup tables (starboard and port turns) have to be used to find the correct turning radius.
Additionally, another lookup table has to be developed to consider the ship reaction regarding different turning radii. In this thesis an average of 0.966 seconds was used as reaction delay but to create a more precise system this all reactions for all turns have to be examined.

The control laws are both based on the heading of the ship. As described in the discussion, the use of the COG can result in a rather different rudder set-point. It is therefore important to explore which value, COG or heading, is best in the system. This choice can depend on the usage of the system, i.e. it depends if the system is just used as a haptic system or also as an autopilot.
Furthermore, the control laws are developed with two PID controllers, one in the waypoint and one in the XTE controller, to create a smooth vessel reaction. These values are based on experiments with only a constant current. To develop a more robust system, the correct PID values, when sailing in waves or with a variable current, have to be investigated.
Another point of notice is that the control laws are now based on an implemented route. A

possible option is a haptic system based on safe and forbidden zones. When the electronic chart is used as input for the haptic system, it may be possible to use safe zones instead of route following. It should be possible to use an isobath as a regional constraint. Note that probably another control law has to be used instead of the control laws in this thesis. This new control law probably requires lookahead capabilities to react to the upcoming forbidden zone.

In the haptic part of the model, the force feedback created is similar for every participant. It is possible that when the feedback is adjusted to an individual operator, the performance will increase [7]. Therefore, different forces for different participants have to be tested to create the most optimal usage of a haptic shared control system.

9.2 Hardware

The experiments are conducted with two haptic levers designed by the Delft Haptics Lab. These levers were initially developed to do experiments with an ASD tug with two azipods. This means that the experiments in this thesis are conducted with steering equipment based on a tug instead of a FRISC. This difference in steering equipment could lead to other final results.
Furthermore, a participant conducts the experiment in a class room with no movement of any kind. To create more reliable results, the testing environment has to be similar to the actual sailing environment. This can be created by using the motion platform of MARIN. This is probably the simulator most similar to the real world.

9.3 Experiment

During the experiments a constant current was used. To show the capability of the system, the system needs to be tested with a variable current in direction and force.
Additionally, the system needs to be tested in waves. All wave heights, up to sea state 5 (maximum operating wave height, Table 1.2), have to be tested to find the limitations of the haptic system. It is possible that with high waves, the operator does not agree with the steering reaction of the system. If this is the case, a solution has to be found.
During this thesis only a small group of participants tested the system. Therefore, more testing should be performed to increase the reliability of the results and ensure the conclusions drawn are similar as stated in this thesis.
Another haptic system developed during this research but not tested, is a warning system. It could be relevant to examine the influences of the warning system solely. When these influences are known, the combination of the warning system and active constraints could be tested. The results can be compared to the results found by using the active constraints or warning signals.
If using a haptic shared control system shows advantages, the experiments should be expanded to a more realistic environment. This means that a motion platform, as indicated before, with actual FRISC operators is a good starting point for good accurate results before the system would be implemented onboard an actual vessel.
When these results also show benefits, the haptic feedback can be implemented and extensively tested onboard an actual FRISC.

A. Main console FRISC

Figure A.1 and A.2 show the main console with the multiple tools the operator and navigator use during sailing, together with the corresponding descriptions.

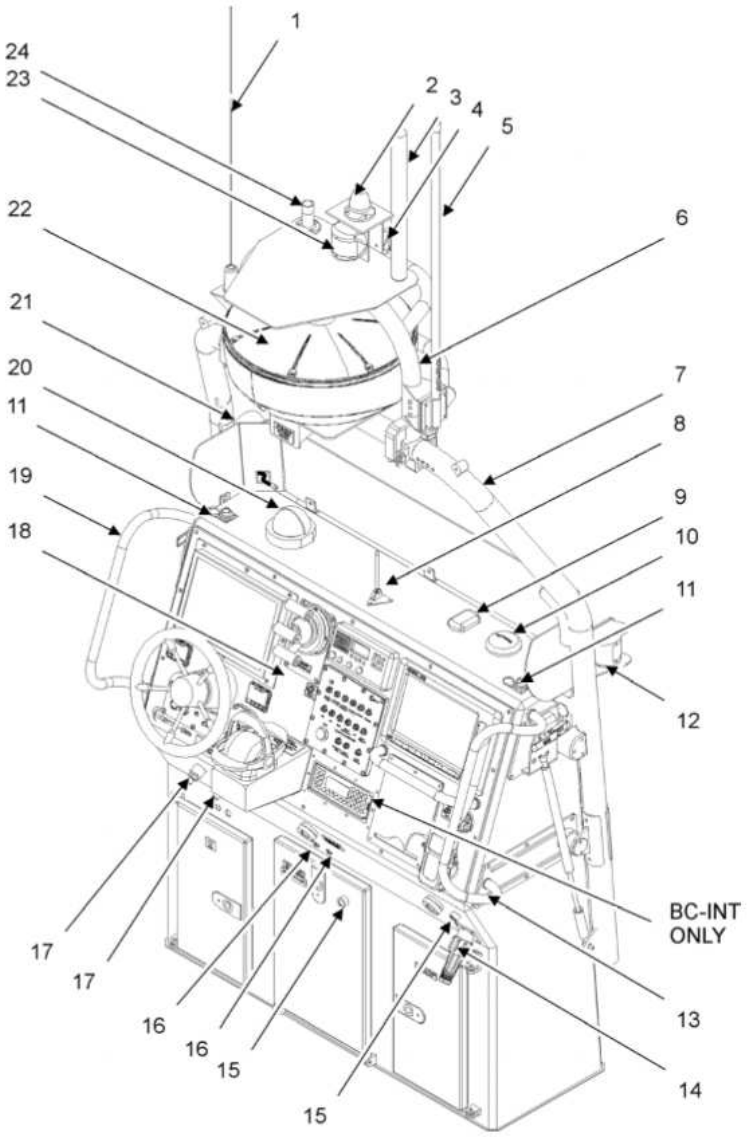

Figure A.1: Main console [3].

Table A.1: Item locations main console [3].

Item No.	**Description**
1	Vtronix VHF Whip Antenna MD-20
2	Anchor light
3	Echomax Radome
4	Mast Navigation Light
5	Comrod AIS (VHF & GPS) Antenna
6	Arch Antenna
7	Over Console Arch Assembly
8	Searchlight Bracket
9	DAGR GPS
10	Raystar GPS
11	Bulgin DP Power Socket (Qty 2) - for the Searchlight
12	Starboard Navigation Light
13	Starboard Console Grab Rail
14	Shore Power Connector
15	Anti Condensation Valves
16	Savox Dummy Connectors (Qty 2)
17	Volvo Lanyard Switches (Qty 2)
18	Main Console Facia (Figure A.2)
19	Port Console Grab Rail
20	Ritchie SS-1002 SuperSport Compass
21	Port Navigation Light
22	Raymarine RD418HD Radome
23	Stern Navigation Light
24	Procom FLG Antenna Mount

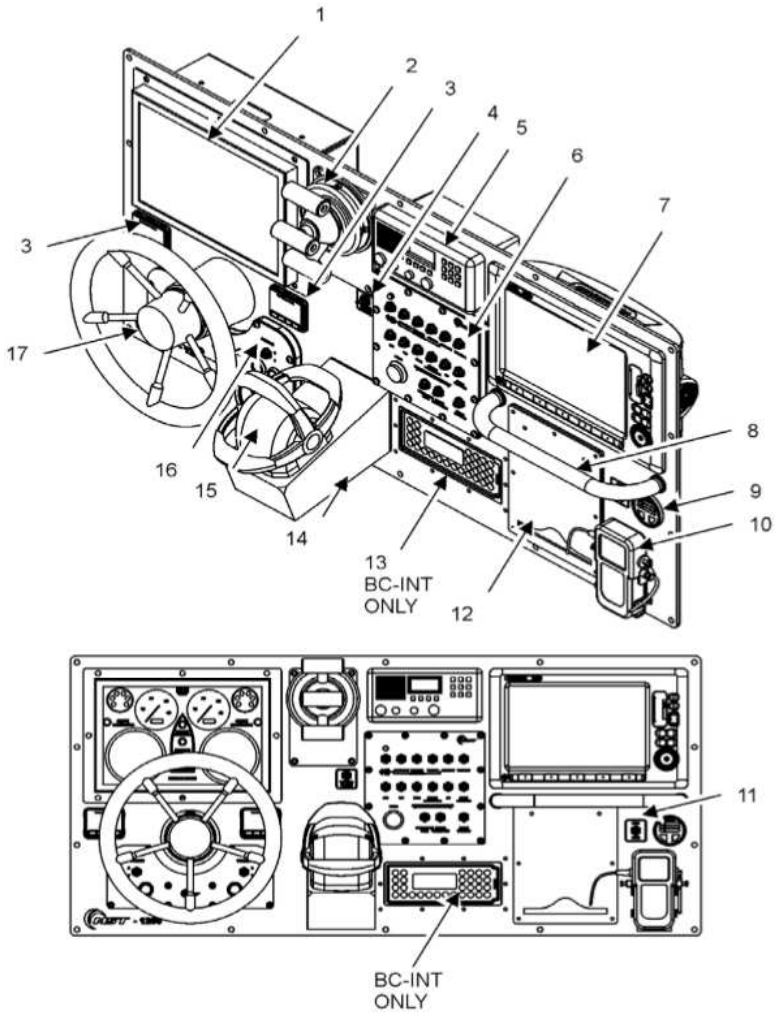

Figure A.2: Main console facia [3].

Table A.2: Item locations main console facia [3].

Item No.	Description
1	Volvo Twin Glazing Panel behind which the following are Installed: • Port and Starboard Engine Tachometers Port • Port and Starboard Engine Warning Clusters • Port and Starboard Engine Displays • Port and Starboard Engine "Check Cooling Level" • Warning LEDs • Bow, Midships and Engine Bay Bilge Alarm LEDs
2	Remote Release Handle
3	Electronic Vessel Control (EVC) Trim Control Panel
4	Twin Fall Release Switch
5	ICOM IC-603
6	FRISC Switch Panel Assembly
7	Raymarine E120W Display
8	Console Facia Grab Rail
9	SeaFire Display (Fire Extinguisher System)
10	Defence Advanced GPS Receiver (DAGR)
11	DGPS/DAGR Selector Toggle Switch
12	A5 Perspex Document Holder
13	C2000 Radio Mount (BC-INT Only)
14	Throttle Control Horizontal Mounting Block
15	Volvo Engine Diesel Control (EDC) Unit, (Throttle)
16	Engine Twin Start Panel
17	Helm Wheel, mounted on Seastar Hydraulic Helm Pump

B. Experimental Setup

In this appendix an elaboration is given on the subsystem *heading controller* created in MATLAB Simulink (Figure B.1). The complete subsystem with its corresponding blocks/subsystems is given in detail. The subsystems are given in multiple paragraphs separately.

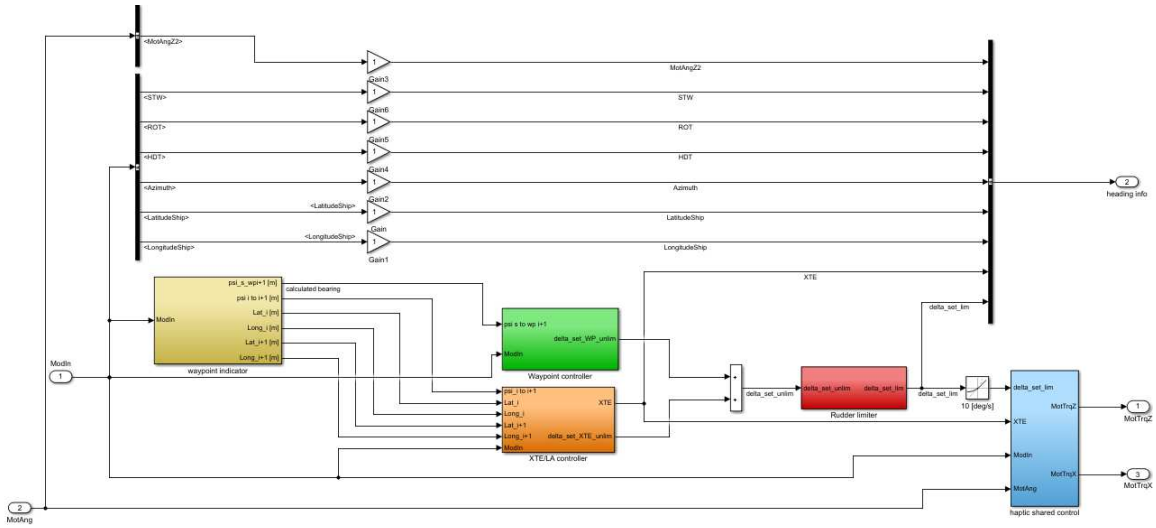

Figure B.1: Subsystem heading controller.

Waypoint indicator

The subsystem *waypoint indicator* (yellow block in Figure B.1) corresponds with the waypoint indicator of Figure 3.4. As mentioned in Section 4.2, this block exists out of multiple subsystems, e.g. bearing calculations and distance from ship to wheel over line. In the following paragraphs a detailed description is given of the multiple subsystems in the waypoint indicator. The different calculations conducted were explained in Section 4.2.

Waypoints

The route prepared in the simulator, has fixed waypoint positions. These positions are presented in degrees and minutes in the MARIN simulator. To use the waypoints in the Simulink model their positions are converted to latitudinal and longitudinal degrees and placed in the model in a matrix called the waypoint database [deg]. Thereafter, the positions are converted to meters (step 1, Paragraph 4.2.1) and the first waypoint is used as the origin of the coordinate system (waypoint database [m]). Figure B.2 shows the total conversion of the positions from degrees to meters, and to the new coordinate system (first waypoint as origin).

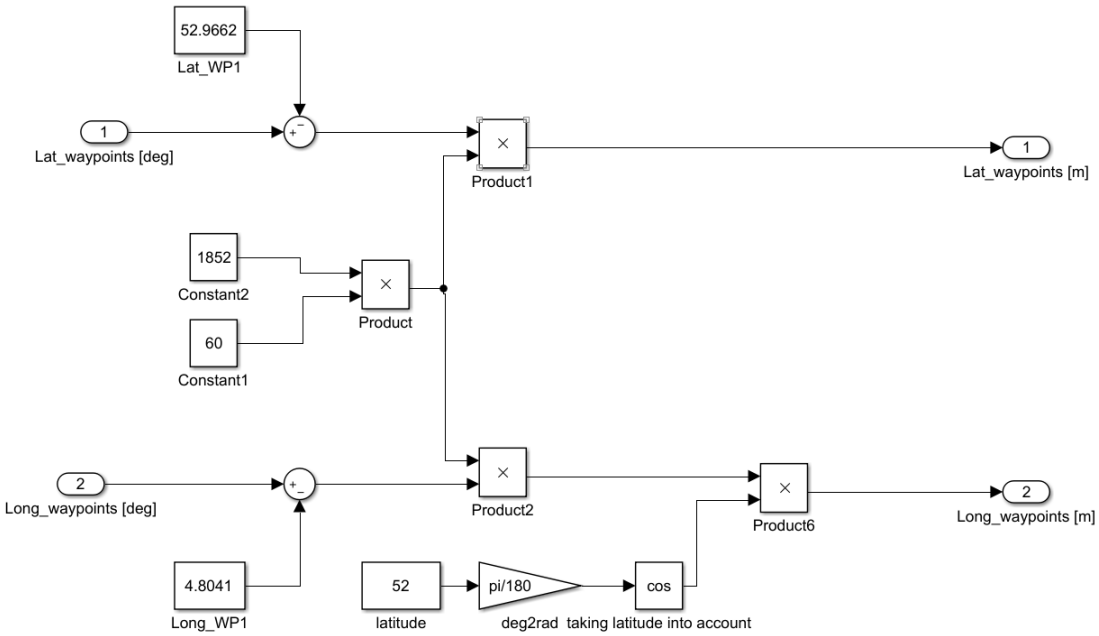

Figure B.2: Position conversion.

The database is used, together with the current track indicator (i), as input for the waypoint selector. The waypoint selector selects the waypoints needed for the upcoming calculations. The output of the waypoint selector, as mentioned in Figure 4.2, are the positions of waypoint i, i+1 and i+2.

Bearing calculations

As mentioned in Paragraph 4.2.1, a bearing is indicated as a direction between two points. In the subsystem *bearing calculations*, the bearings between ship and upcoming waypoint ($\psi_{s->i+1}$), the first and second waypoint ($\psi_{i->i+1}$) and the second and third waypoint ($\psi_{i+1->i+2}$) are calculated. Figure B.3 shows the calculations to determine the multiple bearings. The bearing from ship to waypoint is used later in the subsystem *waypoint controller* and, $\psi_{i->i+1}$ and $\psi_{i+1->i+2}$ are used to determine the wheel over point and wheel over line respectively.

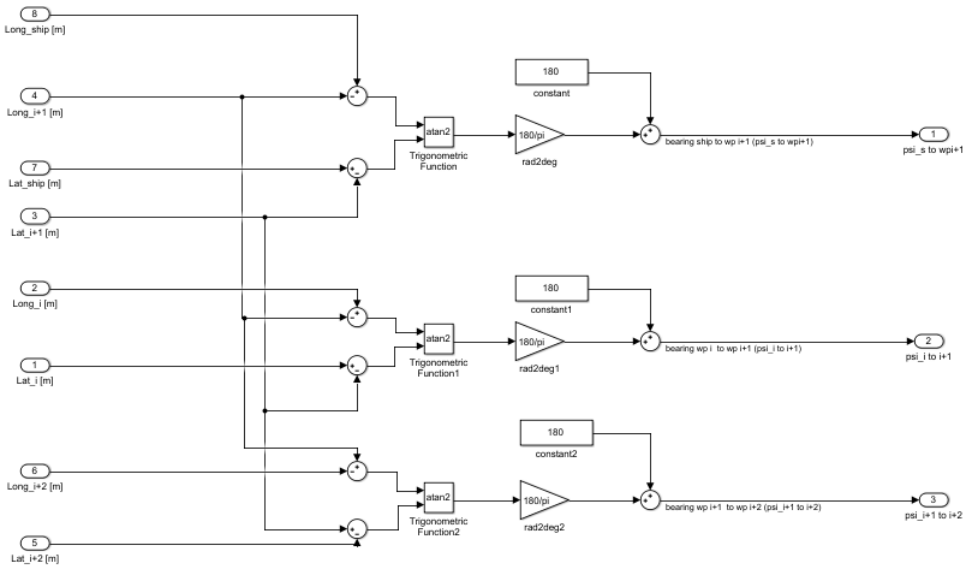

Figure B.3: Bearing calculations.

Determine position WOP

The wheel over point is the turning position of the vessel. To follow a preplanned route, the correct turn radius of the craft must be used (Paragraph 4.2.2). Figure B.4 shows the calculation conducted in the model to determine the position of the WOP.
In the model, the heading is compared to the bearing from waypoint i+1 towards i+2 ($\psi_{i+1->i+2}$). This ensures the most accurate turning angle of the vessel to its new course because the information about the upcoming turn is known.
The PID-controller is used to find the rudder set-point the vessel will use when it turns. The output of the PID-controller, together with the speed of the ship through the water are used as input for the lookup table to find the correct turning radius. This means that the distance from wheel over point to waypoint can be calculated. The PID-controller can use multiple P, I and D values depending on the used control law.
Besides the radius, the reaction time of the vessel has to be taken into account otherwise the vessel starts turning to late. The average reaction time of the vessel (0.996s) is determined during different rudder angles and speeds as mentioned in Paragraph 4.2.2. The update rate of the system is 5Hz which means that the vessel should have its input 0.2 seconds before the actual turning point. Therefore, the reaction times are multiplied by the speed of the vessel in meters per second to determine the reaction distance. This distance is added by the distance q, mentioned in Paragraph 4.2.2, to gain the total distance from waypoint to wheel over point. The total distance is used to find the position of the WOP with the use of Pythagoras.

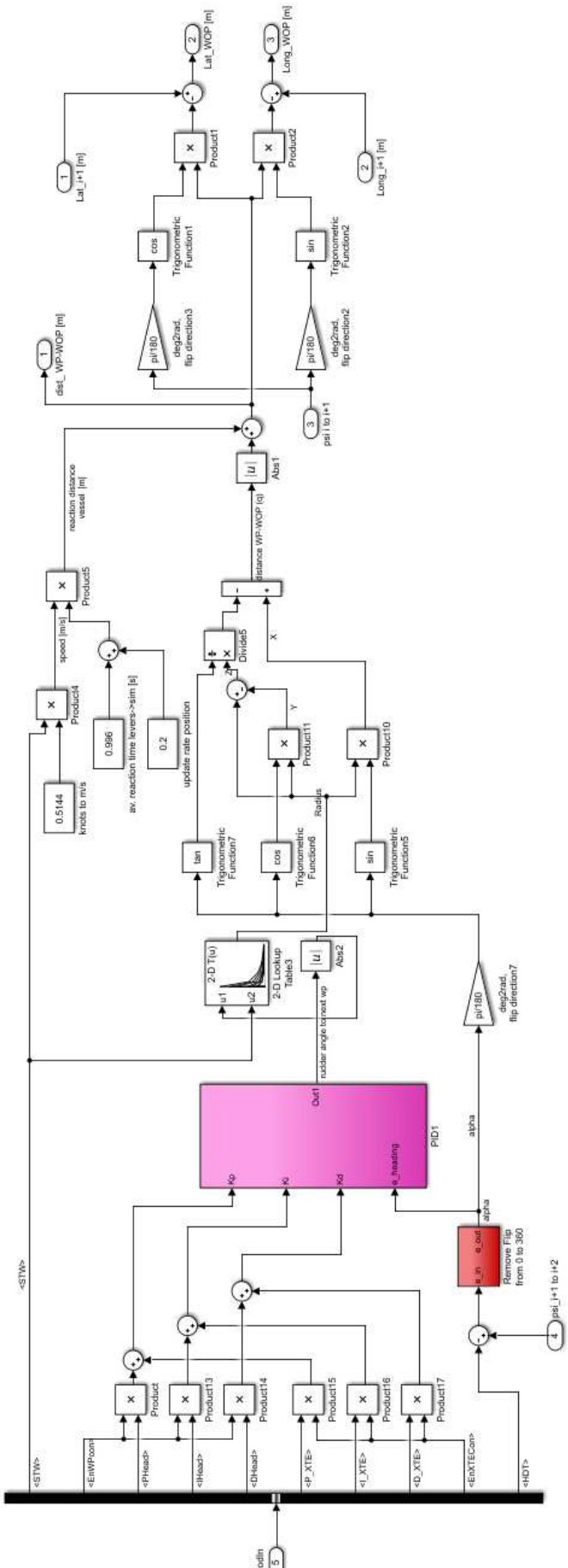

Figure B.4: Position determination WOP.

Determine position WOL

Because the position of the wheel over point is determined, the position of the wheel over line can be calculated. With the bearing between waypoint i+1 and i+2 ($\psi_{i+1->i+2}$) and the position of the WOP, two positions on the WOL can be calculated. Figure B.5 shows the calculation as described in Paragraph 4.2.3.

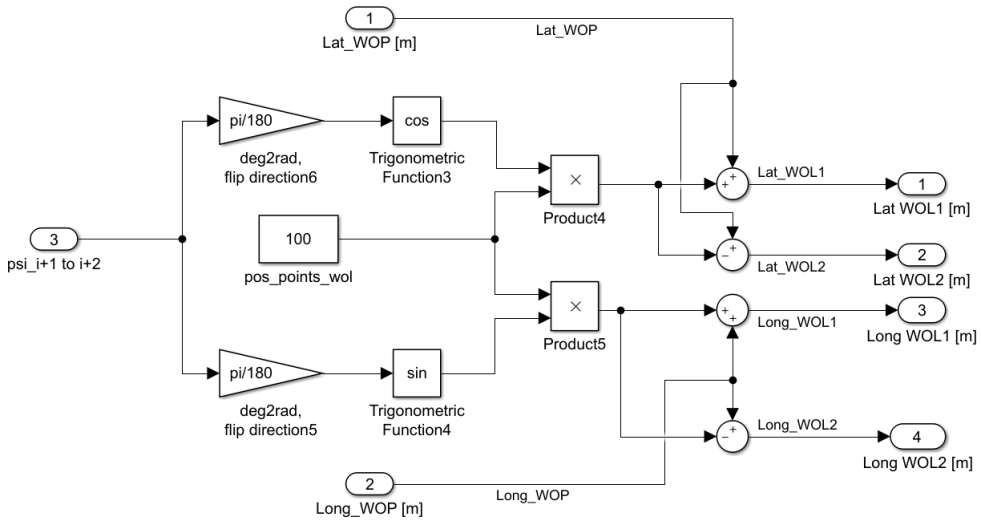

Figure B.5: Position determination WOL.

Distance ship and WOL

The wheel over line determines the turning point of the ship. Therefore, the distance between the vessel and the wheel over line is important and is calculated according Equation 4.10. Figure B.6 shows how this equation is used in the model.

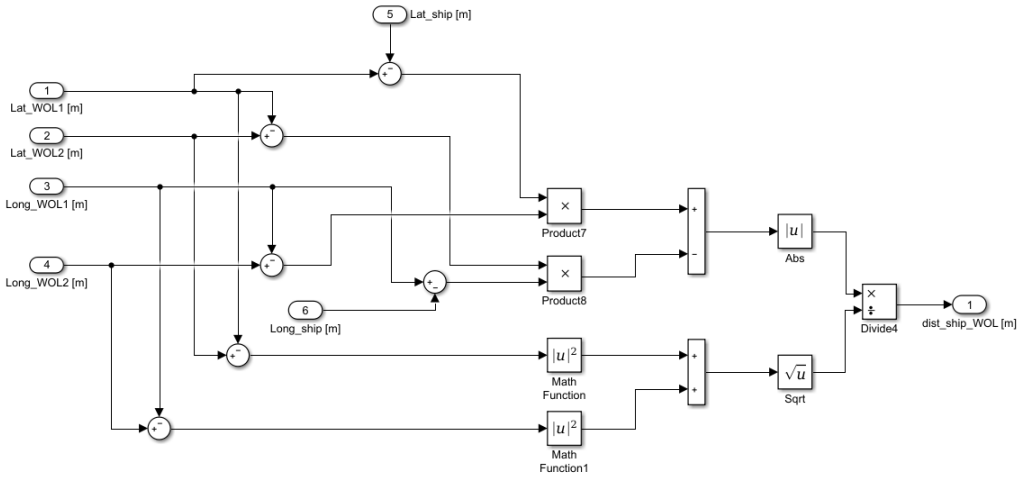

Figure B.6: Distance determination.

Track selector

The track selector determines the value of the current track indicator. When the distance between the ship and the WOL is smaller than 3 meters, a 1 is send to the edge detector. With the unit delay, this 1 is added to the track indicator of the last time step. The track indicator starts at 1 and when all tracks are passed, the indicator has a value of n (in this thesis n=10).
Note that the distance of 3 meters is due to the update rate as mentioned in Paragraph 4.2.5.

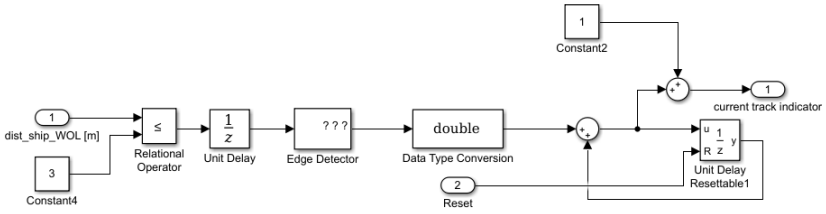

Figure B.7: Constraints waypoint.

Control laws

Two different control laws are used to follow the route as indicated in Section 4.3. Both the waypoint controller and XTE controller are described in the forthcoming paragraphs.

Waypoint controller

The waypoint controller uses one part of the output of the waypoint indicator as input, namely the bearing from ship to waypoint ($\psi_{s->i+1}$).
In the subsystem *waypoint controller* (green block Figure B.1) the unlimited rudder set-point and bearing to the next waypoint ($\psi_{s->i+1}$) is determined (Figure B.8). As mentioned in Paragraph 4.3.1 the error (e_ψ) is determined by subtracting the heading of the craft (ψ_{ship}) from the bearing ($\psi_{s->i+1}$).
Two bearing options can be chosen to calculate the rudder set-point. The first option is to use the calculated bearing $\psi_{s->i+1}$, the other option can be indicated in the GUI (0-360 degrees) of the model. This means that an indicated bearing, for example 260, is used as bearing and compared to the heading. The ship will sail in the direction of 260 degrees. For the latter option, there is no preplanned route necessary and this can be useful to tune the PID-controller without following the planned route.

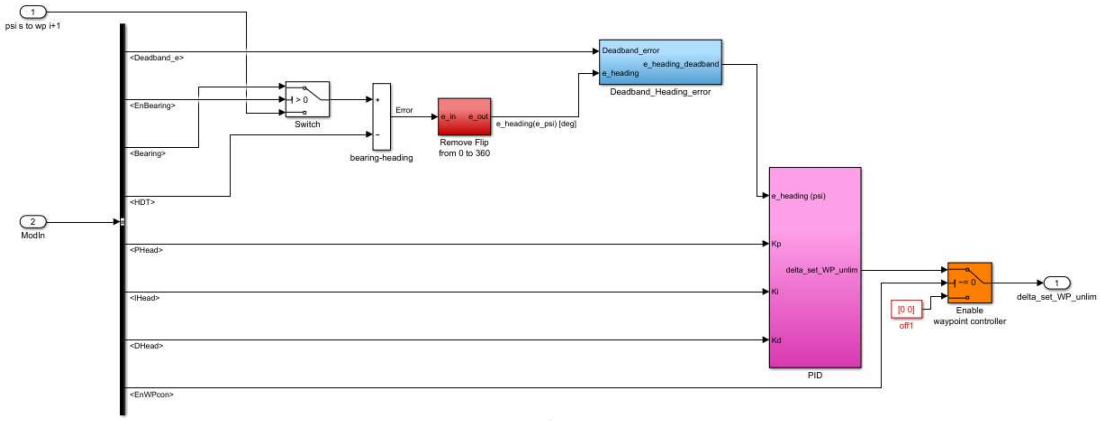

Figure B.8: Subsystem waypoint controller.

This heading error is thereafter sent to the red block (*remove flip*) in Figure B.8 to ensure the heading error is always between -180 and 180 degrees, depending on the steering direction (port or starboard), this block is shown in detail in Figure B.9.
When the error meets the requirement the output results in 1, when it does not, it results in 0. This number is multiplied by -360/360 depending on the constraint. All three numbers are summed, resulting in the correct heading error between -180/180 degrees.

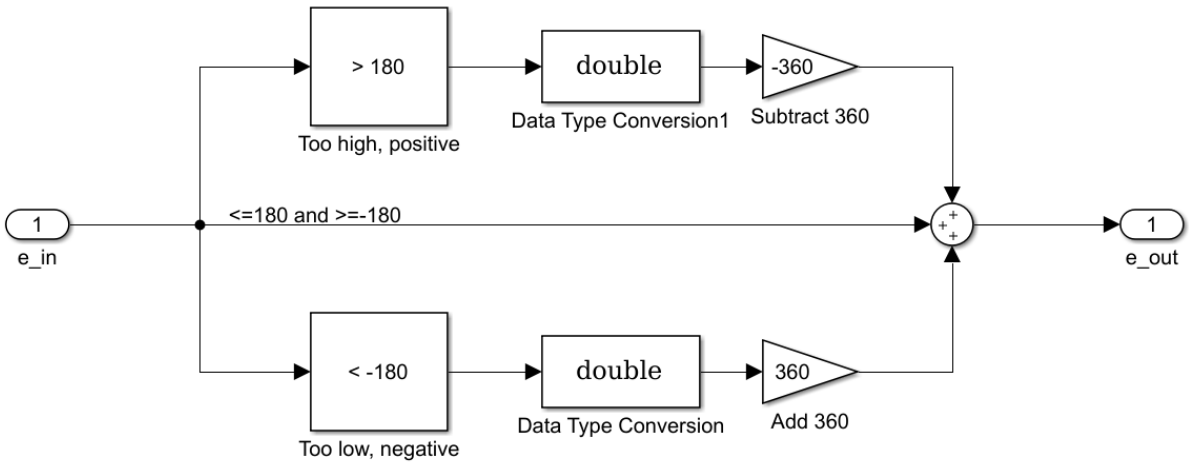

Figure B.9: Subsystem remove flip.

When the heading error is determined, it is compared to a deadband, blue block (*deadband heading error*) in Figure B.8. Figure B.10 shows the determination of the error after passing the deadband. The deadband (deadband error in Figure B.10 can be adjusted in the GUI as preferred. A small deadband results in a very accurate response of the vessel, a larger deadband results in just a response during a large error. For example, when the error is smaller than a deadband of 2°, the heading error sent to the PID-controller is 0°. If the error is larger than 2°, the error as determined, is sent to the PID-controller.

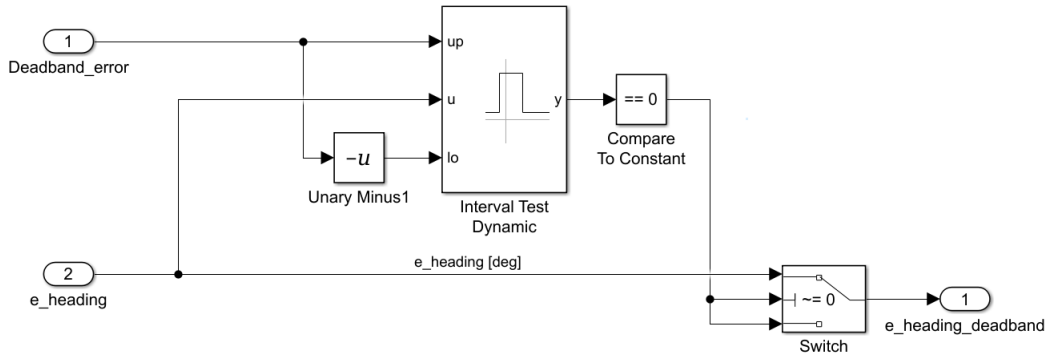

Figure B.10: Subsystem deadband heading error.

The PID-controller (pink block in Figure B.8) ensures the error to alter smoothly and create a steady system. It uses the heading error as input for the multiplications with the proportional ($k_p = 0.45$), integral ($k_i = 0.00015$) and derivative gain ($k_d = 0.245$).
The output of the PID-controller is the unlimited rudder set-point. This means the output can have a value of 35 degrees, which is not possible due to the maximum rudder angle of the vessel. When it leaves the waypoint controller, the unlimited set-point goes through a limiter (red block Figure B.1) which limits the set-point at -25 and +25 degrees (maximum rudder angle of the FRISC in the Marin simulator), resulting in the limited rudder set-point which can be used in a control option.

XTE controller

The XTE controller is the other control law which can be used to determine the rudder set-point. The bearing is in this case based on the cross track error and the speed of the vessel (Paragraph 4.3.2). In the XTE controller, the XTE is calculated and used to determine the desired heading angle (ψ_{set}). Figure B.11 shows the calculation of the XTE. The position of the vessel is compared to that of the relevant track. The equation given in Paragraph 4.3.2 is used to determine the distance (d_{XTE}) from the vessel to the course line.

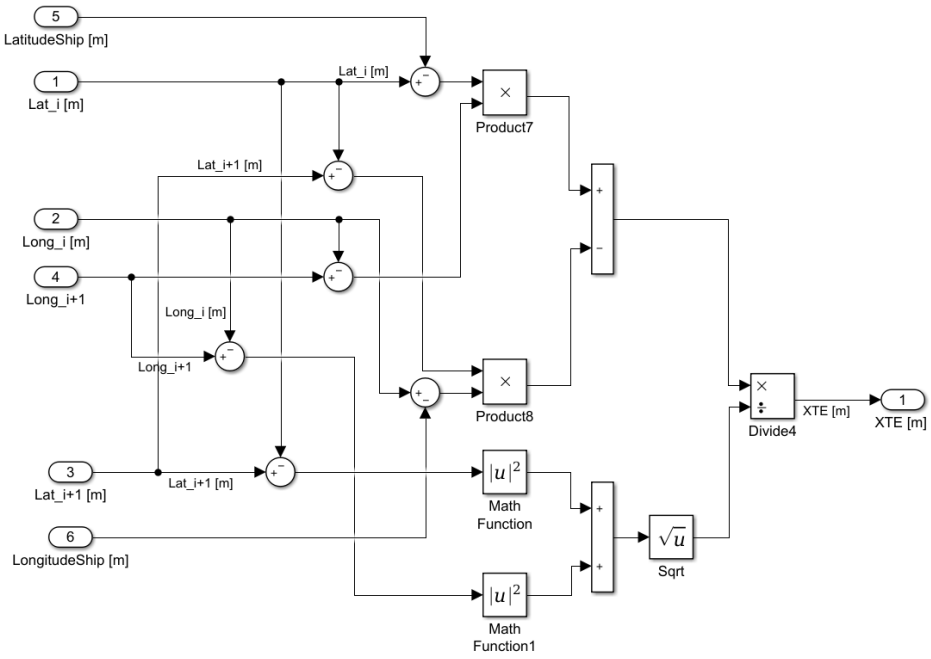

Figure B.11: Subsystem determine XTE.

The XTE is thereafter used to determine the heading set-point. Just as in the waypoint controller, the heading set-point is compared to the heading of the ship and the error is calculated. The heading error is sent through the *remove flip* block, the *deadband* and the *PID-controller*. Note that this PID-controller uses different values than the PID-controller used in the waypoint controller, $k_p = 0.605$, $k_i = 0.0.00005$ and $k_d = 0.245$.
The unlimited rudder set-point is again sent to the limiter to determine the limited rudder set-point which can be used as input for a control option.

Control options

Autopilot

The limited rudder set-point can be used for the autopilot when the haptic shared control is not used. The model uses, as input for the simulator, the limited rudder set-point as the value for the lever angle (MotAngZ). The simulator converts the rudder set-point to a rudder angle. The set-point value is used for both the rudders, this means that the rudders react exactly the same in the same circumstances. When the autopilot is not used, the model uses the MotAngZ2 (azimuth angle of 1 lever) as input for the simulator. Note that the output of the model must be encoded to the correct NMEA-sentences, will the simulator be able to use this value as an input. Figure B.12 shows the autopilot in the model.

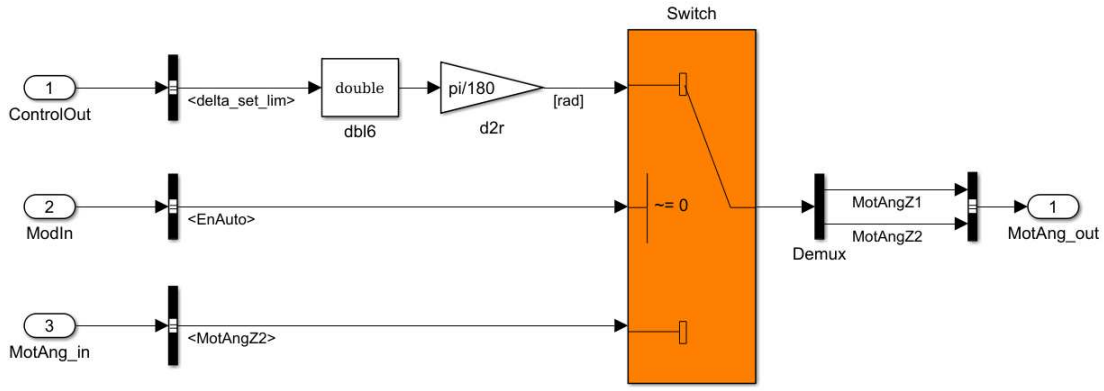

Figure B.12: Autopilot.

Haptic shared control

To provide the operator with haptic feedback and warning signals, the haptic shared control system is used, blue block Figure B.1. Figure B.13 shows the implementation of the controller in the Simulink model.
The input of this haptic system is the limited rudder set-point (-25 to +25 degrees). This is not directly used as input for the lever movements; an adjustable deadband (positive and negative) is inserted to be able to influence the movements of the lever when it is within a certain amount of accuracy. So, with a deadband of 2° and a set-point of 12°, and the position of the lever is within 10-14°, the lever does not move. The result of the summation of the set-point and the deadband is used as the new set-points which are compared with the actual azimuth angle of the levers and are sent through a limiter to turn the levers in the right direction. Thereafter, the set-points are multiplied with a spring constant, creating two torques which are sent to the levers.
With a side path it is possible to insert damping in the system causing the levers to only turn within an indicated range. Again, the set-points (after passing the deadband) are sent to a limiter and put through a discrete derivative with a limiter, resulting in the velocity in azimuth direction of the lever. The velocity is multiplied by a damping constant, resulting in a torque to reduce the vibrations of the lever around the indicated azimuth angle. These two torques are summed and multiplied by the azimuth boundary causing the lever to position correctly and only move within its realistic angles.
The two torques calculated after the multiplication with the spring constant and the damping are summed and sent through a limiter to indicate the maximum torque the levers can encounter. The result after the last limiter is the actual torque sent to the levers, so the levers turn and move the ship in the right heading direction.
Note that this subsystem just provides the correct amount of torque to move the lever to its set-point, the operator is still in control of the levers and the vessel uses the lever angle as input for the simulator.

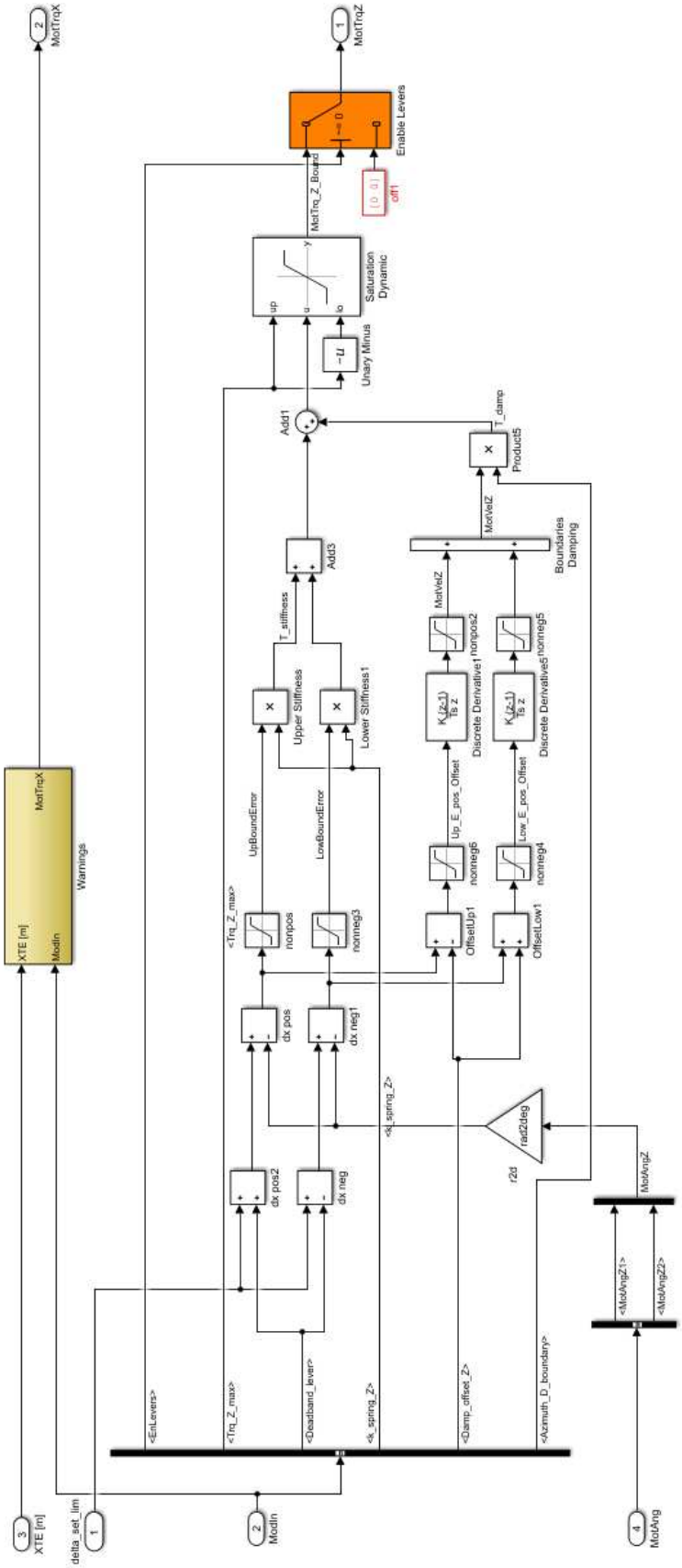

Figure B.13: Subsystem haptic shared control.

Besides the force feedback in the levers, the system is equipped with a warning system. As mentioned in Section 4.4.2 the warning signals are based on the cross track error of the vessel. The system can warn the operator when the ship has a too large XTE. Figure B.14 show the subsystem *warning* in Figure B.13.

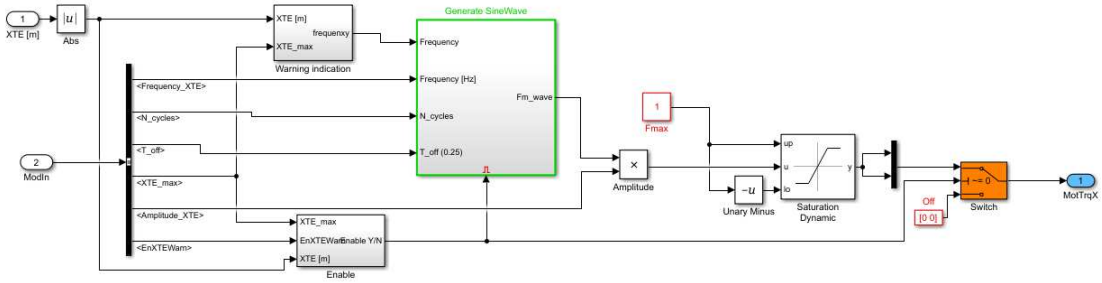

Figure B.14: Subsystem warnings.

The warning indications determine which vibration intensity the operator feels. Depending on the value of the XTE, 0.5, 1 or 1.5 times the frequency indicated in the model (50 Hz) is used as vibration frequency. Note that the warning signals are not used in this thesis because it could interfere with the results of the feedback system.

C. Graphical User Interface

This appendix describes the Graphical User Interface (GUI) used to control the compiled MATLAB Simulink model. The GUI is shown in Figure C.1. Only the buttons used during this thesis will be explained.

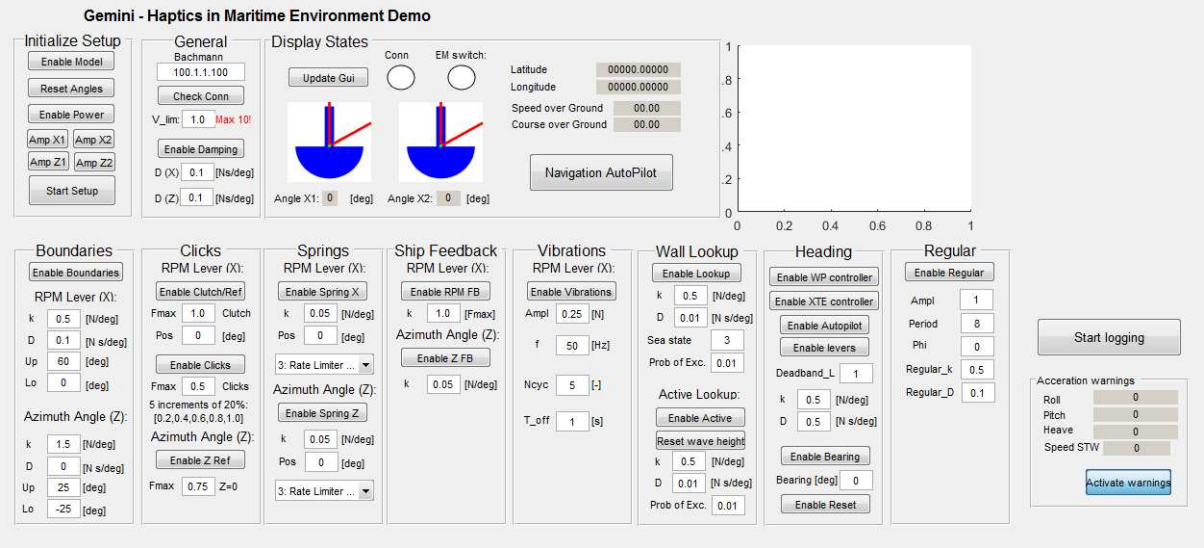

Figure C.1: Graphical User Interface.

At the top left, Initialize Setup, the model can be activated. The buttons are discussed from top to bottom. The top button, *Enable Model*, activates the complete model. When this button is not activated the model is not working. With the button *Reset Angles*, the lever angles are reset. The current lever position is used as the zero-point position. The Maxon motors coupled to the levers are switched on and off by the *Enable Power* button. The individual motors for the rpm and azimuth direction can be activated by the buttons *Amp X1*, *X2*, *Z1* and *Z2* respectively. Additionally, all the buttons discussed above can be activate at once with the *Start Setup* button.
At the right of the Initialize Setup, in the General part and the Display Sates, information about the lever settings can be found. At V-lim, the input voltage of the motors can be adjusted with a maximum of 10 volts. The *Enable Damping* button activates the damping in the levers in rpm and azimuth direction to ensure the levers move in such a way they will not get damaged.
The visual lever information is given in the Display States. With the button *Update Gui*, the visuals in the GUI are updated to the actual lever position. At the bottom of the Display States, the actual lever position in rpm direction is shown for each lever (Angle X1 an X2). The part at the right in Display States, the vessel information (i.e. coordinates, SOG and COG) and the *Navigation AutoPilot* button are not used.
At the bottom left of the GUI, the boundaries of the levers can be adjusted. To use the boundaries, the *Enable Boundaries* button has to be activated. The spring constant, damping and upper and lower boundaries can be adjusted for as well the rpm as the

azimuth direction.
The last part used in the GUI is that of the heading. This part controles the control laws developed in the MATLAB Simulink model. The two controllers, waypoint controller and XTE controller, can be activated separately with the buttons *Enable WP controller* and *Enable XTE controller*.
Furthermore, a choice can be made to let the craft sail with the autopilot (*Enable Autopilot*) or to use the haptic shared control (*Enable Levers*). For the latter, the lever deadband, the spring constant and the damping of the levers can be adjusted as preferred.
Additionally, a bearing can be activated separately with the use of the waypoint controller. This means that this part of the model is not coupled to the implemented route. This part of the model can be activated with the button *Enable Bearing* and the bearing can be indicated. The last button in the Heading part is the *Enable Reset* button which resets the current track indicator to 1. This is used to be able to use the model again without compiling the complete model again.
To be able to log the data during an experiment the button *Start Logging* can be used and the data can be viewed afterwards.

D. Participant form

Participant form

Name:.....

Age:.....

Gender:.....

Are you in possession of a navigation license (vaarbewijs)?: YES / NO

Do you have experience on the water (sailing or otherwise)?: YES / NO

Date (D/M/Y):...../...../.....

Assigned experimental order:.....

Signature:.....

E. NASA-TLX

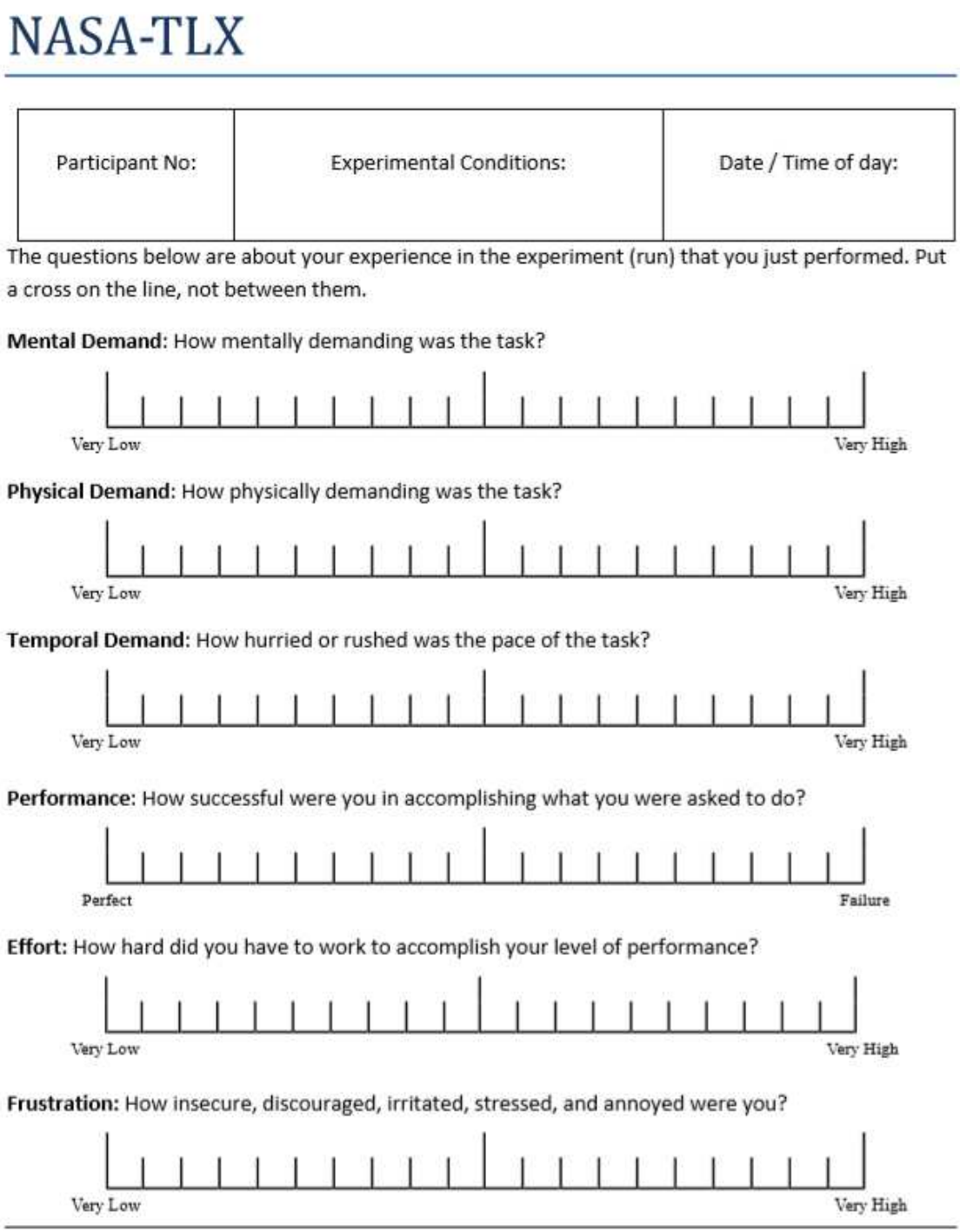

NASA-TLX

Participant No:	Experimental Conditions:	Date / Time of day:

The questions below are about your experience in the experiment (run) that you just performed. Put a cross on the line, not between them.

Mental Demand: How mentally demanding was the task?

Very Low — Very High

Physical Demand: How physically demanding was the task?

Very Low — Very High

Temporal Demand: How hurried or rushed was the pace of the task?

Very Low — Very High

Performance: How successful were you in accomplishing what you were asked to do?

Perfect — Failure

Effort: How hard did you have to work to accomplish your level of performance?

Very Low — Very High

Frustration: How insecure, discouraged, irritated, stressed, and annoyed were you?

Very Low — Very High

Figure E.1: NASA-TLX questionnaire.

Bibliography

[1] Barry Kirwan. Human error identification techniques for risk assessment of high risk systems-part 1: review and evaluation of techniques. *Applied Ergonomics*, 29(3):157–177, 1998.

[2] Frisc-motorboot. Retrieved from https://www.defensie.nl/onderwerpen/materieel/schepen/frisc-motorboot-fast-raiding-interception-and-special-forces-craft [Online; accessed 03-12-2017].

[3] Marine Specialised Technology Limited, Unit 2, Atlantic Way, Brunswick Business Park, Liverpool, L3 4BE. *Operator Manual FRISC, Boarding Craft Variant*, June 2012.

[4] Marine Specialised Technology Limited, Unit 2, Atlantic Way, Brunswick Business Park, Liverpool, L3 4BE. *Operator Manual FRISC, Suport Craft Caribbean Variant*, 2012.

[5] Stuart A. Bowye, Brian L. Davies, and Ferdinando Rodriguez y Baena. Active constraints/virtual fixtures: A survey. *IEEE TRANSACTIONS ON ROBOTICS*, 30(1):138–157, 2014.

[6] Frank Flemisch, Johann Kelsch, Christian Löper, Anna Schieben, and Julian Schindler. Automation spectrum, inner / outer compatibility and other potentially useful human factors concepts for assistance and automation. *Factors for assistance and automation*, pages 1–16, 2008.

[7] Mark Mulder, David A. Abbink, and Erwin R. Boer. Sharing control with haptics: Seamless driver support from manual to automatic control. *Human Factors*, 54(5):786–798, October 2012.

[8] D.A. Abbink and M. Mulder. *Neuromuscular Analysis as a Guideline in designing Shared Control*, chapter 27, pages 499–516. INTECH, April 2010.

[9] Thor I. Fossen. *Handbook of Marine Craft Hydrodynamics and Motion Control*. Wiley, 2011.

[10] Conventional ship testing. Retrieved from http://www.ivt.ntnu.no/imt/courses/tmr7/lecture/ship˙model˙testing.pdf [Online; accessed 12-03-2018].

[11] De frisc is er nog lang niet, June 2012. Retrieved from https://marineschepen.nl/dossiers/FRISC-is-er-nog-lang-niet.html [Online; accessed 07-12-2017].

[12] Stafbureau Personeelslogisitek. *Operationele evaluatie FRISC*. Royal Netherlands Navy, Rijkszee- en Marinehaven, 1780CA Den Helder, October 2015.

[13] Royal Netherlands Navy. *VCZSK DOPS NLMF STC 167.1*, November 2016. Zeemanschap deel 1.

[14] Juergen Sauer, David G. Wastell, G. Robert J. Hockey, C. Mmartin Crawshaw, Mai Ishak, and Jonathan C. Downing. Effects of display design on performance in a simulated ship navigation environment. *Ergonomics*, 45(10):329–347, 2002.

[15] Ada W.S. Leung, Chetwyn C.H. Chan, Jimmy J.M. Ng, and Peter C.C. Wong. Factors contributing to officers' fatigue in high-speed maritime craft operations. *Applied Ergonomics*, 37(2006):565–576, 2005.

[16] Gerald Matthews, D. Roy Davies, Stephen J. Westerman, and Rob B. Stammers. *Human Performance - Cognition, stress and individual differences*. Psychology Press, 2000.

[17] S. de Stigter, M. Mulder, and M.M. van Paassen. Design and evaluation of a haptic flight director. *Journal of Guidance Control and Dynamics*, 30(1):35–46, January 2007.

[18] Paul G. Griffiths and R. Brent Gillespie. Sharing control between humans and automation using haptic interface: Primary and secondary task performance benefits. *HUMAN FACTORS*, 47(3):574–590, 2005.

[19] David A. Abbink, Mark Mulder, and Erwin R. Boer. Haptic shared control: smoothly shifting control authority? *Cognition, Technology and Work*, 14(1):19–28, March 2012.

[20] F. Hoeckx, A. Vrijdag, and D.A. Abbink. Development of a test setup for exploring the potential of haptic feedback for maritime operations. In *Marine Electrical and Control Systems Safety*, November 2017. Marine Electrical and Control Systems Safety Conference (MECSS) 2017.

[21] Royal Netherlands Navy. *Hand-out FRISC*, version 1.13 edition.

[22] D. Stapersma, J. Pinkster, J.W. Frouws, et al. Design of advanced marine vehicles (reader), October 2000. Delft University of Technology.

[23] Defensie Materieel Organisatie. *Binationaal Gebruiksplan Fast Raiding, Interception and Special Forces Craft*, October 2013.

[24] Pedro Antao and C. Guedes Soares. Causal factors in accidents of high-speed craft and conventional ocean-going vessels. *Reliability Engineering and System Safety*, 93(9):1292–1304, 2008.

[25] P. Antao and C. Guedes Soares. Analysis of high speed craft accidents. In *Conference: Safety & Reliability, At Bedford & van Gelder (Eds.)*, volume 1, pages 37–44, July 2003.

[26] Bengt Schager. Increased safety for high-speed marine craft by focusing on operators and organization. *Marine Profile*, 1998. Marine Profile UK. Ltd., Londen, UK.

[27] Raluca Apostol-Mates and Alina Barbu. Human error - the main factor in marine accidents. *Naval Academy Scientific Bulletin "Mircea cel Batran" Naval Academy*, 19(2):451–454, 2016.

[28] Kristian S. Gould, Bjarte Knappen Roed, Vilhelm F. Koefoed, Robert S. Bridger, and Bente E. Moen. Performance-shaping factors associated with navigation accidents in the royal norwegian navy. *Military Psychology*, 18(sup1):S111–S129, 2006. Lawrence Erlbaum Associates, Inc.

[29] Report on the investigation of the grounding at high speed of the leisure powerboat sea snake, March 2006. Retrieved from https://assets.publishing.service.gov.uk/media/547c7092ed915d4c0d0000b1/Sea˙Snake.pdf [Online; accessed 16-04-2018].

[30] Report on the investigation of the grounding at high speed of the rib sooty, October 2009. Retrieved from https://assets.publishing.service.gov.uk/media/547c6fd240f0b60244000043/SootyReport.pdf [Online; accessed 16-04-2018].

[31] Rib-tocht strandt op de rassen, knrm brengt 51 mensen in veiligheid. Retrieved from https://www.pzc.nl/zeeuws-nieuws/rib-tocht-strandt-op-de-rassen-knrm-brengt-51-mensen-in-veiligheid a987059a/ [Online; accessed 16-04-2018].

[32] Snelle rib vastgelopen in het amsteldiep. Retrieved from https://www.knrm.nl/nieuws/knrm-reddingstation-texel-de-cocksdorp/snelle-rib-vastgelopen-in-het-amsteldiep [Online; accessed 16-04-2018].

[33] Twee schepen vastgelopen. Retrieved from https://www.knrm.nl/nieuws/knrm-reddingstation-lemmer/twee-schepen-vastgelopen [Online; accessed 16-04-2018].

[34] Report on the investigation of the ejection of six people from the rigid inflatable boat milly, January 2014. Retrieved from https://assets.publishing.service.gov.uk/media/547c6f30e5274a4290000011/Milly.pdf [Online; accessed 16-04-2018].

[35] G.R.J. Hockey, A. Healy, M. Crashaw, D.G. Wastell, and J. Sauer. Cognitive demands of collision avoidance in simulated ship control. *Human Factors*, 45(2):252–265, 2003.

[36] Erik Hollnagel. *Cognitive Reliability and Error Analysis Method (CREAM)*. Elsevier Ltd., 1998.

[37] Jaewhan Kim and Wondea Jung. A taxonomy of performance influencing factors for human reliability analysis of emergency tasks. *Journal of Loss Prevention in the Process Industries*, 16:479–495, 11 2003.

[38] Megha Goyal, Dimple Saproo, Asha Bagashra, and Kumar Rahul Dev. Haptics: Technology based on touch. *International Journal of Scientific Research Engineering & Technology*, 2(8):468–471, November 2013.

[39] Robert J. Stone and Example Corliss. Haptic feedback: A potted history, from telepresence to virtual reality. *Haptic Human-Computer Interaction*, pages 1–7, 2000.

[40] Frederick P. Brooks, Ming Ouh-Young Jr., James J. Battert, and P. Jerome Kilpatrick. Project grope - haptic displays for scientific visualization. *Computer Graphics*, 24(4):177–185, August 1990.

[41] B. H. McCormick. Visualization in scientific computing. *ACM SIGBIO Newsletter*, 10(1):15–21, March 1988.

[42] Jonathan C. Roberts and Sabrina Panëels. Where are we with haptic visualization? In *Second Joint EuroHaptics Conference and Symposium on Haptic Interfaces for Virtual Environment and Teleoperator Systems*. IEEE Computer society, March 2007.

[43] Carolina Passenberg, Raphaela Groten, Angelika Peer, and Martin Buss. Towards real-time haptic assistance adaptation optimizing task performance and human effor. In *World Haptics Conference*, pages 155–160, 2011.

[44] Sebastiaan M. Petermeijer, David A. Abbink, Mark Mulder, and Joost C. F. de Winter. The effect of haptic support systems on driver performance: A literature survey. *IEEE Transactions on Haptics*, 8(4):467–479, October 2015.

[45] Frank Beruscha, Klaus Augsburg, and Dietrich Manstetten. Haptic warning signals at the steering wheel: a literature survey regarding lane departure warning systems. *Haptics-e*, 4(5), March 2011.

[46] Jordan Navarro, Franck Mars, Jean-François Forzy, Myriam El-Jaafari, and Jean Michel Hoc. Objective and subjective assessment of warning and motor priming assistance devices in car driving. *Human Factors for assistance and automation*, pages 273–283, 2008.

[47] Jake J. Abbott, Panadda Marayong, and Allison M. Okamura. Haptic virtual fixtures for robot-assisted manipulation. In Sebastian Thmn, Rodney Brooks, and Hugh Durrant-Whyte (Eds.), editors, *Robotics Research. Springer tracts in advanced robotics*, volume 28, pages 49–64. Springer, 2007.

[48] David A. Abbink, Diane Cleij, Mark Mulder, and Marinnus M. van Paassen. The importance of including knowledge of neuromuscular behaviour in haptic shared control. In *Systems, Man and Cybernetics (SMC)*. IEEE International Conference on Systems, Man, and Cybernetics, October 2012.

[49] Louay Saleh, Philippe Chevrel, Fabien Claveau, Jean-Francois Lafay, and Franck Mars. Shared steering control between a driver and an automation: Stability in the presence of driver behavior uncertainty. *IEEE Transactions on intelligent transportation systems*, 14(2):974–983, June 2013.

[50] Eric J. Rossetter and J. Christian Gerdes. Lyapunov based performance guarantees for the potential field lane-keeping assistance system. *Journal of Dynamic Systems, Measurement, and Control*, 128(3):510–522, 2006.

[51] Franck Mars, Mathieu Deroo, and Jean-Michel Hoc. Analysis of human-machine cooperation when driving with different degrees of haptic shared control. *IEEE Transactions on haptics*, 7(3), July 2014.

[52] Mark Mulder, David A. Abbink, and Erwin R. Boer. The effect of haptic guidance on curve negotiation behavior of young, experienced drivers. In *IEEE International Conference on Systems, Man and Cybernatics*, 2008.

[53] Mark Mulder and David A. Abbink. Sharing control with elderly drivers: Haptic guidance during curve negotiation. *IFAC Proceedings Volumes*, 43(13):310–315, 2010.

[54] Pilot assist en lane keeping aid. Retrieved from https://support.volvocars.com/nl/Pages/article.aspx?article=3395a91b40bddd9ac0a801511916dab3 [Online; accessed 01-02-2018].

[55] Lane assist. Retrieved from https://www.volkswagen.nl/over-volkswagen/technieken [Online; accessed 01-02-2018].

[56] Audi active lane assist. Retrieved from https://www.audi.nl/nl/web/nl/innovatie/assistentiesystemen/cruise-control/lane-assist.html [Online; accessed 01-02-2018].

[57] Volvo lane keeping aid. Retrieved from https://www.youtube.com/watch?v=JlP6˙t7KVJ4 [Online; accessed 01-02-2018].

[58] Cnt204/x function modules. Retrieved from https://www.bachmann.info/fileadmin/media/Produkte/Steuerungssystem/Produktblaetter/CNT204˙en.pdf [Online; accessed 06-20-2018].

[59] Mh200 processor modules. Retrieved from https://www.bachmann.info/fileadmin/media/Produkte/Steuerungssystem/Produktblaetter/MH200-series˙en.pdf [Online; accessed 06-20-2018].

[60] Retrieved from www.automationworld.com/article/technologies/communication-protocols-standards/m1-controller-system-bachmann-speaks-all [Online; accessed 06-25-2018].

[61] Klaus Betke. The nmea 0183 protocol, May 2000. Retrieved from http://www.tronico.fi/OH6NT/docs/NMEA0183.pdf [Online; accessed 06-20-2018].

[62] Analog input/ output modules. Retrieved from https://www.bachmann.info/fileadmin/media/Produkte/Steuerungssystem/ Produktblaetter/GIO212˙en.pdf [Online; accessed 06-20-2018].

[63] J.B. Koolmees. *DOLPHIN user's guide*. MARIN, 6700 AA Wageningen, 4.2.1 edition, January 2018.

[64] L.E. Dubins. On curves of minimal length with a constraint on average curvature, and with prescribed initial and terminal positions and tangents. *American Journal of Mathematics*, 79(3):497–516, July 1957.

[65] C.A. de Groot. Basiselementen der navigatie. Royal Netherlands Navy, October 2013.

[66] Manoeuvring committee of 23rd ITTC. Ittc - recommended procedures. In *International towing tank conference*, 2002.

[67] Eric Weisstein. Point-line distance 2 dimensional, May 2018. Retrieved from http://mathworld.wolfram.com/Point-LineDistance2-Dimensional.html [Online; accessed 22-05-2018].

[68] Thor I. Fossen. *Guidance and Control of Ocean Vehicles*. John Wiley and Sons, 1994.

[69] Cheng Chew Lim. *Autopilot design for ship control*. PhD thesis, Loughborough University of Technology, 1980.

[70] prof.ir. J. Gerritsma. Golven, scheepsbewegingen, sturen en manoeuvreren 1. Delft University of Technology.

[71] Job van Amerongen. *Adaptive steering of ships: a model-reference approach to improved manoevring and economical course keeping*. PhD thesis, Delft University of Technology, 1982.

[72] A.J. de Winter. Design and implementation of a path following system for an autonomous vehicle. Master's thesis, Delft University of Technology, February 2017.

[73] Anastasios M. Lekkas and Thor I. Fossen. A time-varying lookahead distance guidance law for path following. *IFAC Proceedings Volumes*, 45(27):398–403, 2012. 9th IFAC Conference on Manoeuvring and Control of Marine Craft.

[74] James V. Bradley. Complete counterbalancing of immediate sequential effects in a larin square design. *Journal of the American Statistical Association*, 53(282):525–528, 1958.

[75] Human Performance Research Group. *Task Load Index*. NASA.

[76] Difference between gps and dgps, June 2017. Retrieved from http://grindgis.com/blog/difference-between-gps-and-dgps [Online; accessed 03-06-2018].